

JOURNAL OF CAVE AND KARST STUDIES

March 2019
Volume 31, Number 1
ISSN 1090-6924
A Publication of the National
Speleological Society



DEDICATED TO THE ADVANCEMENT OF SCIENCE,
EDUCATION, EXPLORATION, AND CONSERVATION

**Published By
The National Speleological Society**

<http://caves.org/pub/journal>

Office

6001 Pulaski Pike NW
Huntsville, AL 35810 USA
Tel:256-852-1300
nss@caves.org

**Editor-in-Chief
Malcolm S. Field**

National Center of Environmental
Assessment (8623P)
Office of Research and Development
U.S. Environmental Protection Agency
1200 Pennsylvania Avenue NW
Washington, DC 20460-0001
703-347-8601 Voice 703-347-8692 Fax
field.malcolm@epa.gov

**Production Editor
Scott A. Engel**

Knoxville, TN
225-281-3914
saecaver@gmail.com

**Journal Copy Editor
Linda Starr**

Albuquerque, NM

The *Journal of Cave and Karst Studies*, ISSN 1090-6924, CPM Number #40065056, is a multi-disciplinary, refereed journal published four times a year by the National Speleological Society. The *Journal* is available by open access on its website, or check the website for current print subscription rates. Back issues are available from the NSS office.

POSTMASTER: send address changes to the National Speleological Society Office listed above.

The *Journal of Cave and Karst Studies* is covered by the following ISI Thomson Services Science Citation Index Expanded, ISI Alerting Services, and Current Contents/Physical, Chemical, and Earth Sciences.

Copyright © 2019
by the National Speleological Society, Inc.

BOARD OF EDITORS

Anthropology

George Crothers
University of Kentucky
Lexington, KY
george.crothers@utk.edu

Conservation-Life Sciences

Julian J. Lewis & Salisa L. Lewis
Lewis & Associates, LLC.
Borden, IN
lewisbioconsult@aol.com

Earth Sciences

Benjamin Schwartz
Texas State University
San Marcos, TX
bs37@txstate.edu

Leslie A. North

Western Kentucky University
Bowling Green, KY
leslie.north@wku.edu

Mario Parise

University Aldo Moro
Bari, Italy
mario.parise@uniba.it

Carol Wicks

Louisiana State University
Baton Rouge, LA
cwicks@lsu.edu

Exploration

Paul Burger

National Park Service
Eagle River, Alaska
paul_burger@nps.gov

Microbiology

Kathleen H. Lavoie

State University of New York
Plattsburgh, NY
lavoiekh@plattsburgh.edu

Paleontology

Greg McDonald

National Park Service
Fort Collins, CO
greg_mcdonald@nps.gov

Social Sciences

Joseph C. Douglas

Volunteer State Community College
Gallatin, TN
615-230-3241
joe.douglas@volstate.edu

Book Reviews

Arthur N. Palmer & Margaret V Palmer

State University of New York
Oneonta, NY
palmeran@oneonta.edu

Front cover: Miocene neritic limestone layers in Turkey. . See Şener and Öztürk in this issue.

OBSERVATIONS ON THE POPULATION ECOLOGY OF THE CAVE SALAMANDER, *EURYCEA LUCIFUGA* (RAFINESQUE, 1822)

J. Gavin Bradley¹ and Perri K. Eason²

Abstract

Salamanders are potentially important constituents of subterranean ecosystems, but relatively little is known about their effects in caves. A common facultative hypogean salamander in the eastern United States is the Cave salamander, *Eurycea lucifuga* (Rafinesque, 1822). Despite being common and widespread, little more than basic information exists for this species. Herein, we provide new data concerning open population modeling, demographics, wet-biomass, and density estimation for a population in a small Kentucky spring cave. We have found population abundances of this species to be much higher than previously reported, and describe low capture probabilities and high survival probabilities. Average wet-weight per individual was 2.90 g, and estimated seasonal population wet-biomass peaked at 1426.8 g. Mean salamander density and wet-biomass density are 0.08 salamanders m⁻² and 0.22 g m⁻², respectively. The data we provide indicate that Cave salamanders have important ecological impacts on small spring cave systems.

Introduction

The Cave salamander, *Eurycea lucifuga* (Rafinesque, 1822), is a facultative cave dweller that is native to the eastern United States (Hutchison, 1958; Williams, 1980; Petranksa, 1998; Camp et al., 2014). The classification scheme of cave-dwelling organisms is in flux due to a lack of consensus for terminology that defines the gradations of dependency that organisms have on cave environments. Troglobites, or troglobionts, are wholly dependent upon cave environments and cannot persist outside of them. Facultative cave-dwelling organisms may be broadly defined as troglophilic and troglonexic. Troglophiles are able to persist entirely in or outside of caves, whereas troglonexes are frequently found in caves but must leave at some point during their life cycle to obtain one or more epigeal resources. *Eurycea lucifuga* must leave caves to obtain sufficient food resources from surface environments, but may otherwise persist in subterranean environments. Under the classical troglobite-troglophile-troglonex-accidental scheme (e.g., Barr Jr. 1968; Barr and Holsinger 1985; Trajano and Carvalho 2017), *E. lucifuga* is classified as a troglonex. A slightly different classification scheme has been suggested recently: troglobiont-eutroglophile-subtroglophile-troglonex (e.g., Lanza et al. 2006; Sket 2008; Lunghi et al. 2014) according to which *E. lucifuga* is classified as a subtroglophile. Categories of these two classification schemes (classic versus newer) are somewhat synonymous: troglobite is synonymous with troglobiont, troglophile is similar to eutroglophile, troglonex is similar to subtroglophile, and accidental is similar to troglonex. However, there are discrepancies within the two naming systems as to the meaning of troglophile and troglonex, leading to confusion of these terms. Therefore, here we simply refer to *E. lucifuga* as a facultative cave-dwelling organism, one that is dependent upon epigeal food resources.

Cave salamanders are relatively common, but little more than some natural history, morphology, physiology, taxonomy, behavior, and basic ecological information exists for this species. Cave salamanders may be important constituents of subterranean ecosystems, since salamanders are generally considered to be key ecological components in certain ecosystems (Davic and Welsh, 2004; Semlitsch et al., 2014). We collected data on a population of Cave salamanders from a Kentucky cave to report basic demographic information, and to calculate seasonal abundance estimates, capture probabilities, and survival probabilities using open-population models. These abundances were used to estimate seasonal wet-biomass, and we estimated wet-biomass density and salamander density from the same cave. This represents the first approximation of these characteristics for this species.

Population modeling and estimates of biomass and density provide important species information, which facilitates a greater understanding of the ecological influence a species has in its ecosystem. This is important because the impact of cave-dwelling salamanders on cave ecosystems is poorly understood. Populations of obligate cave species (i.e., troglobites) are typically small, due to the lack of available energy within their habitat (Venarsky et al., 2014). However, facultative cave species, such as Cave salamanders, use the epigeal environment, where abundant energy is accessible, likely supporting larger populations of these organisms. This may have great implications for cave ecosystem dynamics. Estimates of population model parameters, biomass, and density of facultative cave-dwelling salamanders may provide important insights that can inform cave ecology and conservation.

¹Elizabethtown Community and Technical College, Biology Department, 600 College Street Road, Elizabethtown, KY 42701, jbradley0127@kctcs.edu

²University of Louisville, Department of Biology, Life Sciences Building, Room 139, Louisville, KY 40208, perri.eason@louisville.edu

Methods

We monitored a population of *E. lucifuga* in two mostly crawlway-sized passages, 99 m (main passage) and 82.3 m (side passage), of Sauerkraut Cave, a small spring cave in E.P. “Tom” Sawyer State Park, Louisville, Kentucky, USA. (Specific location details are not given in an effort to reduce potential disturbance and vandalism to the cave, but may be obtained upon request from the Kentucky Speleological Survey). This cave was historically used as a springhouse, and was modified extensively with the construction of troughs and brick walls that spanned much of the entrance (Ford and Ford, 1882). The perennial stream was channelized to the west side of the main passage through a brick trough. The water exits the cave, then is immediately routed underground by a pipe.

Surveys were generally conducted weekly from March 2015 to February 2017, but survey dates were modified occasionally due to flooding or scheduling difficulties. In each passage, we searched the walls, floor, ceiling, and standing water for terrestrial (adult and juvenile) salamanders using red-filtered light during daylight hours (typical start time between 1100 to 1230). Hutchison (1958), Williams (1980), and Briggler and Prather (2006) similarly conducted surveys of this species during daylight hours. We counted all individuals found and used an Olympus TG-4 digital camera (Olympus America Inc., Center Valley, Pennsylvania, USA) to photograph the dorsal spot pattern of the head and neck of each salamander in plain sight. These images were used for individual identification in the pattern-recognition software Interactive Individual Identification System-Spot version 4.0.2 (I³S-S) (van Tienhoven et al., 2007; den Hartog and Reijns, 2014). This method of individual identification has been found to be successful for this species (Bradley and Eason, 2018) and closely related *E. longicauda longicauda* (Jonas et al., 2011; Nazdrowicz, 2015). We also photographed the entire dorsal surface of individuals next to metered tape to create scaled images. From these images we measured snout-furrow length (SFL), a body metric similar to snout-vent length (SVL) (unpublished data, Bradley), in millimeters (\pm SE) using image analysis software, ImageJ 1.48v (Schneider et al., 2012). We determined gender by secondary sexual characteristics (males: swollen mental gland and elongated oral cirri; females: ovaries visible through the body wall) that are particularly evident from July to November. Additionally, we estimated age classes (adult and juvenile) by SFL; referencing measurements of SVL at sexual maturity, reported by Hutchison (1966) and Carlyle et al. (1998) for Cave salamanders, we classified individuals ≥ 49 mm SFL as adults.

Summary statistics are presented as the mean (\pm SE). A χ^2 goodness-of-fit test was conducted using R statistical software 3.4.1 (R Core Team, 2017) to determine if the observed sex ratio of this population differed ($\alpha = 0.05$) from the expected 1:1 ratio. We estimated population parameters (i.e., abundance, capture and survival probabilities) using recapture histories in open (Jolly–Seber) population models. Open population models allow births, deaths, immigration and emigration to occur, and are more realistic for long-term studies. The repeated surveys resulted in recapture histories for those individuals that were seen and marked (i.e., photographed) more than once. We conducted model estimation by season: spring (March to May), summer (June to August), fall (September to November), and winter (December to February). Population models were analyzed using Rcapture (Baillargeon and Rivest, 2007) in R. We assessed model fit with Akaike Information Criterion and by refitting models with Pearson residuals ≥ 2 (Baillargeon and Rivest, 2007; Beck et al., 2013). Estimates for each sampling period within a season were pooled to provide a single mean (\pm SE) value of each parameter for each season.

To estimate salamander population biomass, we modified the equation $W = aSVL^b$ (Salvidio, 1998; Huntsman et al., 2011) by substituting SVL with SFL (i.e., $W = aSFL^b$), to calculate individual salamander weight (W). For estimating the constants, a and b , we collected, weighed, and measured salamanders from March to April 2017, after the original study period. For these salamanders, we measured SFL as described above using ImageJ. To obtain individuals' W, we directed salamanders by hand, or an aquarium net, into a tared, plastic bag containing a paper towel wetted with cave water and then weighed them in grams (\pm SE) using a Pesola Micro-Line spring scale. We then released them at the site of capture. Also, we noted gender during this procedure, using similar sexual characteristics as described above; individuals too small to exhibit sexual characteristics were classified as juveniles. Capture and handling followed guidelines by Shaffer et al. (1994), HACC (2004), and Stasiak (2015).

We developed regressions (predictor variable = SFL; response variable = W) for males ($n = 36$), females ($n = 20$), and juveniles ($n = 4$), using log-transformed data for preliminary comparisons to determine whether there were differences in regressions between males vs. females and adults vs. juveniles. We analyzed these comparisons using ANCOVA in R. Since no significant differences in the relationship between SFL and W were detected among groups (see Results), one common regression equation was developed using non-log-transformed data. We used that equation and SFL measurements acquired from March 2015 to February 2017 to estimate individuals' W for the study population. Next, we calculated the mean individual W, then multiplied the mean W by seasonal abundances to estimate seasonal wet-biomass, following Salvidio (1998) and Crawford and Peterman (2013). We estimated mean (\pm SE) wet-biomass density (g m^{-2}) by first multiplying mean W by the mean salamander count, then dividing this number by the available surface area of the walls and floor of the cave. Subsequently, we estimated mean (\pm SE) salamander density (salamanders m^{-2}) by dividing the mean salamander count by the same available cave surface area.

Results

The mean salamander count per survey was 66.10 ± 4.00 (range: 10 to 245; $n = 73$) and the mean number of salamanders photographed per survey was 38.40 ± 2.97 (range: 0 to 172; $n = 72$), with a total of 1127 individual salamanders identified. The numbers of individuals identified as males and females were 97 and 106, respectively. The sex ratio is 1:1.1, which does not deviate significantly from a 1:1 ratio ($\chi^2 = 0.40$, $df = 1$, $p = 0.528$). Mean SFL was 55.26 ± 0.41 mm (range: 25.84 to 74.77; $n = 380$) in study year one (March 2015 to February 2016), with 80.3% of captured individuals sexually mature (≥ 49 mm SFL). Similarly, mean SFL was 56.82 ± 0.37 mm (range: 35.95 to 73.91; $n = 364$) in study year two (March 2016 to February 2017), with 81.6% ≥ 49 mm SFL. Open population models revealed that salamander abundance was highest in spring 2016, with the maximum abundance estimated at 492 ± 77.2 individuals (Table 1, Fig. 1).

Capture probabilities (Table 1) were correspondingly low in spring 2016 (0.04 ± 0.01 probability); the probability of being captured in the cave was also relatively low in summer (0.13 in 2015 and 2016), but higher in fall and winter (range: 0.20 to 0.29). Prob-

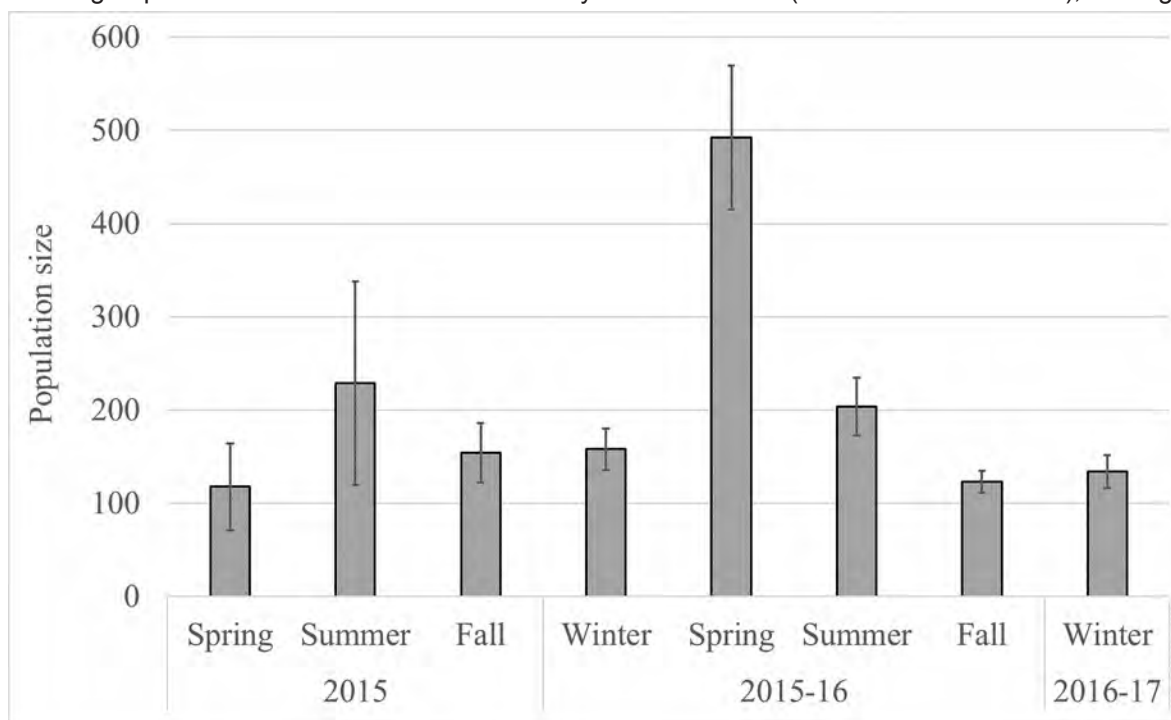


Figure 1. Seasonal estimates of the population size (\pm SE) of Cave salamanders in Sauerkraut Cave in from 2015 to 2017.

Table 1. Parameters calculated in open population models in the Rcapture package of R. Values are presented as the mean \pm SE.

Season	Year	Abundance	Capture Probability	Survival Probability
Spring	2015	118 \pm 46.5	0.068 \pm 0.029	0.923 \pm 0.095
Summer	2015	229 \pm 109	0.126 \pm 0.063	0.961 \pm 0.352
Fall	2015	154 \pm 31.8	0.204 \pm 0.048	0.709 \pm 0.063
Winter	2015 – 16	158 \pm 22.6	0.227 \pm 0.032	0.858 \pm 0.043
Spring	2016	492 \pm 77.2	0.038 \pm 0.010	0.930 \pm 0.024
Summer	2016	204 \pm 31.1	0.127 \pm 0.024	0.798 \pm 0.040
Fall	2016	123 \pm 11.8	0.292 \pm 0.038	0.730 \pm 0.037
Winter	2016 – 17	134 \pm 17.8	0.208 \pm 0.029	0.850 \pm 0.026

SFL from March 2015 to February 2017 was 2.90 ± 0.042 g (range: 0.27 to 6.31 g; $n = 649$). Estimates of seasonal wet-biomass (Table 2) showed high biomass in spring 2016 and relatively low biomass in fall and winter, as would be expected given the numbers of salamanders seen during respective surveys.

The total available surface area of walls and floor in Sauerkraut Cave is 853.4 m² (main passage: 468.8 m²; side passage: 384.6 m²). Mean wet-biomass density was 0.22 ± 0.014 g m⁻² (range: 0.03 to 0.83; $n = 73$). Mean sal-

ability of survival was high in spring and summer 2015 and spring 2016 (range: 0.92 to 0.96) and lowest in fall (0.71 and 0.73 for 2015 and 2016, respectively).

Regressions of SFL and W showed that the relationship between length and weight did not differ significantly in either males vs. females or adults vs. juveniles ($F = 0.37$, $df = 1$, $p = 0.55$ for males vs. females; $F = 1.58$, $df = 1$, $p = 0.21$ for adults vs. juveniles). Thus, we used a common regression line for all individuals, $W = 0.0155(\text{SFL})^{3.0042}$ (Fig. 2). Mean calculated W for salamanders with measured

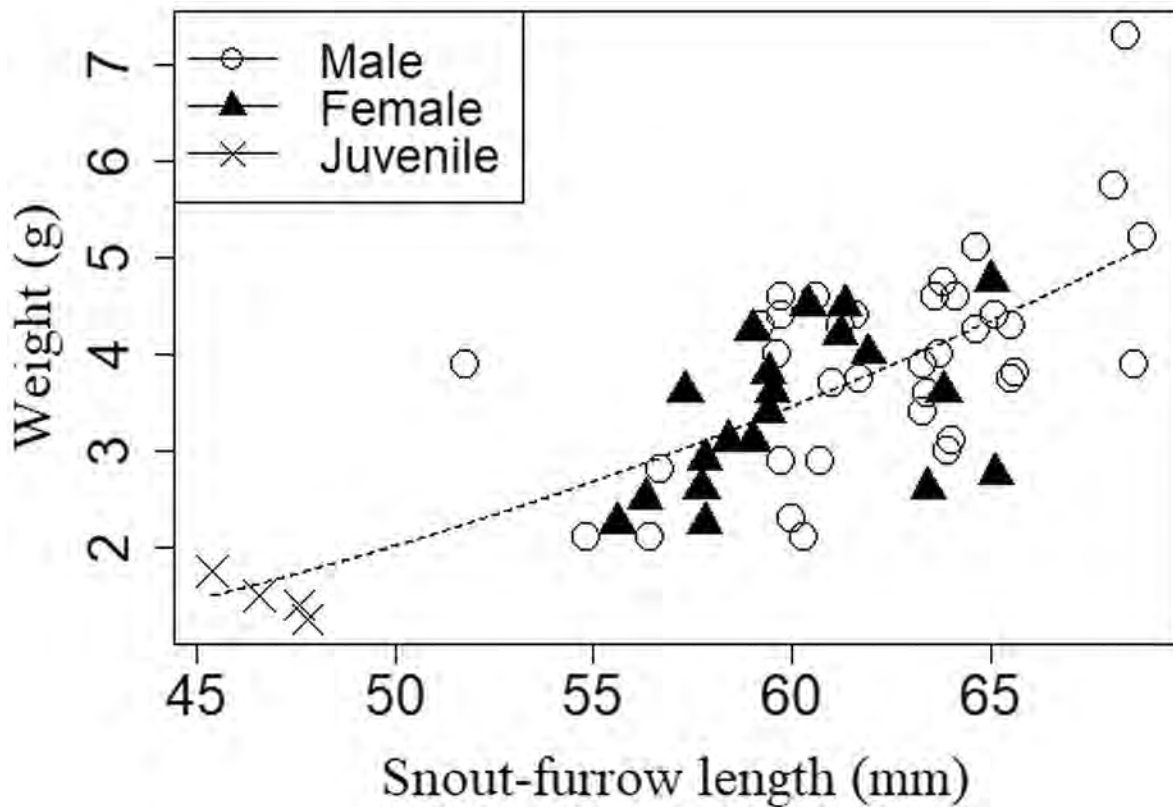


Figure 2. Scatterplot and power trendline, $W = 0.0155(SFL)^{3.0042}$, for the relationship between SFL and W for male, female, and juvenile Cave salamanders.

Table 2. Estimates of seasonal population wet-weight biomass for Cave salamanders at Sauerkraut Cave.

Season	Year	Wet-Weight Biomass, g
Spring	2015	342.2
Summer	2015	664.1
Fall	2015	446.6
Winter	2015 – 16	458.2
Spring	2016	1426.8
Summer	2016	591.6
Fall	2016	356.7
Winter	2016 – 17	388.6

(1958) found that males were more dominant in his study with a ratio of 1.6:1, mentioning there was no apparent reason for this deviation. He suggested that gravid females may become less active and/or more secluded than males during the breeding season to explain part of this bias. However, Hutchison (1958) sampled 11 months out of one year and consistently found more males than females regardless of season. No evidence was found in this study to support Hutchison's suggestion. Mean snout-furrow length (SFL) for this population of Cave salamanders is similar to snout-vent length measures reported by Hutchison (1958), Williams (1980), Carlyle et al. (1998) and Juterbock (2005) for other Cave salamander populations. Mean SFL and the proportion of salamanders ≥ 49 mm SFL indicates adults are numerically dominant in this population with a relatively low presence of juveniles (19.7 % in study year

Table 3. Wet-weight biomass density and salamander density of Cave salamanders in Sauerkraut Cave.

Passage	n	Wet-Weight Biomass Density (g m ⁻²)			Salamander Density (individuals m ⁻²)		
		Mean	SE	Range	Mean	SE	Range
Main	76	0.34	0.022	0.04 – 1.37	0.12	0.007	0.01 – 0.47
Side	73	0.09	0.007	0.00 – 0.38	0.03	0.003	0.00 – 0.13
Total	73	0.22	0.014	0.03 – 0.83	0.08	0.005	0.01 – 0.29

one and 18.4 % in study year two). Juveniles composed 11.35 % of marked individuals in Hutchison (1958), and Nazdrowicz (2015) found that juveniles of *E. l. longicauda* comprised 11 to 35 % of total populations. This pattern is characteristic of other plethodontid salamanders as well (Hairston Sr., 1987).

To our knowledge, this study provides the first estimates of abundance using open population models for *E. lucifuga*, and the first account of capture and survival probabilities for this species. Previously, Hutchison (1958) provided esti-

amander density was 0.08 ± 0.005 salamanders m⁻² (range: 0.01 to 0.29; n = 73). Mean wet-biomass density and salamander density for each passage separately are shown in Table 3.

Discussion

The sex ratio is near the expected 1:1, which is near the estimation of 1.125:1 (male:female) by Williams (1980) for another population of this species. Hutchison

mates of population size for *E. lucifuga* using a closed (Lincoln-Peterson) population model. His estimates of population size (36 to 63 individuals from four caves in Virginia, USA) are low compared to ours, likely because he only sampled from the twilight zone of his study caves. *Eurycea lucifuga* is known to inhabit both the dark and twilight zones of caves (Green et al., 1967), and population distribution patterns change seasonally within these zones (Hutchison, 1958; Williams, 1980; Camp et al., 2014). Our observations in the dark zone of Sauerkraut Cave indicated that a substantial proportion of the population occurs there depending upon the time of year. Hutchison (1958) also pooled counts and recaptures for his entire study year. This practice violates the assumption of closure and, thus, results in poor model estimation. He acknowledged the inadequacies of using this model, suggesting rough estimates at best. We have found that population size estimates for cave-inhabiting *E. lucifuga* may be much larger, and probably more accurate, when individuals from both the dark and twilight zones are included in open population modeling. We believe our estimates are reasonable because they are within range of estimates for other species of salamanders occupying caves (Huntsman et al., 2011; Fenolio et al., 2014; Taylor et al., 2015) or similar habitats, i.e., springhouses (Nazdrowicz, 2015) and wet rock faces (Salvidio, 1998; Crawford and Peterman, 2013) (Table 4).

Table 4. Population estimates and densities of salamander species that inhabit caves or similar habitat (i.e., springhouses and rock faces).

Source	Species	Population Estimate	Density (salamanders m ⁻²)
Salvido (1998)	<i>Hydromantes [Speleomantes] strinatii</i>	155	0.8
Huntsman et al. (2011)	<i>Gyrinophilus palleucus</i>	109, 215	0.03 & 0.10
Crawford and Peterman (2013)	<i>Desmognathus</i> spp.	496	14.69
Fenolio et al. (2014)	<i>Eurycea spelaea</i>	342, 507	0.04 & 0.12 (larvae & adults)
Nazdrowicz (2015)	<i>Eurycea longicauda</i>	29–1410	...
Taylor et al. (2015)	<i>Plethodon albagula</i>	157	0.61–1.14

Our highest seasonal abundance estimates, which occurred in spring 2016, followed by summer of both years, generally reflect trends that others have found for *E. lucifuga*, with monthly (May to June: Hutchison, 1958; May: Williams, 1980) or seasonal (spring: Camp et al., 2014; summer: Briggler and Prather, 2006) highest counts and average counts similarly reported at these times. These earlier authors studied Cave salamanders in the twilight zone of their study caves, and given that Cave salamanders predominantly reside in this area of caves in spring and summer (Hutchison, 1958; Williams, 1980) it is unsurprising that their studies found highest abundance then.

In our study, the lowest seasonal abundance occurred in spring 2015, which is probably atypical for the spring season. Two factors, flooding and temperature, may account for this discrepancy. A substantial flood (ca. 17.3 cm rainfall in two days) occurred in April 2015 that likely explains the low counts of salamanders in subsequent surveys that month (Fig. 3) because salamanders probably retreated to other areas of the cave or were flushed out; this, undoubtedly, affected abundance estimates for spring 2015. Furthermore, average temperature in February and March of 2015 (−3.2 and 6.9 °C, respectively) for Louisville, Kentucky was lower than the central state average (3.4 and 8.2 °C, respectively), and lower that year than in 2016 (3.9 and 11 °C, respectively) (UKAWC,

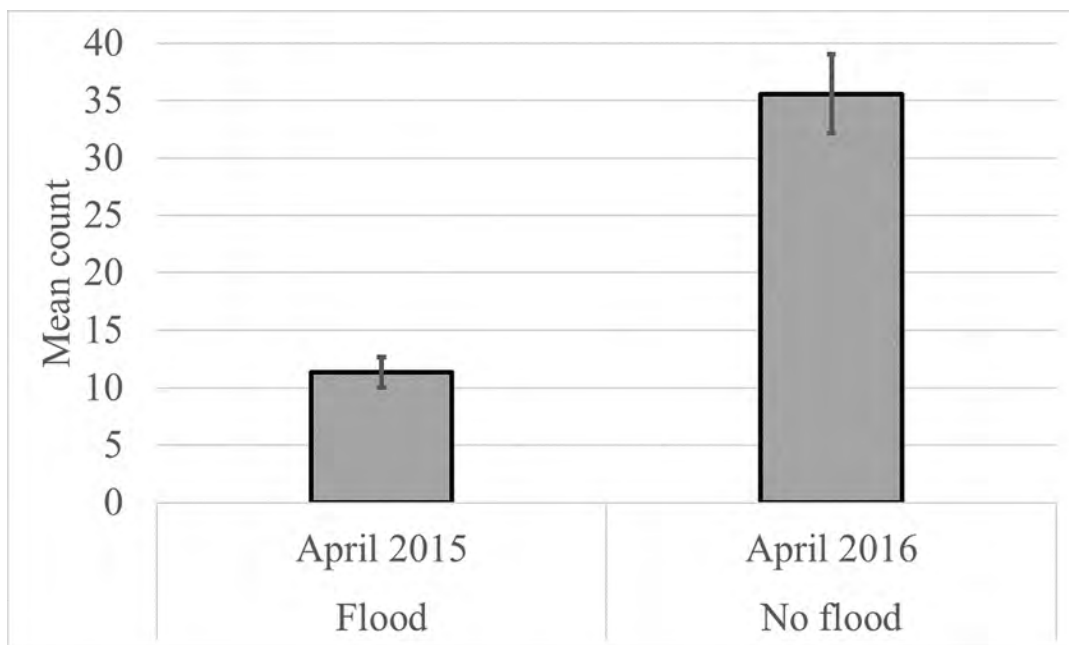


Figure 3. Mean counts (± SE) of Cave salamanders in Sauerkraut Cave in April 2015, when there was a substantial flood, and April 2016, when there was no substantial flood.

2017). This may have influenced the distribution and activity of Cave salamanders within the cave, especially in the twilight zone, where surface environmental fluctuations are most apparent. Our next lowest abundance estimate was in fall 2016. In two studies that focused on the twilight zone, the lowest counts for this species were reported in winter (Hutchison, 1958; Camp et al., 2014); Cave salamanders are rarely found in the twilight zone of caves during winter because the population has moved to the dark zone to escape the inhospitable (i.e., cold and dry) environment near the cave entrance (Hutchison, 1958; Williams, 1980). In a third study that also found the lowest counts in winter, Briggler and Prather (2006) likely surveyed the dark zone of some study caves, but it is unclear how many of their study caves included the dark zone or how far they penetrated. It is uncertain why low abundance occurred in fall in our study, but this result may be associated with low survival probabilities (discussed below).

Capture probabilities for salamanders are generally low due to reduced levels of detectability (O'Donnell and Semlitsch, 2015) and have been shown to vary temporally for both epigeal (Bailey et al., 2004; Price et al., 2012; Muncy et al., 2014) and hypogean (Fenolio et al., 2014) species. As expected, capture probabilities in our study were also low and variable, being lowest in spring 2015 and 2016. Cave salamanders often leave caves in spring to explore adjacent epigeal habitats for foraging or may emigrate (Petranka, 1998), thus being unavailable for capture in the cave. High capture probability occurred in fall and winter of 2015 and was highest in fall 2016. Cave salamanders reinvade deeper portions of the twilight zone for courtship and/or to escape approaching inhospitable climate at these times of year (Hutchison, 1958; Williams, 1980; Petranka, 1998), making them relatively accessible for capture in the cave.

Our estimates of survival probability are generally similar to those reported for other plethodontids (Price et al., 2012; Fenolio et al., 2014; Muncy et al., 2014). The low probabilities of survival we observed during the fall of both study years may be due to decreasing food availability as salamanders move farther back into the dark zone and to movement of potential predators into the cave for eventual torpor (e.g., Black rat snakes [*Pantherophis (Elaphe) obsoleta*] and Green frogs [*Rana (Aquarana) clamitans*] were seen in Sauerkraut Cave in fall). We observed an anecdotal increase in individual tail loss in this season, which may have been a result of interactions with these potential predators. Highest survival probability occurred in spring and summer 2015 and in spring 2016, in seasons when epigeal and twilight zone climates are equitable and food is readily available.

Total biomass and biomass density of cave-inhabiting salamanders have seldom been reported. Huntsman et al. (2011) reported biomass density for a troglobitic species as 0.18 g m^{-2} and 0.03 g m^{-2} ash-free dry mass in two caves in Alabama, USA. Salvidio (1998) reports average total wet-biomass and wet-biomass density for a facultative cave-dwelling salamander in Liguria, Italy as 238.48 g and 1.25 g m^{-2} , respectively. An assemblage of *Desmognathus* spp. at a wet rock face (a similar habitat to caves, albeit likely having higher food densities), had estimated wet-biomass of 916.56 g and wet-biomass density of 27.16 g m^{-2} (Crawford and Peterman, 2013), respectively, in North Carolina, USA. Our study indicates seasonally variable wet-biomass in this population of Cave salamanders, which likely has important implications for energy distribution within the cave. Dead individuals were rarely observed (nine in total for the study period), but those that were seen were occupied by invertebrates, and all but vertebrae were gone the following survey one week later. Given this short amount of time that dead individuals may be visible before being consumed, and that we could not survey the entire cave, it is likely that more individuals died in the cave without being noticed. This may represent an important pulse nutrient resource for cave-inhabiting organisms. Salamanders may also supply energy through fecal deposition (Bohonak and Whiteman, 1999; Lilleskov and Bruns, 2005) in caves, and we regularly observed salamander feces in Sauerkraut Cave in spring. This contribution may be substantial with greater levels of population biomass.

Salamander densities have been reported for troglobites (Huntsman et al., 2011; Fenolio et al., 2014) and facultative cave dwellers (Salvidio, 1998; Crawford and Peterman, 2013; Taylor et al., 2015) (Table 4). Our densities are most similar to densities reported for troglobitic species (Huntsman et al., 2011; Fenolio et al., 2014), likely because our study took place exclusively within a cave system. Although Taylor et al. (2015) similarly investigated a population of facultative cave-dwelling salamanders in a cave system, they mention that individuals often congregated in a pit, which may have inflated density estimates; our highest density estimate (0.47 m^{-2}) approaches their lowest (0.61 m^{-2}). Densities of those populations studied at rock faces (Salvidio, 1998; Crawford and Peterman, 2013) were higher than our estimates, which may be due to the limited surface area and probable higher food abundance of this habitat compared to a cave system. Rock outcrops are important habitat for many fauna (Fitzsimons and Michael, 2017) and may provide an accessible, safer refuge than what can be found on the ground, making this ideal habitat for salamanders. Likewise, many individuals may utilize this habitat, trading off space for safety, which may explain increased densities at rock faces.

Conclusion

There is much yet to be learned about the natural history and ecology of *Eurycea lucifuga*, and facultative cave-dwelling salamanders in general. It is likely, though not well established, that these cave inhabitants play important ecological roles in cave ecosystems. This is an important consideration as caves, and the organisms restricted to them, are

often of conservation concern. Unraveling the ecological dynamics of facultative cave-dwelling salamanders will surely provide valuable information that can be used to manage and conserve these fascinating habitats.

Acknowledgements

We thank Paige Wilson, Danica Shepherd, Faith Bowers, and Nick Callahan for assistance in data collection and the developers of Rcapture, Sophie Baillargeon and Louis-Paul Rivest, for their timely explanations and help with R. We thank the staff at E.P. “Tom” Sawyer State Park for facilitating this research. Procedures for handling salamanders were reviewed and approved by the University of Louisville Institutional Animal Care and Use Committee (IACUC #17005). This study was approved by Kentucky Department and Fish and Wildlife (permit # SC1711045) and the Kentucky Department of Parks (permit # 1412).

References

- Bailey, L.L., Simons, T.R., Pollock, K.H., 2004, Comparing population size estimators for plethodontid salamanders: *Journal of Herpetology*, v. 38, no. 3, 370–380. <https://dx.doi.org/10.1670/194-03A>.
- Baillargeon, S., Rivest, L.-P., 2007, Rcapture: Loglinear models for capture-recapture in R: *Journal of Statistical Software*, v. 19, no. 5, 1–31. <https://doi.org/10.11168.1620>.
- Barr, Jr., T.C., 1968, Cave ecology and the evolution of troglobites: pp. 35–102 in T. Dobzhansky, M. K. and Hecht, W. C. Steere, eds., *Evolutionary Biology*. Boston, Springer.
- Barr, Jr., T.C., and Holsinger, J.R., 1985, Speciation in cave faunas: *Annual Review of Ecology and Systematics*, v. 16, p. 313–337. doi:10.1146/annurev.es.16.110185.001525.
- Beck, H., Snodgrass, J.W., Thebpanya, P., 2013, Long-term enclosure of large terrestrial vertebrates: Implications of defaunation for seedling demographics in the Amazon rainforest: *Biological Conservation*, v. 163, 115–121. <https://doi.org/10.1016/j.biocon.2013.03.012>.
- Bohonak, A.J., Whiteman, H.H., 1999, Dispersal of the fairy shrimp *Branchinecta coloradensis* (Anostraca): Effects of hydroperiod and salamanders: *Limnology and Oceanography*, v. 44, no. 3, 487–493. <https://doi.org/10.4319/lo.1999.44.3.0487>.
- Bradley, J.G., Eason, P.K., 2018, Use of a non-invasive technique to identify individual Cave Salamanders, *Eurycea lucifuga*: *Herpetological Review*, v. 49, no. 4, 660–665.
- Briggler, J.T., Prather, J.W., 2006, Seasonal use and selection of caves by Plethodontid salamanders in a karst area of Arkansas: *The American Midland Naturalist*, v. 155, no. 1, 136–148. [https://doi.org/10.1674/0003-0031\(2006\)155\[0136:SUASOC\]2.0.CO;2](https://doi.org/10.1674/0003-0031(2006)155[0136:SUASOC]2.0.CO;2).
- Camp, C.D., Wooten, J.A., Jensen, J.B., Bartek, D.F., 2014, Role of temperature in determining relative abundance in cave twilight zones by two species of lungless salamander (family Plethodontidae): *Canadian Journal of Zoology*, v. 92, 119–127. <https://doi.org/10.1139/cjz-2013-0178>.
- Carlyle, J.C., Sanders, D.E., Plummer, M.V., 1998, *Eurycea lucifuga* (Cave Salamander). *Reproduction: Herpetological Review*, v. 29, no. 1, 37–38.
- Crawford, J.A., Peterman, W.E., 2013, Biomass and habitat partitioning of *Desmognathus* on wet rock faces in the southern Appalachian mountains: *Journal of Herpetology*, v. 47, no. 4, 580–584. <https://doi.org/10.1670/13-044>.
- Davic, R.D., Welsh, H.H., 2004, On the ecological roles of salamanders: *Annual Review of Ecology, Evolution, and Systematics*, v. 35, 405–434. <https://doi.org/10.1146/annurev.ecolsys.35.112202.130116>.
- Fenolio, D.B., Niemiller, M.L., Bonnett, R.M., Graening, G.O., Collier, B.A., Stout, J.F., 2014, Life history, demography, and the influence of cave-roosting bats on a population of the Grotto salamander (*Eurycea spelaea*) from the Ozark plateaus of Oklahoma (Caudata: Plethodontidae): *Herpetological Conservation and Biology*, v. 9, no. 2, 394–405. <https://doi.org/10.1146/annurev.ento.51.110104.151107>.
- Fitzsimons, J.A., Michael, D.R., 2017, Rocky outcrops: A hard road in the conservation of critical habitats: *Biological Conservation*, v. 211, 36–44. <https://doi.org/10.1016/j.biocon.2016.11.019>.
- Ford, H.A., Ford, K., 1882, Anchorage: Page 33 in *History of the Ohio falls cities and their counties*, v. 2. Cleveland, Ohio, USA, L. A. Williams & Co.
- Green, N.B., Brant Jr., P., Dowler, B., 1967, *Eurycea lucifuga* in West Virginia: Its distribution, ecology, and life history: *Proceedings of the West Virginia Academy of Science*, v. 39, 297–304.
- HACC: Herpetological Animal Care and Use Committee, 2004, Guidelines for use of live amphibians and reptiles in field and laboratory research, 2nd Ed: American Society of Ichthyologists and Herpetologists.
- Hairton Sr., N.G., 1987, *Community ecology and salamander guilds*: Cambridge, England, UK, Cambridge University Press, 230 p.
- den Hartog, J., Reijns, R., 2014, I3S Spot Manual: Interactive Individual Identification System version 4.0.2: http://www.reijns.com/i3s/download/I3S_Spot.pdf. [accessed February 20, 2015].
- Huntsman, B.M., Venarsky, M.P., Benstead, J.P., Huryn, A.D., 2011, Effects of organic matter availability on the life history and production of a top vertebrate predator (Plethodontidae: *Gyrinophilus palleucus*) in two cave streams: *Freshwater Biology*, v. 56, 1746–1760. <https://doi.org/10.1111/j.1365-2427.2011.02609.x>.
- Hutchison, V.H., 1958, The distribution and ecology of the cave salamander, *Eurycea lucifuga*: *Ecological Monographs*, v. 28, no. 1, 1–20. <https://doi.org/10.2307/1942273>.
- Hutchison, V.H., 1966, *Eurycea lucifuga*: *Catalogue of American Amphibians and Reptiles*, v. 24.1, 24.1–24.2.
- Jonas, M., Bowman, J.L., Nazdrowicz, N.H., 2011, Using spot pattern to identify individual long-tailed salamanders: *Herpetological Review*, v. 42, no. 4, 520–522.
- Juterbock, J.E., 2005, *Eurycea lucifuga* Rafinesque, 1822, Cave Salamander: Pages 750–753 in M. Lannoo, ed. *Amphibian Declines: The Conservation Status of United States Species*. Berkeley, California, USA, University of California Press.
- Lanza, B., Pastorelli, C., Laghi, P., Cimmaruta, R., 2006, A review of systematics, taxonomy, genetics, biogeography and natural history of the genus *Speleomantes* Dubois, 1984 (Amphibia Caudata Plethodontidae): *Atti del Museo Civico di Storia Naturale di Trieste*, v. 52, p. 5–135.
- Lilleskov, E.A., Bruns, T.D., 2005, Spore dispersal of a resupinate ectomycorrhizal fungus, *Tomentella subliilacina*, via soil food webs: *Mycologia*, v. 97, no. 4, 762–769. <https://doi.org/10.1080/15572536.2006.11832767>.
- Lunghi, E., Manenti, R., Ficetola, G.F., 2014, Do cave features affect underground habitat exploitation by non-troglobite species? *Acta Oecologica*, v. 55, p. 29–35. doi:10.1016/j.actao.2013.11.003.

- Muncy, B.L., Price, S.J., Dorcas, M.E., 2014, Capture probability and survivorship of the Southern two-lined salamander (*Eurycea cirrigera*) in drought and non-drought conditions: *Copeia*, v. 2014, no. 2, 366–371. <http://doi.org/10.1643/CE-13-139.1>.
- Nazdrowicz, N.H., 2015, Ecology of the eastern long-tailed salamander (*Eurycea longicauda longicauda*) associated with springhouses: PhD Dissertation. University of Delaware, Newark, Delaware, USA, 129 p.
- O'Donnell, K.M., Semlitsch, R.D., 2015, Advancing terrestrial salamander population ecology: The central role of imperfect detection: *Journal of Herpetology*, v. 49, no. 4, 533–540. <https://doi.org/10.1670/14-100>.
- Petranka, J.W., 1998, Salamanders of the United States and Canada: Washington, DC, USA, Smithsonian Books, 587 p.
- Price, S.J., Eskew, E.A., Cecala, K.K., Browne, R.A., Dorcas, M.E., 2012, Estimating survival of a streamside salamander: Importance of temporary emigration, capture response, and location: *Hydrobiologia*, v. 679, 205–215. <https://doi.org/10.1007/s10750-011-0882-2>.
- R Core Team, 2017, R: A language and environment for statistical computing: Vienna, Austria, R Foundation for Statistical Computing.
- Salvidio, S., 1998, Estimating abundance and biomass of a *Speleomantes strinatii* (Caudata, Plethodontidae) population by temporary removal sampling: *Amphibia-Reptilia*, v. 19, no. 2, 113–124. <https://doi.org/10.1163/156853898X00412>.
- Schneider, C.A., Rasband, W.S., Eliceiri, K.W., 2012, NIH Image to ImageJ: 25 years of image analysis: *Nature Methods*, v. 9, no. 7, 671–675. <https://doi.org/10.1038/nmeth.2089>.
- Semlitsch, R.D., O'Donnell, K.M., Thompson III, F.R., 2014, Abundance, biomass production, nutrient content, and the possible role of terrestrial salamanders in Missouri Ozark forest ecosystems: *Canadian Journal of Zoology*, v. 92, 997–1004. <https://doi.org/10.1139/cjz-2014-0141>.
- Shaffer, H.B., Alford, R.A., Woodward, B.D., Richards, S.J., Altig, R.G., Gascon, C., 1994, Quantitative sampling of amphibian larvae: pp. 130–141 in W. R. Heyer, M. A. Donnelly, R. W. McDiarmid, L.-A. C. Hayek, and M. S. Foster, eds. *Measuring and Monitoring Biological Diversity: Standard Methods for Amphibians*. Washington, DC, USA, Smithsonian Institution Press.
- Sket, B., 2008, Can we agree on an ecological classification of subterranean animals? *Journal of Natural History*, v. 42, no. 21–22, p. 1549–1563. [doi:10.1080/00222930801995762](https://doi.org/10.1080/00222930801995762).
- Stasiak, I., 2015, Standard Operating Procedure (SOP): Prevention of disease transmission in amphibians: Kentucky Department of Fish and Wildlife Resources.
- Taylor, S.J., Krejca, J.A., Niemiller, M.L., Dreslik, M.J., Phillips, C.A., 2015, Life history and demographic differences between cave and surface populations of the western slimy salamander, *Plethodon albagula* (Caudata: Plethodontidae), in Central Texas: *Herpetological Conservation and Biology*, v. 10, no. 2, 740–752.
- Trajano, E., Carvalho, M.R., 2017, Towards a biologically meaningful classification of subterranean organisms: A critical analysis of the Schiner-Racovitza system from a historical perspective, difficulties of its application and implications for conservation: *Subterranean Biology*, v. 22, 1–26. <https://doi.org/10.3897/subtbiol.22.9759>.
- van Tienhoven, A.M., den Hartog, J.E., Reijns, R.A., Peddemors, V.M., 2007, A computer-aided program for pattern-matching of natural marks on the spotted raggedtooth shark *Carcharias taurus*: *Journal of Applied Ecology*, v. 44, 273–280. <https://doi.org/10.1111/j.1365-2664.2006.01273.x>.
- UKAWC: University of Kentucky Agricultural Weather Center, 2017, Kentucky Climate Data: http://www.wagwx.ca.uky.edu/ky/data.php#KY_Climate_Data. [accessed February 2, 2017].
- Venarsky, M.P., Huntsman, B.M., Huryn, A.D., Benstead, J.P., Kuhajda, B.R., 2014, Quantitative food web analysis supports the energy-limitation hypothesis in cave stream ecosystems: *Oecologia*, v. 176, no. 3, 859–869. <https://doi.org/10.1007/s00442-014-3042-3>.
- Williams, A.A., 1980, Fluctuations in a population of the cave salamander *Eurycea lucifuga*: *NSS Bulletin*, v. 42, 49–52.

GEOLOGICAL AND HYDROGEOLOGICAL EFFECTIVE FACTORS IN THE HIGH PERMEABILITY ZONES OF SEVERAL DAM SITES OF THE ZAGROS REGION, IRAN

Behnaz Shabab Boroujeni¹, Javad Ashjari² and Haji Karimi³

Abstract

Stratigraphical, discontinuity and hydraulic characteristics of a karstic region are crucial factors in solution development, producing areas with strong contrasts in permeability with probable water seepage from dam foundations and abutments. The aim of this study is to explore the effect of these elements on karstic dam sites of the Zagros region in Iran. Although the Asmari Formation is inherently fractured, according to the distribution of boreholes and dams, and there is no case that is merely controlled by one of these elements; therefore, all factors are unequally responsible for creating a high-permeable zone. The river and adjacent karst connect in three possible ways: water flows from the river to the adjacent rock mass, the river gets water from the adjacent rock mass, and there is no hydraulic connection between the river and adjacent karst areas. The settlement of impermeable layers, such as marly limestone and marl inside carbonate bodies, may create suitable places for water collection and initiation of dissolution. Finally, at the borehole scale, it is possible to find some high-permeable zones controlled only by one of the three mentioned elements, but there is no borehole or no dam site in which all high permeable zones are controlled by only one of these elements.

Introduction

Karst is a special type of landscape developed particularly on soluble rocks such as limestone, marble, and gypsum (Ford and Williams, 1989; Stevanović, 2015) and containing caves and extensive underground water systems. Karst is often characterized by karrens, sinkholes, shafts, poljes, caves, ponors, caverns, estavelles, intermittent springs, submarine springs, lost rivers, dry river valleys, intermittently-inundated poljes, underground river systems, denuded rocky hills, karst plains, and collapses (Milanović, 2004; Parise and Gunn, 2007; Parise and Lollino, 2011). Karst conduits form the main path for water loss, and problems arise because these conduits are difficult to find. The development of karst conduits is not random within a rock mass but is a dissolution process that follows specific geological features (Wright, 1991; Palmer, 2007). Primary flow paths follow discontinuities such as joints, faults, and bedding planes (Kiraly, 1975). Water loss through the foundations and abutments of dams constructed in karstic areas leads to considerable economic costs and a loss in reservoir capacity (Milanović, 2000, 2002; Zhou and Beck, 2011; Gutierrez et al., 2014; Parise et al., 2015). The numbers of investigations related to impacts of evaporite and carbonate karst on dams (James, 1992; Romanov et al., 2003; Johnson, 2008; Milanović, 2011; Cooper and Gutierrez, 2013; Gutierrez et al., 2003, 2015) is limited. The main focus of Johnson (2008) was on gypsum karst and dam constructions in the USA. Problems associated with construction of dams and reservoirs in karstic area, and some special approaches such as grouting and geophysical investigations, have to be assumed to prevent seepage as discussed by Milanović (2011). Cooper and Gutierrez (2013) reviewed collapsing dams, violently flooding mines, tunnels, and other hazards in gypsum karstic area with some of the measures that can be considered to reduce them. Romanov et al. (2003) presented a model simulation of karstification below dams by coupling equations of dissolutional widening of fractures to hydrodynamic flow that showed increasing leakage with time. Gutierrez et al. (2003) demonstrated that one of the main causes of failure of an earth dam in the NE of Spain was subsidence by dissolution of the 4 m thick detrital cover with a gypsum content of about 40 %. Gutierrez et al. (2015) analyzed distribution of leakage paths, subsidence along the main leakage path, and origin of karst in La Loteta Dam, a reservoir built in a large karst depression developed on Tertiary evaporites. The karst features can hinder the ability of a dam to hold water in a reservoir, and can even cause collapse of a dam (Johnson, 2008). The objective of this study is to investigate the likely relationship between geology, hydraulic elements, and highly-permeable zones as water leakage paths in dam sites at borehole scale. This paper focuses on karstic dam sites in the Zagros region of Iran and used both borehole logs and hydrogeological investigations. In the Zagros, perennial high-discharge rivers originating from non-karstic watersheds traverse the karst formations and develop deep valleys. The rivers flow generally from north to south to discharge their water into the Persian Gulf at the regional base level. The dams in this study were constructed or are under construction to provide drinking water, agricultural water, and energy supplies in karstic regions (Ashjari, 2007). The main problem with these dams is water seepage from abutments or foundations.

¹Geology Department, Tehran University, Iran. behnaz.shabab@modares.ac.ir

²Abanrood-Tadbir Company, Tehran, Iran. Javad_Ashjari@yahoo.com

³University of Illam, Iran. haji.karimi@gmail.com

Approach

The main focus of this study is to represent the zones with high leakage potential in geological and hydrogeological perspectives. First, we need to define the terms used in this paper. Seepage or leakage zones are zones having permeability of greater than 30 Lugeon units, as considered by Houlsby (1976) in the classification of highly permeable rocks. Stratigraphy describes the overall thickness of soluble rocks (mainly limestone and dolomite) and impermeable interbeds such as shales, marl, and marly limestone. A fracture or discontinuity is any kind of joint or fault that divides the rocks into several parts. Local base level is the lowest hydraulic level of a karst aquifer that groundwater can flow through and exit as a spring or discharge to rivers without any barrier.

Karst is a network of conduits imbedded in a matrix that come together to store and transfer water underground. The presence of impermeable layers often impede water flow vertically or laterally and lead to the development of conduits or drainage horizons along bedding planes which can make seepage horizons. Therefore, it is very likely that the conduits follow bedding plane horizons completely (Fig. 1).

Discontinuities are significant with regards to seepage if they are sufficiently open to permit water to flow under a reasonable hydraulic gradient. As the pattern of conduit development is most likely controlled by large aperture fracture density and configurations, it is likely to expect that water seepage horizons follow the fracture pattern at dam sites (Fig. 2).

This paper is limited to karst areas of dam sites. Since dams are constructed over rivers with high water flow rates, the hydraulic relationship between the river and the adjacent carbonate aquifer is crucial. If the aquifer is surrounded by impermeable formations, the hydraulic connectivity of the aquifer with following aquifers is reduced, and the groundwater can flow into the river in the absence of any geological barrier (Ashjari, 2007). Therefore, rivers can act as the main local base level, which is important in understanding karst conduit development or seepage horizon (Fig. 3). Furthermore, it is possible that the river recharges the aquifer under conditions where the base level of the aquifer is not the river, the riverbed is permeable, groundwater level is lower than the river, and there is no impermeable layer between the river bed and groundwater. Over a long period of time, water infiltration around the river may lead to karst conduit development under the riverbed and between the river and groundwater level. For simplicity, the hydraulic interaction of groundwater and river as either a recharge or a discharge hydraulic factor is considered.

This case study is on different places with specific geology and hydrogeology characteristics. Borehole data were used to describe the stratigraphy of each site vertically and horizontally, with particular geological properties due to the high heterogeneity of karst. To simply compare the three major factors affecting the high-permeable horizon from bore-

hole scale to dam site scale and regional scale, a triangular diagram was defined. It is important to mention that karst development is a complicated process that cannot be exhaustively covered by these three elements. For simplicity and to present the results, a triangular diagram with three apexes of stratigraphy, fractures, and hydraulics was assumed as shown in Figure 4. First, the diagram was drawn based on the data of boreholes for each site. Then the average of each site was determined and pre-

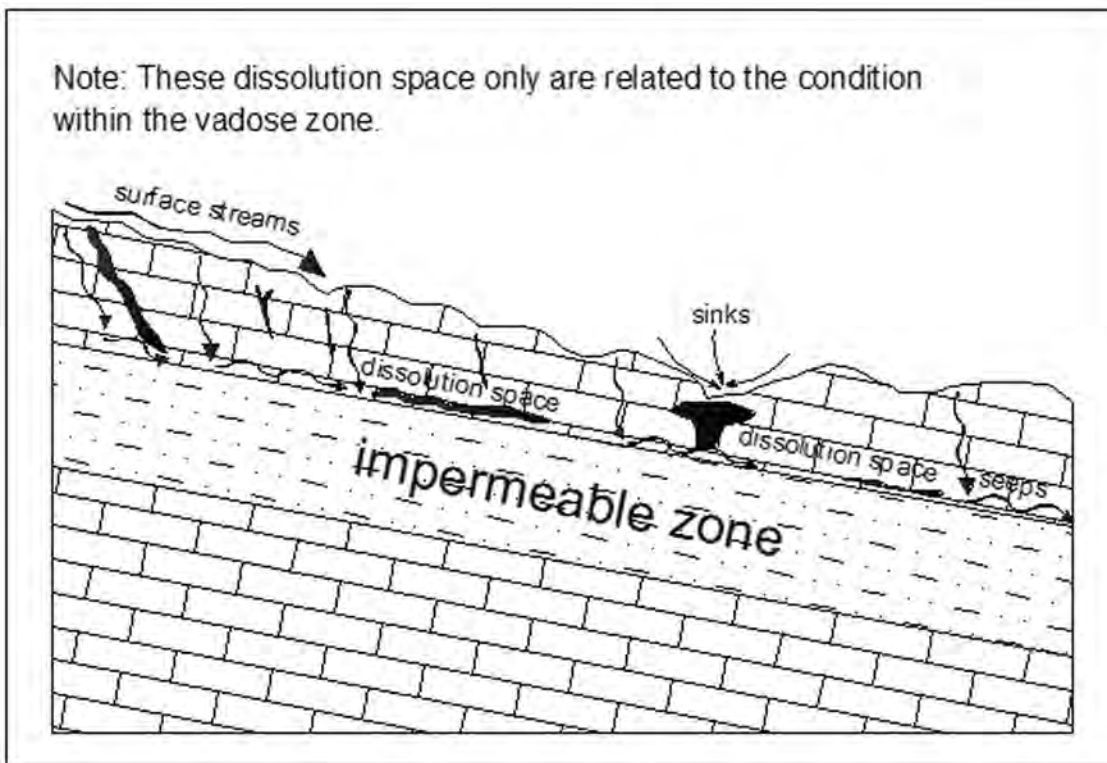


Figure 1. Role of the stratigraphy element in guiding the water flow and conduit development.

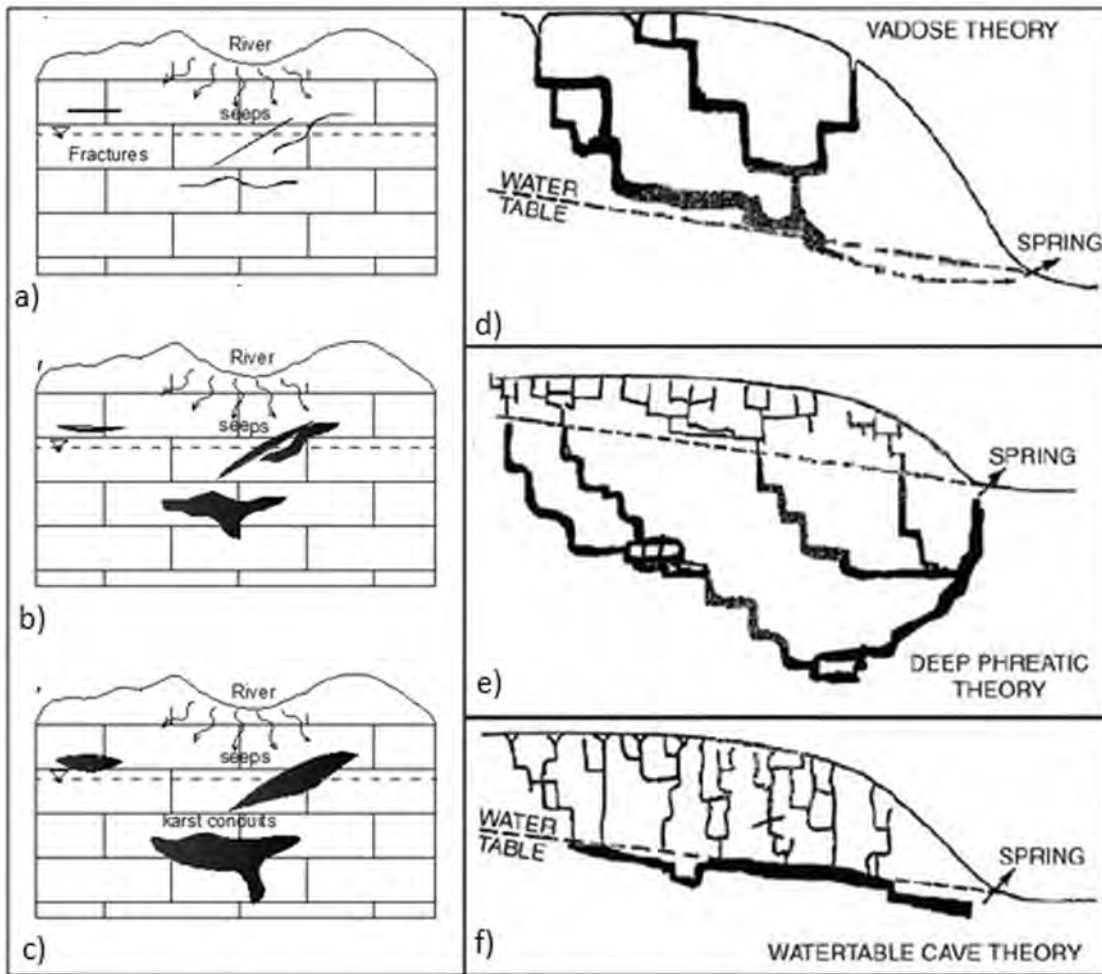


Figure 2. Role of the fractures in guiding water flow and conduit developing. A,B, and C show the steps of developing of the solution space from fractures, respectively.

contains radiolarites, ophiolites, and very small amounts of basic igneous rocks of upper Cretaceous age (Falcon, 1974). The combination of halite, anhydrite, limestone, dolomite and igneous rock forms Folded Zagros. These lithological

presented as a regional diagram which contains all the dam sites.

Geological setting

The Zagros area extends from the west to the south and southeast of Iran. Zagros consists of a combination of faulted and folded rocks with various carbonate and non-carbonate formations. It is the result of three major successive tectonic events which resulted in the formation of two main zones. From northeast to southwest, these include the Thrust Zone (High Zagros) which is limited by the main Zagros thrust in the northeastern boundary, and the Folded Zagros (known as outer Zagros) in the southwest. The Thrust Zone contains

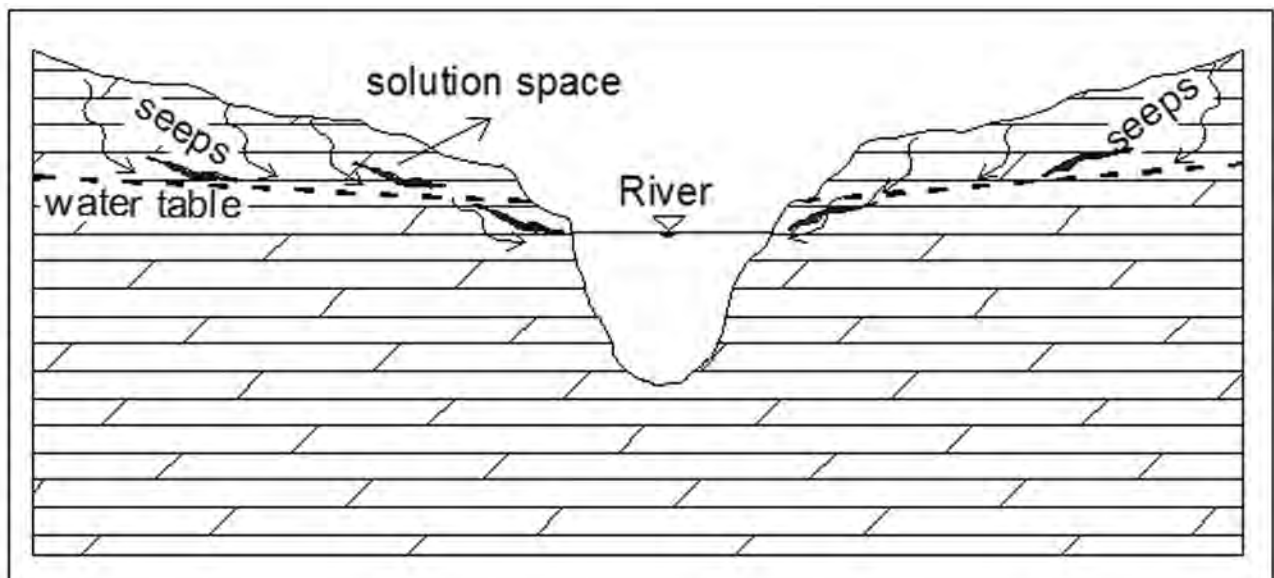


Figure 3. Role of the hydraulic element in situation of solution space.

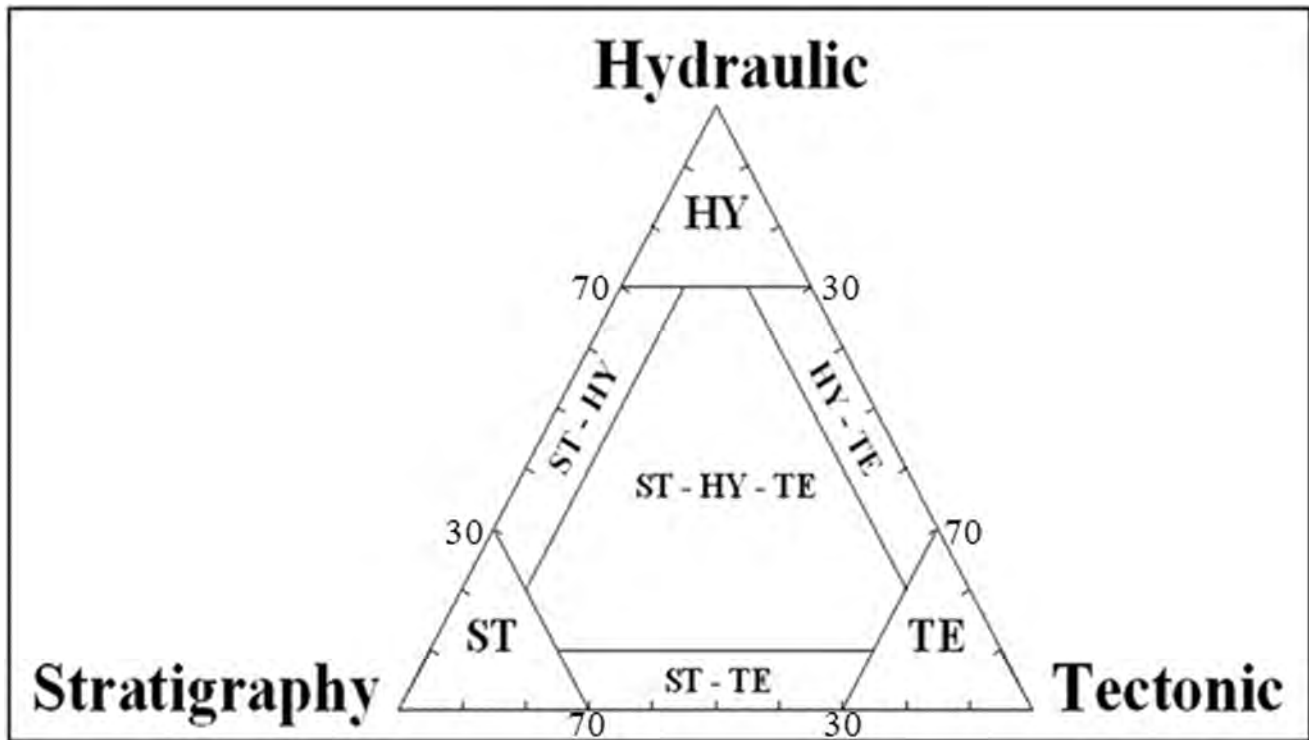


Figure 4. The assumption triangular diagram showing the role of ST, HY and TE element. (HY: Hydraulic Control range. TE: Tectonic Control range. ST: Stratigraphy Control range. ST-HY: Stratigraphy and Hydraulic Control range. HY-TE: Hydraulic and Tectonic control range. ST-TE: Stratigraphy and Tectonic control range. ST-HY-TE: Stratigraphy, Hydraulic and Tectonic Control range).

units are from upper Precambrian to middle Cambrian with 115 salt domes of late Jurassic (Aghanabati, 2004). The study areas are situated in different zones, mainly in the western parts of Zagros (Fig. 5).

The stratigraphical and structural characteristics of the Zagros sedimentary sequences have been described in detail by Stocklin and Setudehnia (1971) and Alavi (2004). In the following sections, the main outcropping formations of the study areas are discussed in decreasing order of age (Stocklin and Setudehnia, 1971; Alavi, 2004). The Gurpi, Upper Cretaceous, is composed of 350 m of marl, marly limestone and claystone. Pabdeh, Eocene-Paleocene, consists of 800 m of calcareous shale, marl, and lime mudstone with subordinate shaly limestone. Facies grade towards the southwest into the Shahbazan carbonates. The Shahbazan, Middle-Upper Eocene, is composed of 485 m cliff-forming dolomite interbedded with dolomitic limestone. Facies grade towards the east into the Jahrum carbonates. Eocene in age, they are composed of 485 m of dolomite interbedded with dolomitic limestone. The thickness of the Asmari Formation, Oligocene-Miocene, varies from a few meters up to 500 m, consisting of medium-bedded to thick-bedded and well-jointed limestone. The

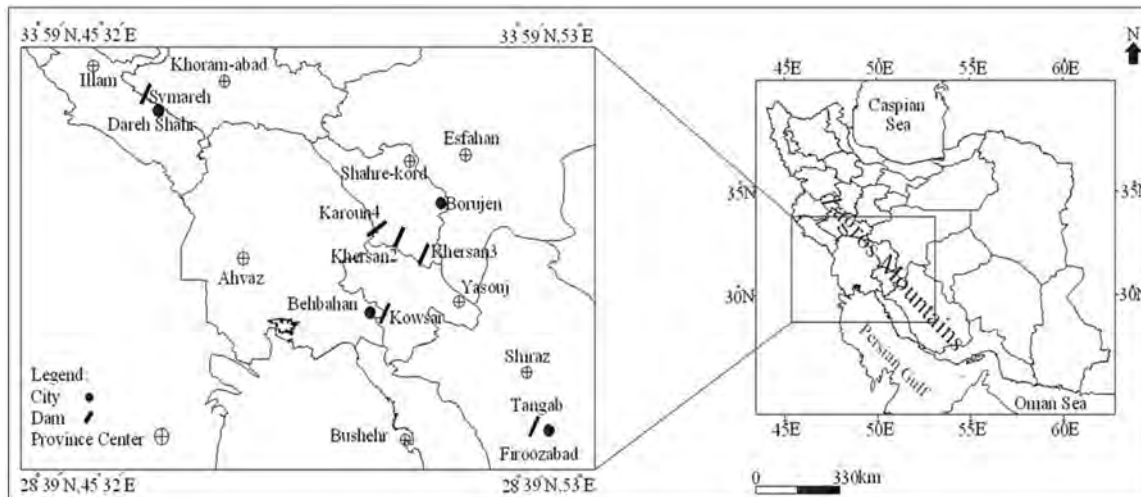


Figure 5. Location of dams in the study area, Zagros, Iran.

Gachsaran Formation, Miocene, is composed of multiple sequences of variable thicknesses (up to 1900 m) and lithologies, including alternations of evaporites (gypsum, anhydrite and subordinate halite), shale, marl, and locally conglomeratic calcarenite. The Mishan Formation,

Miocene, is composed of marl, calcareous shale, siltstone, and sandstone. The Aghajari Formation, Upper Miocene, is a thick, up to 3000 m succession, composed of carbonate-clast and polymict conglomerate, calcarenite, sandstone, siltstone, marl, and lime-mudstone. The younger sediments are composed mainly of conglomerate and recent alluvium (Fig. 6).

Carbonate formations control the geomorphology of the Zagros. They form cylindrical anticlines which plunge beneath younger permeable or impermeable sediments at both sides (Ashjari and Raeisi 2006). According to Ashjari and Raeisi (2006), the anticlines are bare on the top while their bottoms are bounded by impermeable layers that disconnect the hydraulic connectivity of each limb. Just in few cases, they proposed that the groundwater flow is likely to occur between two flanks at sites where the elevations of bedrocks are low enough in relation to the groundwater level of the limes. This kind of hydraulic interaction of the limbs is often detectable around the plunges or main rivers.

Method of Study

The selected dams lie in various positions in the Zagros region. Geology maps of the dam sites were prepared based on geology maps of 1/100,000 Oil Companies and Geology Surveys of Iran. The geotechnical data of drilled boreholes, such as geological logs, RQD (rock quality designation), Lugeon tests, geomorphologic data, and the size of dissolution pores and their relative location to main geological and hydraulic elements in the sites were collected. The following data and reports were gathered: flow system and hydrogeological characteristics of the sites, water level measurements in boreholes in karstic rock mass or wells, springs location and discharge, water tracing results, isotopic studies outcome, river flow rate and water level, and rainfall of the area. The main source of data was the Water Resource Management Office of Iran.

Geological logs and geotechnical data were used to find the potential horizon of conduit developments. Lugeon test results were used to find high-permeability zones in a borehole and the relation of the leakage zone to the geological characteristics of the dam sites.

From a geotechnical standpoint, permeability greater than 3 Lugeon units denotes the presence of water leakage potential, and permeability higher than 30 Lugeon units denotes a high seepage volume (Houlsby, 1976). The locations with permeability higher than 30 Lugeon units are considered the Main Seepage Zone (MSZ). The vertical variations

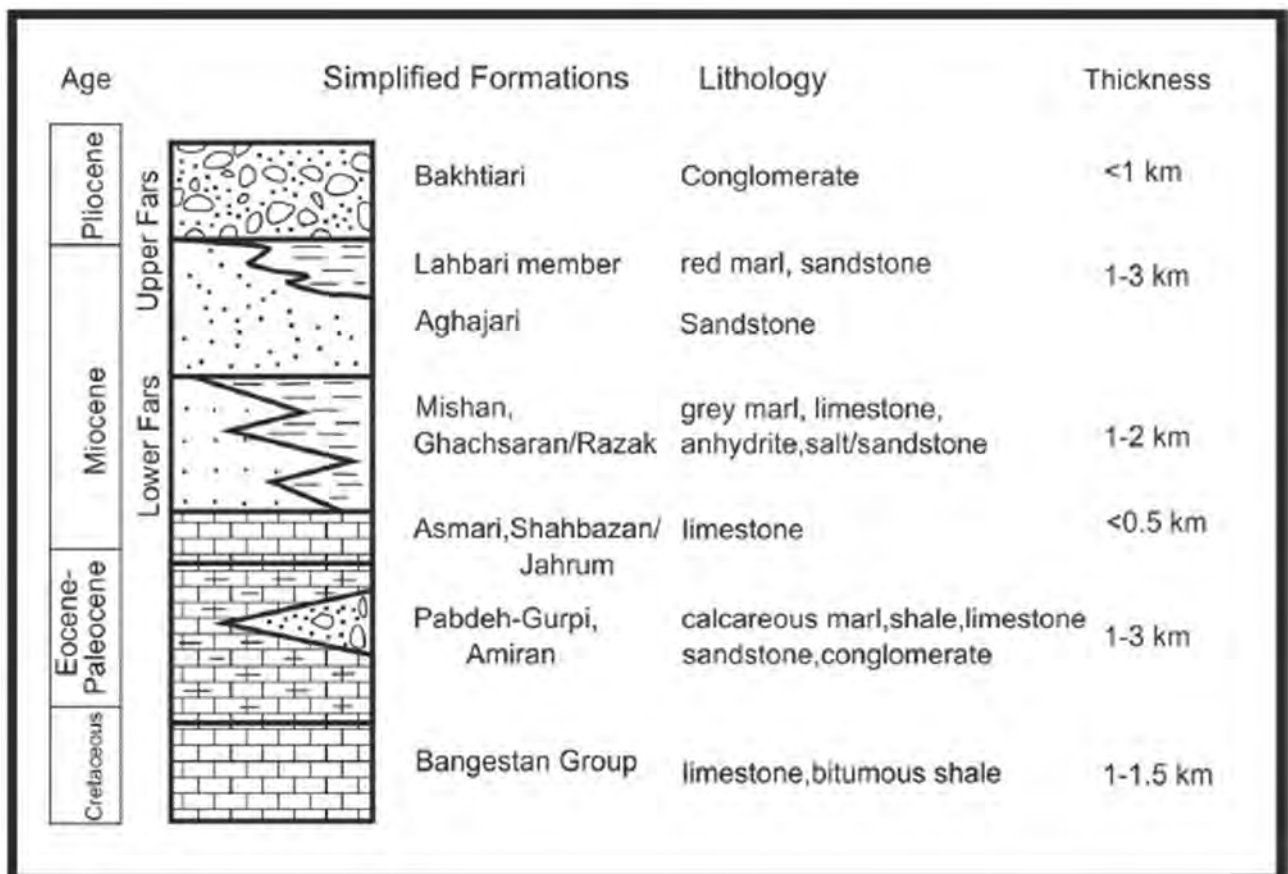


Figure 6. Simplified stratigraphy column of formations in understudy area.

of permeability of each borehole were checked and horizons higher than 30 Lugeon units were marked as MSZ. Then, geological data of the same level of each MSZ of borehole were extracted from core logs. The presence or absence and frequency of fractures, cavity, lithology of rock within the MSZ, as well as above or below it, were determined.

The water levels of boreholes were used to find the potential hydrogeological relationship of riverbeds and aquifers or subaquifers of the dam sites, in other words, to understand if the river is the local base level of the aquifer or the river is a recharging aquifer. The method has been discussed in detail by Ashjari and Raeisi (2006). The hydrogeological results, geological investigation and geotechnical data were compiled to show the role of various elements in making water seepage horizons through dam sites at borehole scale.

A triangular diagram was used to display the results. In a ternary plot, the proportions of the three elements, fracture, stratigraphy, and hydraulic must sum up to 1.0 or 100 %. Every point on a diagram shows different compositions of the three variables. Based on this study, it was rarely observed that a MSZ in a specific borehole is merely controlled by one factor. Therefore, the controlling elements of each MSZ are determined. The presence or absence of each element is more important than frequency. For example, it is possible that an MSZ is located at highly fractured point, the impermeable layer of shale is detected adjacent to MSZs, and the hydraulic play a role. In such case, the weight of every element would be equal to 33.33 %. If only two elements play roles in the creation of MSZs, the weight of each of them would be 50 %. Then the length of each MSZ is measured, and the value of each element in a borehole was calculated based on the MSZ length. The next step was to draw borehole data on a ternary diagram. The apexes of diagram show the points in which each element has the weight of 100 %, and the sides of triangles were divided from 0 % to 100 %, which reduce from apex toward the facing side. The further away from the apex, the effect of the element decreases in creating MSZs. Finally, based on the calculated percentage of each element, the boreholes were plotted on the diagram. In reality, the diagram shows the prevailing controlling factor of MSZ at the scale of the dam site. To plot the data on a regional scale, the same method was used. Instead of using a weighting method for just one borehole, it is used for all boreholes together.

Results

Six dams were studied in this research. In all the cases, the abutment(s) and/or foundation of the dams are located on Asmari Formation. The study focuses on high seepage locations (more than 30 Lugeon units) that are considered to be MSZ. More detailed information is provided by Shabab-Boroujeni (2012). The controlling agents of all MSZs are determined based on the available information (Lugeon tests, RQD, geological information, etc.). The MSZs are plotted on the proposed triangular diagram for each borehole individually and resultant factors at dam site scale, separately. The results show that there are cases, at borehole scale, controlled barely by one of these elements while there are no cases merely controlled by one element at dam site scale. It should be noted that MSZs in the different boreholes are not the same, but belong to different leakage features. All cases are distributed in the intermediate part of the diagram, near the half side of the tectonic-stratigraphy line (Fig. 7). Therefore, it is not possible to classify the dams according to the prevailing

controlling factor of MSZ. To find out the role of the three elements in MSZ, three cases were selected to be discussed in more detail.

Symareh Dam

The Symareh Dam was constructed on the Symareh River, with an average discharge of $109 \text{ m}^3 \text{ s}^{-1}$ and flowing perpendicular to the Ravandi Anticline axis. The anticline consists of Asmari Formation

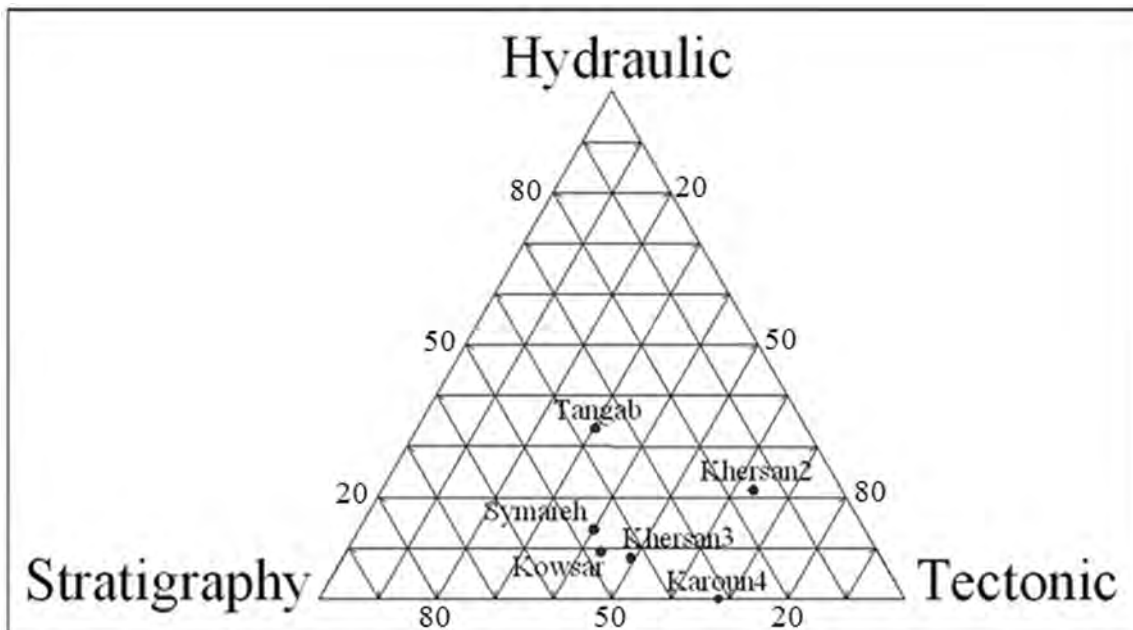


Figure 7. Diagram of classification of under study dams based on the controlling factor of MSZ.

(well-jointed limestone) with $\sim 61 \text{ km}^2$ exposed surface, which is the main aquifer of the area. The aquifer is surrounded by Gachsaran impervious formation (marl and gypsum) at the surface and marly layers of Pabdeh-Gurpi as bedrock. The river flows on Gachsaran and through a narrow and vertical cliff valley in the Asmari Formation (Fig. 8a). The river water level varies from 598 m.a.s.l to 610 m.a.s.l in response to precipitation, which usually occurs in the form of snow.

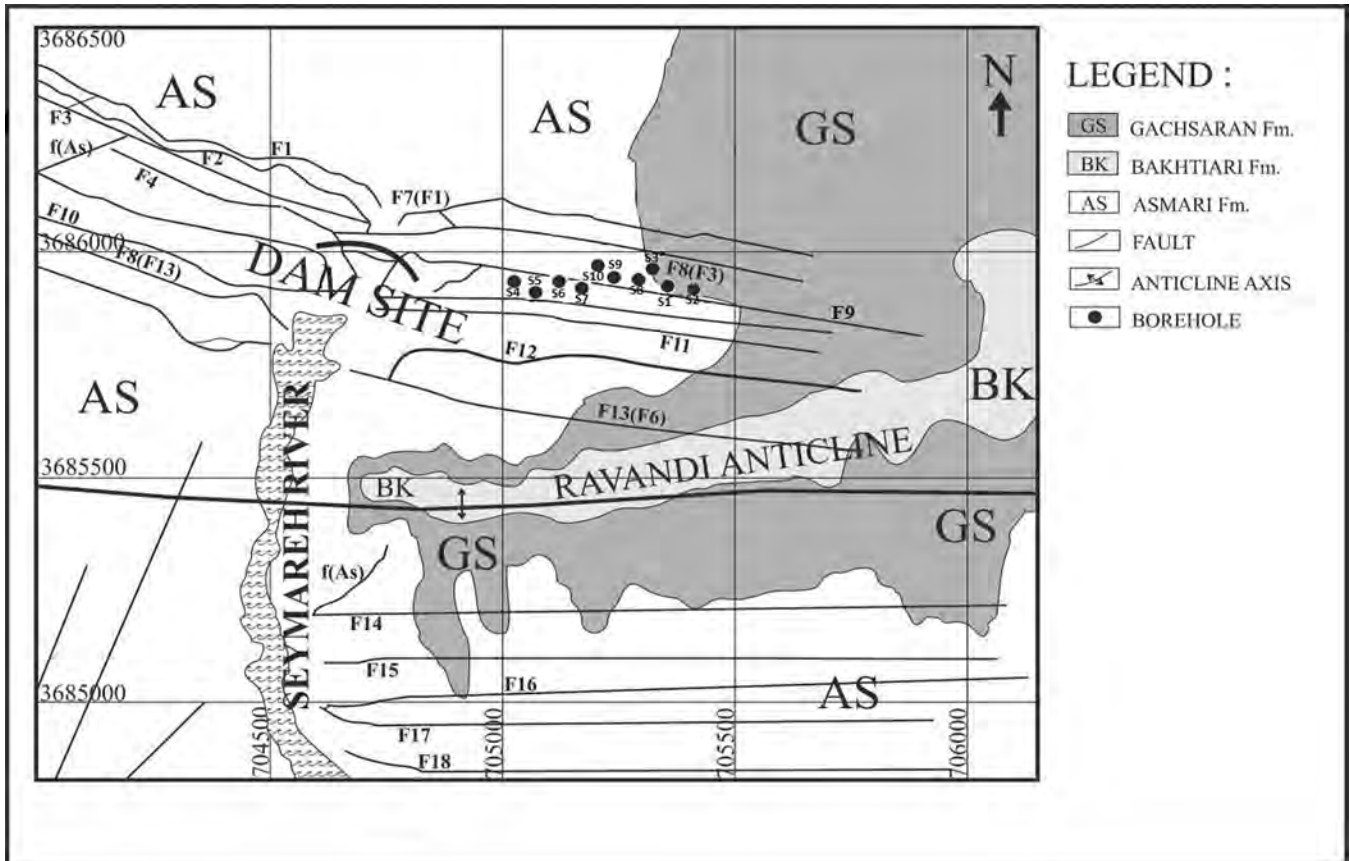


Figure 8a. Geology map of Symareh Dam Site and location of boreholes (Iran Water and Power Resources Development Co., 2008).

Hydrogeologically, karst water of Asmari's aquifer discharges only into Symareh River via 39 springs on the eastern and 2 springs on the western bank (Karimi et al., 2005). The impervious Pabdeh-Gurpi Formations (marl, shale, and marly limestone) is the bedrock of the aquifer and is located below the river level. The groundwater level fluctuates between 598 and 620 m.a.s.l, as measured in the boreholes near the river. The river acts as the local base-level of the aquifer (Ashjari and Raeisi, 2006).

Reliable data on 10 boreholes from the left abutment of Symareh Dam were obtained. The boreholes have extensive information on lithology, fracture density, cavities, Lugeon test, and RQD, with records of every 2 m to 5 m. A summary of borehole data is presented in Table 1. The results show that the permeability of rocks is less than 30 Lugeon units at boreholes S1, S2, S5, and S6; however, the core logs of the boreholes show the presence of fracture and impermeable layers, or both, at different depths. Therefore, no MSZ exists. Only one point is reported to have a permeability >30 Lugeon at boreholes S4, S7, and S10, and more than one point at boreholes S3, S8, and S9.

Our analysis does not include locations with permeability lower than 30 Lugeon units. For clarification, boreholes S7 and S4 are located about 420 and 240 m to the east of the Symareh River at elevations of 642 m.a.s.l and 637 m.a.s.l at depths of 142 m and 125 m, respectively. The results of the Lugeon test of S7 show that the permeability of different levels is <10 Lugeon units except at spacing of 632 m to 637 m which exhibited 85 Lugeon units. The core log analysis shows that there is a thin layer of marly limestone below the MSZ. Small cavities and fractures are also observed at that level. Examination of the differences of this level with the rest of the boreholes reveals that the frequency of fractures is very low. Although cavities were observed in other parts of the borehole, the size of cavities, at the scale of the core specimen, is bigger than the others. S4 has only one high-permeable place at the level of 611 m to 617 m. The water level of the river fluctuates between 592 m.a.s.l to 612 m.a.s.l. and the groundwater level varies from 598 m to 620 m in the observed wells. No fracture was reported in that horizon, but cavities were observed. The high-permeable horizon is located in the fluctuation zone of the groundwater level. Furthermore, there is potential of water injection from river to

Table 1. Summary of boreholes in Symareh Dam Site.

Borehole Name	Borehole Level ^a	Number of Seepage Horizons ^b	Elevation of Seepage Horizons ^a	Cavity ^c	Fractured Zone ^c	Presence of Impurity Adjacent to Horizons	Effect of Hydraulic Factor
S1	648–708	0	–	–	–	–	–
S2	653–703	0	–	–	–	–	–
S3	632–682	2	675	N	Y	Mudstone	N
			635	Y	N	Marly Limestone	N
S4	512–637	1	615	Y	N	Stylolite Horizon	N
S5	501–636	0	–	–	–	–	–
S6	550–636	0	–	–	–	–	–
S7	500–642	1	635	Y	N	Marly Limestone	N
S8	500–639	5	596	Y	Y	Stylolite Horizon	N
			591	Y	Y	Stylolite Horizon	N
			586	Y	N	Stylolite Horizon	N
			581	Y	Y	N	N
			571	Y	Y	N	N
			619	Y	N	Stylolite Horizon Stylolite	N
			609	Y	Y	Horizon Stylolite Horizon	N
			599	Y	Y	Stylolite Horizon	N
S9	500–636	6	584	Y	Y	N	Y
			579	Y	N	N	Y
			544	Y	Y		Y
			614	Y	Y	Stylolite Horizon	Y
			614	Y	Y	Stylolite Horizon	Y
S10	500–637	1	614	Y	Y	Stylolite Horizon	Y

^a The elevations are reported as a.m.s.l.

^b Number of horizon with permeability more than 30 Lugeon units.

^c Y: means presence, and N: means absent.

Note: Symareh River Level = 598–612 m.a.s.l.; Groundwater Level = 598–620 m.a.s.l.

rocks during high flood time. Therefore, it is possible that the hydraulic element plays a crucial role in the development of low-level permeable zone of S4, whereas it is not important for the high-permeable zone of S7. The high-permeable zone of S7 is located beneath a thin layer of the Gachsaran Formation, gypsum and marl. The aggressive precipitation water infiltrates from Gachsaran layer to carbonate formation. The marly limestone interbed impedes the vertical movement of groundwater locally, and allows the water to dissolve carbonate and create the high-permeable zone. Consequently, the presence of the impermeable layer is crucial in the formation of high-permeable zone.

The same analysis was performed for all the boreholes. The MSZs of borehole S3 (2 zones) were limited by marly limestone and mudstone as interbedded inside the Asmari limestone body. Stylolite is common in limestones and is generally marked by insoluble constituents such as clay minerals and pyrite. It is reported to be present in the lithology column of boreholes S4, S8, S9, and S10 at various levels adjacent to high-permeable locations. It seems that this kind of impermeable thin layers may cause the formation of seepage zones.

Six horizons were scattered at the same level of the river and the groundwater level fluctuation zone. It is expected that the presence of MSZs is not extended to elevations lower than the river stage because the river acts as the local base level of the area, so that the possibility of dam-induced karstification is limited and controlled by the river elevation. However, there are three points with MSZ at borehole S9 which are located deeper than the river level at about 10 m to 50 m. Cavities and rod falls were reported in 15 out of the 16 MSZs. These horizons have the highest frequency of fracture, which is sufficient to create a high-permeable zone. These zones could be connected to surface water by interconnected networks of fractures and permit water seepage. A schematic cross section of high-permeable zones is presented in Figure 8b.

Tangab Dam

The Tangab Dam, with a reservoir capacity of 90 Mm³, was constructed over the Firozabad River, 90 km south of Shiraz. The Firozabad River water level varies from 1390 m.a.s.l to 1400 m.a.s.l, flows through the U-shaped Tangab Valley located in the catchment area of Qomp spring. The spring emerges from the central section of the Podenow anticline, which consists of the Asmari Formation (well-jointed limestone) as the main aquifer (Fig 9a). The carbonate formation is surrounded by younger transitional layers of marl and marly limestone and older marly layers of Pabdeh-Gurpi as bedrock. Two dye tests were injected into two boreholes on the left and right abutment of Tangab Dam and they appeared in Qomp spring (Ashjari 2007). The groundwater levels are about 20 m to 27 m below the river at the dam site. The water budget studies by Karimi et al. (2005) shows that the Firozabad River recharges Qomp's spring catchment area about 100 L s⁻¹. Ashjari (2007) demonstrated that the main local base level of aquifers is Qomp Spring. He further reported that the Firozabad River is not the local base level of aquifers in its entrance section to the Tangab Valley in the north, but rather it turns into the local base level of the area after exiting the valley south of the aquifer (Ashjari, 2007).

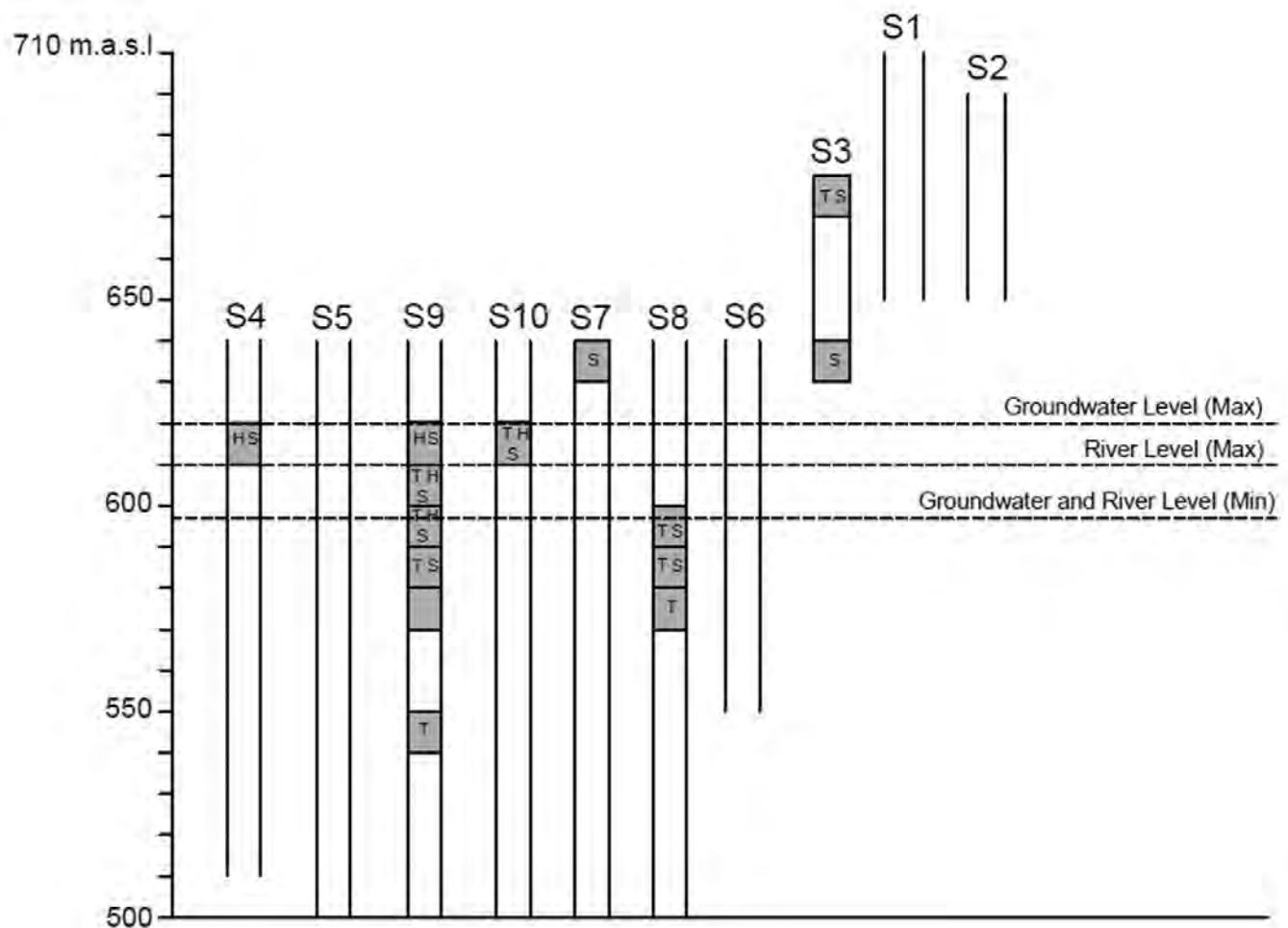


Figure 8b. Fluctuation of groundwater level and river level at boreholes in Symareh Dam Site.

Thirteen boreholes at both abutments of Tangab Dam were studied (Table 2). Fig. 9b shows a schematic cross section of boreholes, groundwater, and river levels. No MSZ was detected in the three boreholes that were drilled more than 70 m away from the river. Eighteen MSZs were found in both abutments of the dam, distributed unevenly from elevations of 1300 m.a.s.l. to 1447 m.a.s.l. Fractures and an impermeable thin layer, represented by marly limestone, were observed in 14 cases. Borehole T1 is located 5 m away from the river, and is the only case without evidence of fractures or an impermeable layer. Four horizons are located in the same level of the river; six horizons are in the space between the river level and groundwater levels; four are detected in the groundwater level fluctuation zone, four horizons are deeper than the water table, and only one horizon is higher than the river.

The deepest horizon, located in borehole T7, is about 50 m below the groundwater level, which is limited by marl limestones at the bottom, while no fracture zone was present nearby. Borehole T7 had another horizon about 10 m below the groundwater level but it is a fractured zone without evidence of an impermeable layer below or above the zone. The remaining deep seated MSZs, at boreholes T12 and T6, are fractured and imbedded by marly limestone. In addition to the deep horizons, in the boreholes drilled very close to the river (less than 10 m), there are one or two horizons with high-seepage at groundwater level or in the space between the river and groundwater. The highest MSZ lies about 5 m above the maximum river stage (70 m away from the river) in a fractured zone next to marly limestone. There is a fairly good relationship between the MSZ depth and distance from the river. The boreholes close to the river have higher permeability, which implies that existence of some passages in depth is more likely.

Although a karst conduit is seldom reported in boreholes logs, there are three exposed caves close to the dam site, and during excavation of the dam's galleries, one hidden shaft was exposed.

Kowsar Dam

Kowsar Dam, with a capacity of 570 Mm³, was constructed on Khirabad River in the Douk anticline to supply the demand for water of two provinces in south Iran. Geologically, the dam abutments and foundation are based on carbonate layers which are covered by gypsum and cemented conglomerate, and recent alluvial sediments (Fig. 10a). The layers

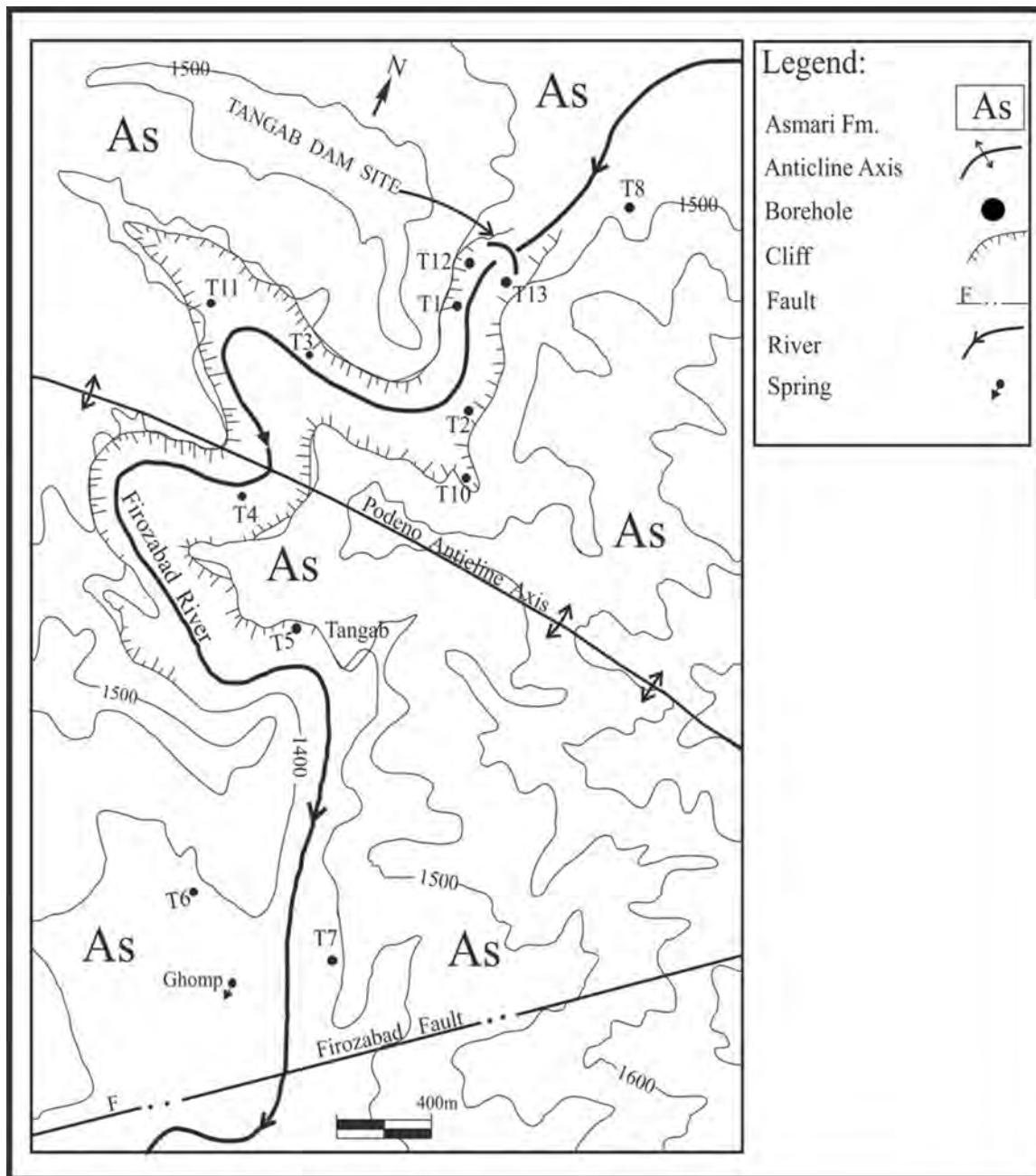


Figure 9a. Geology map of Tangab Dam Site and boreholes (Nadri, 1999).

are approximately horizontal, dipping less than 6° around the dam. The lowest elevation of the exposed part of Asmari (well-jointed limestone), as the main aquifer in the area, is in the southern plunge of the anticline.

Hydrogeologically, Pabdeh-Gurpi (marl, shale, and marly limestone) as bedrock does not inhibit the hydrogeological relationship of both flanks of the anticline. Although the river has incised the Asmari Formation (well-jointed limestone), at least at the dam site, there is no hydraulic relationship between the river and the aquifer, which has been confirmed by dye test and isotopic analysis (Water Research Centre of Iran, 1997). The general direction of groundwater

flow is towards the southern plunge of the anticline (Rahanjam, 2009). The borehole study reports the presence of 56 MSZs at 8 boreholes distributed at different levels: 45 at higher elevation than the river, 2 MSZs at the groundwater level fluctuation zone, and 7 below groundwater level (Table 3). The space between the river's bedrock and the groundwater level is too thin to hold any horizon inside it and the absence of hydraulic connectivity between the river and the aquifer results in a non-seepage zone.

A schematic cross section of high-permeable zones is presented in Figure 10b. The impermeable layers, here consisting of marls and marly limestones, were adjacent to 32 out of 56 MSZs (~57%), and 28 horizons are in fractured zones. Neither fractured zones nor impermeable layers were observed in 12 horizons distributed in different levels. The three deepest horizons lie 15 m to 20 m below the river level which is limited by marly limestones, with one horizon fractured.

Cavities of different sizes are reported inside 39 horizons. In three horizons, no cavity, impermeable layer or fracture was observed. Therefore, it is possible to find a MSZ without any evidence of primary elements of karst development. The cause of MSZ can be removed by excessive development of one passage which erodes the impermeable layers, or when several minor passages combine into one passage.

Table 2. Summary of boreholes in Tangab Dam Site.

Borehole Name	Borehole Level ^a	Number of Seepage Horizons ^b	Elevation of Seepage Horizons ^a	Cavity ^c	Fractured Zone ^c	Presence of Impurity Adjacent to Horizons	Effect of Hydraulic Factor
T1	1360–1405	2	1390 1365	N N	Y N	Marly Limestone N	Y Y
T2	1360–1406	1	1399	N	N	Marly Limestone	Y
T3	1360–1394	2	1384 1367	N N	Y Y	N N	Y Y
T4	1357–1397	2	1382 1367	N N	N N	Marly Limestone Marly Limestone	Y Y
T5	1330–1364	0	–	–	–	–	–
T6	1325–1387	2	1345 1314	N N	Y Y	Marly Limestone Marly Limestone	N N
T7	1299–1369	3	1356 1339 1305	N Y N	Y Y N	Marly Limestone N Marly Limestone	Y Y N
T8	1327–1447	0	–	–	–	–	–
T9	1292–1442	0	–	–	–	–	–
T10	1300–1430	1	1417	N	Y	Marly Limestone	N
T11	1263–1393	1	1378	N	Y	Marly Limestone	Y
T12	1275–1425	3	1391 1376 1336	Y N N	Y Y Y	Marly Limestone Marly Limestone Marly Limestone	Y Y N
T13	1295–1425	1	1395	N	Y	Marly Limestone	Y

^a The elevations are reported as a.m.s.l.

^b Number of horizon with permeability more than 30 Lugeon units.

^c Y: means presence, and N: means absent.

Note: Tangab River Level = 1390–1400 m.a.s.l.; Groundwater Level = variable.

Discussion

The presence of impermeable layers such as marl, marly limestone, and clay within a permeable section can guide the flow of water along the contact of the impermeable layer and karstifiable rocks (Fig. 1). Subsequently, the dissolution of carbonate rocks can lead to development of karst conduits as main seepage horizons. These horizons are concordant with the inception horizon hypothesis by Lowe (1992). It is noteworthy that this concept was proposed by Ford and Ewers (1978), White (1988), Ford and Williams (1989) and Palmer (1975 and 1991) without using the term “inception horizon”.

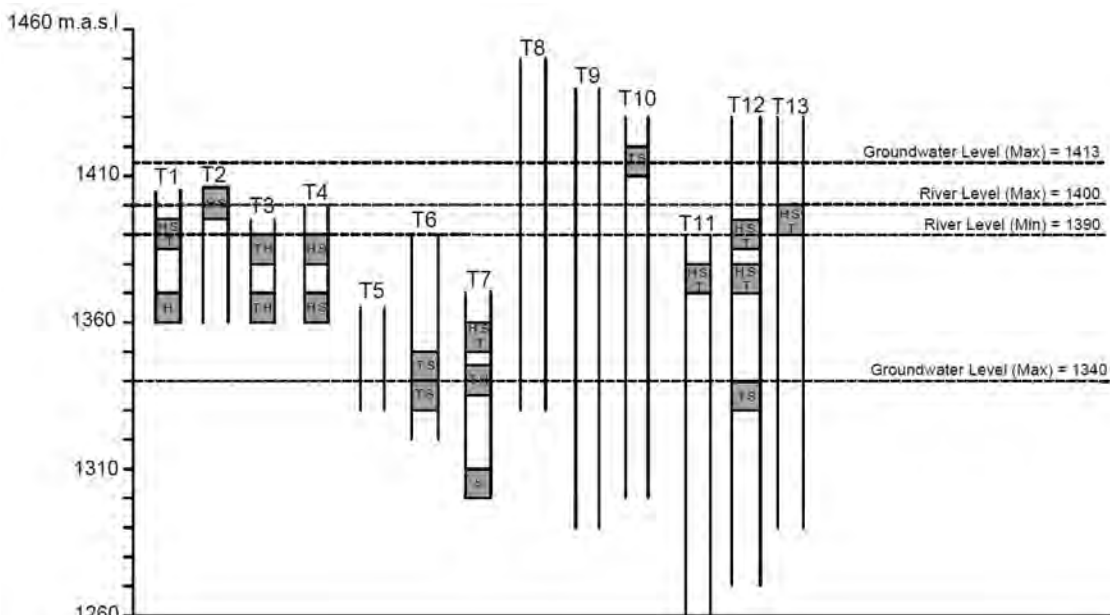


Figure 9b. Fluctuation of groundwater level and river level at boreholes in Tangab Dam Site.

It seems the role of an inception horizon is not too important among the selected dams to plot close to the stratigraphic apex of the triangular diagram (Fig. 7). However, there is only one out of 30 boreholes which absolutely matches this apex. It could be due to two possible factors: a) it is possible that the inception horizons fully control the karst

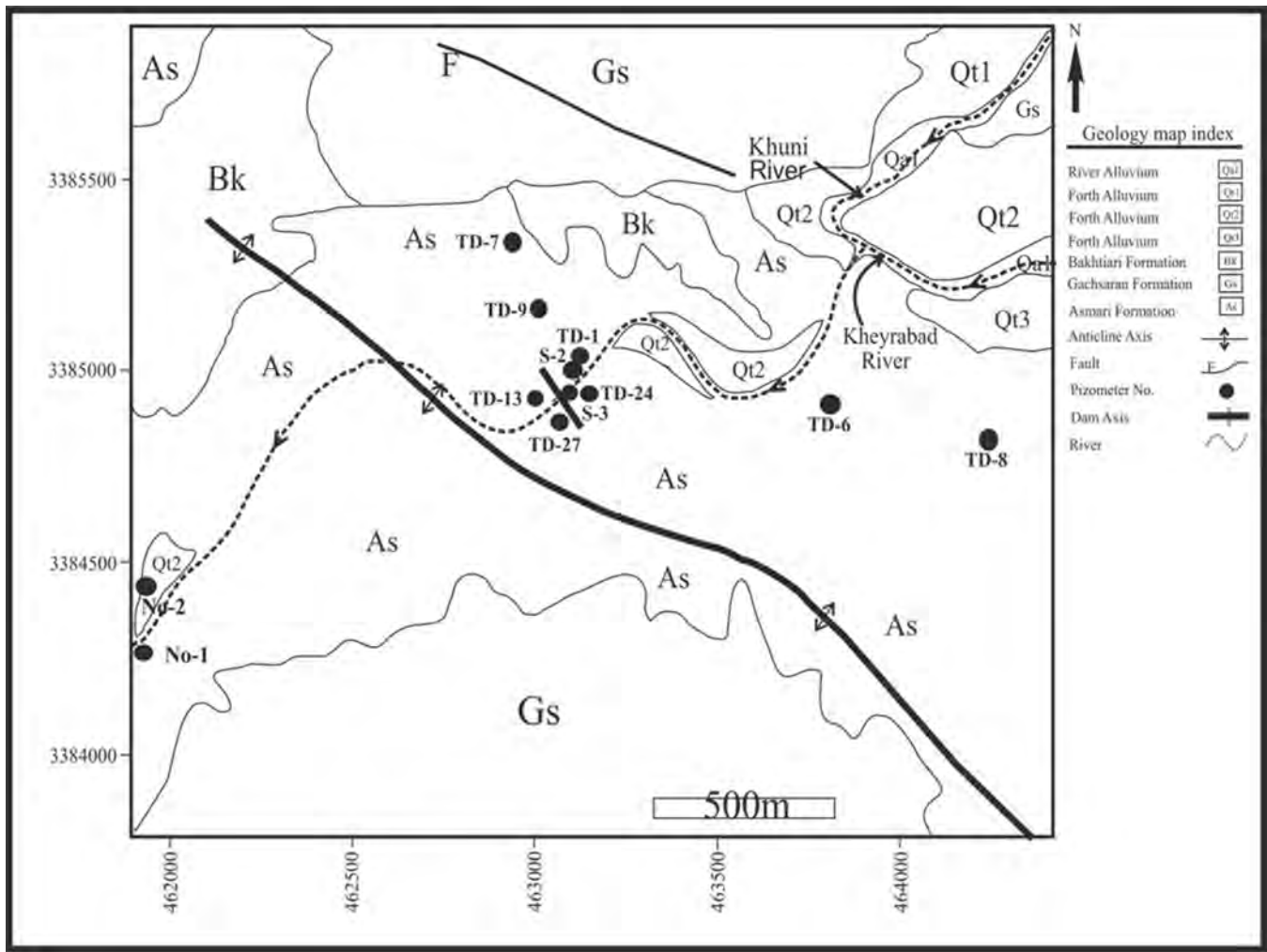


Figure 10a. Geology map of Kowsar Dam Site and boreholes.

conduit development at a zone, but it cannot be the main factor in larger areas such as dam sites or regional scales. It appears that the inception zone is randomly developed by geological elements or our knowledge is not adequate to report a general role for karst development based on inception horizons. Alternatively, the current evidence of ancient inception horizons disappeared due to geological alterations since the formation of these zones or the paleohydraulic history of the region erodes this evidence.

The presence of fractures and impermeable layers in some horizons permits the formation of intensively-developed passages with high-permeability to transfer water. The impermeable layers retard the easy water movement inside the carbonate rocks but this diverts the water to a fracture that connects the two karstic layers. The hydraulic concentration of water in such fractures allows high volumes of water to enter the fractured carbonate rocks; therefore, the passages develop into MSZ.

The role of rivers and their location relative to soluble layers is crucial in making a MSZ. If a river discharges the carbonate rock as an aquifer, such as the Symareh Dam site, the MSZs are most likely to be distributed at the same level of the river, and groundwater level is controlled by the river as well. In such conditions, the probability of MSZ presence in levels higher or lower than the river stage and groundwater table fluctuation zone will decrease. Although the fractures and impermeable layer in the same level of rivers can aggregate the karst conduit development, they are likely to be washed away by water flow. The horizontal extension of MSZ can be very far from the river banks, but it is vertically limited to the river level. For such a situation, the area must be tectonically stable to some extent for a significant geological time. If the region is active, the river will incise the karstic layer faster and the developed karst conduits will be limited to the valley walls as thin and shallow karstic zones.

At Tangab Dam, the river recharges the aquifer because the river is not at the base level of the surrounding karstic aquifer. The high volumes of water seeping from the river's bed are guided by fractures and voids to reach the ground-

Table 3. Summary of boreholes in Kowsar Dam Site.

Borehole Name	Borehole Level ^a	Number of Seepage Horizons ^b	Elevation of Seepage Horizons ^a	Cavity ^c	Fractured Zone ^c	Presence of Impurity Adjacent to Horizons	Effect of Hydraulic Factor
K1	489-579	5	568	Y	Y	N	N
			556	N	Y	N	N
			553	Y	N	N	N
			550	Y	N	N	N
			535	N	N	N	N
K2	456-610	6	602	Y	N	Marly Limestone	N
			567	N	Y	N	N
			562	Y	N	N	N
			547	Y	N	N	N
			542	Y	Y	N	N
			532	Y	N	N	N
K3	538-618	9	605	N	Y	N	N
			595	Y	N	Marly Limestone	N
			590	Y	Y	N	N
			585	Y	Y	N	N
			580	N	Y	N	N
			575	N	N	N	N
			560	Y	N	N	N
			555	Y	Y	N	N
			550	N	N	N	N
K4	477-617	4	604	Y	N	Marly Limestone	N
			599	Y	N	Marly Limestone	N
			589	N	Y	N	N
			584	Y	N	N	N
K5	483-608	3	530	Y	N	Marly Limestone	N
			520	Y	N	N	N
			505	Y	N	N	Y
K6	491-606	16	598	Y	Y	Marly Limestone	N
			593	Y	N	Marly Limestone	N
			588	Y	Y	N	N
			583	Y	N	Marly Limestone	N
			573	N	Y	Marly Limestone	N
			568	Y	N	Marly Limestone	N
			553	Y	Y	Marly Limestone	N
			548	Y	N	N	N
			543	Y	Y	Marl	N
			538	N	Y	Marl	N
			533	Y	Y	Marl	N
			528	N	N	Marly Limestone	N
			513	Y	Y	Marl	N
			508	Y	Y	Marl	Y
			498	Y	Y	Marl	Y
			493	N	Y	Marl	N
K7	480-510	2	492	Y	Y	Marly Limestone	N
			487	N	Y	Marly Limestone	N
K8	458-558	11	550	Y	Y	Marly Limestone	N
			545	Y	Y	Marl	N
			535	N	N	Marl	N
			530	Y	Y	Marl	N
			515	Y	N	Marly Limestone	N
			510	N	Y	Marly Limestone	Y
			505	N	Y	Marl	Y
			500	Y	N	Marly Limestone	Y
			490	N	N	Marly Limestone	N
			485	Y	N	Marly Limestone	N
			480	N	N	Marly Limestone	N

^a The elevations are reported as a.m.s.l.

^b Number of horizon with permeability more than 30 Lugeon units.

^c Y: means presence, and N: means absent.

Note: Kowsar River Level = 505-512 m.a.s.l.; Groundwater Level = 495-502 m.a.s.l.

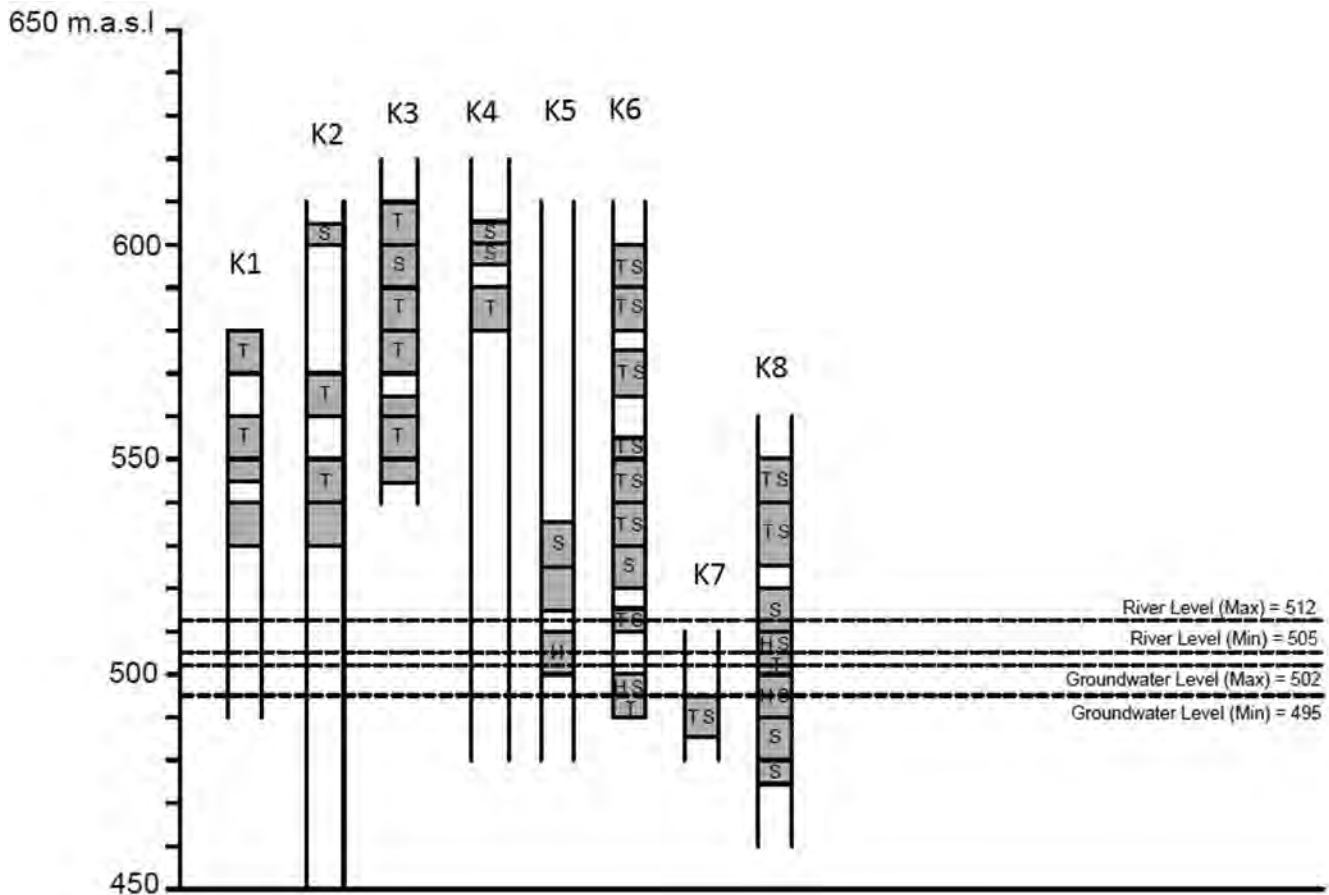


Figure 10b. Fluctuation of groundwater level and river level at boreholes in Kowsar Dam Site.

water, and then the contact of water with voids and fractured surfaces creates an opportunity for the development of some karst conduits as MSZ. Akhondi and Mohammadi (2014) have proposed a geostatistical model based on the Lugeon tests to identify spatial variability at permeability in the Tangab dam site. They concluded that the high Lugeon value placements are concordant with the marl inter-bedded layers in the left abutment of the dam. If the impermeable layers are settled as interbedded among the carbonate layer in the space between the water table and the river's bed, the role of fractures in rupturing water tightness of impermeable layer becomes effective. The karstification extension is mainly limited to river banks horizontally, and to the space between the river's bed and groundwater table vertically.

It is possible that the hydraulic connectivity between river and karstic layer is reduced if: a) insoluble materials such as clay and marl settle at the river's bed and bank to make an impermeable layer, that is, Kowsar case; b) the river has incised the karstic rocks and reached the insoluble and impermeable bedrock of karstic formation. It is apparent that in the past, there was a type of hydraulic connectivity, recharge or discharge, of river and karstic layer. In general, MSZs are mostly located at higher elevations than rivers. Determining their origin is very complex and sometimes ambiguous.

Conclusion

To show the relationship between the three main elements— fracture, stratigraphy, hydraulic, and the main seepage horizons of water in dam sites of Zagros Region, a triangular diagram was presented. The main advantage of this diagram is that it is a simple way to present the extent of the element effects on MSZ formation. There are some MSZs that cannot be related to any of the three main elements presented here. The evidence might have been removed during a geological time in different tectonical and hydrogeological conditions from the present.

Although the Asmari Formation is inherently fractured, according to the distribution of boreholes and dams on the diagram, there is no borehole or dam in which only one element is responsible for creating MSZ. In fact, karst development is a very complicated process, which is not merely governed by interaction of these elements. In summary, Asmari, as a carbonate rock, is soluble but the impermeable layers' settlements (thin layer marly, marly limestone, and clay limestone) inside the formation make some horizons to be prone to conduit development and guide the water to seep from the area.

The hydraulic connectivity of the river with adjacent karstic layers and groundwater level fluctuation zones are very important in developing an MSZ. The gaining rivers are effective in the development of a MSZ at river level and long distances from the river. The water seepage is expected to be more problematic in dam abutments than basements. The recharge rivers widen fractures and dissolve rocks at their basements. The high hydraulic gradient and massive volumes of concentrated water in the space between the river's bed and groundwater level can breach the impermeable interbeds. The main problem with this type of dam is in the foundation.

Although in neutral rivers, there is no hydraulic relationship between river and carbonate rocks, existence of the MSZ shows that there may be some hydraulic relations at some points in the past. This type is a very complex MSZ development.

Finally, at the borehole scale, it is possible to determine a MSZ to be controlled by one of the three mentioned elements. To extend the results at dam site or regional scale, it is necessary to have more information on regional geology and dye-tracing data.

References

- Aghanabati, A., 2004, Geology of Iran: Geological Survey of Iran, p. 619. [Persian]
- Akhondi, M., and Mohammadi, Z., 2014, Preliminary analysis of spatial development of karst using geostatistical simulation approach: *Bulletin of Engineering Geology and the Environment*, v.73, p.11. <https://doi.org/10.1007/s10064-014-0599-3>.
- Alavi, M., 2004, Regional stratigraphy of the Zagros Folds-Thrust Belt of Iran and its proforeland evolution: *American Journal of Science*, v. 304, p. 1–20. <https://doi.org/10.2475/ajs.304.1.1>.
- Ashjari, J., 2007, Classification of Zagros karstic aquifers based on general direction of groundwater flow and physico-chemical properties: [Ph.D. Dissertation]: Shiraz, Iran, University of Shiraz, Iran.
- Ashjari, J., Raeisi, E., 2006, Influences of anticlinal structure on regional flow, Zagros, Iran: *Journal of Cave and Karst Studies*, v. 68, n. 3, p. 118–129.
- Cooper, A.H., Gutiérrez, F., 2013, Dealing with gypsum karst problems: hazards, environmental issues, and planning, *in* Shroder, J. and Frumkin, A., eds., *Treatise on Geomorphology: Karst Geomorphology*, San Diego, Academic Press, v. 6, p. 451–462.
- Falcon, N.L., 1974, Southern Iran: Zagros Mountains: Geological Society, London, v. 4, p. 199–211.
- Ford, D.C., and Ewers, R.O., 1978, The development of limestone cave systems in the dimensions of length and depth: *Canadian Journal of Earth Science*, v. 15, p. 1783–1798. <https://doi.org/10.1139/e78-186>.
- Ford, D.C. and Williams, P., 1989, *Karst Hydrogeology and Geomorphology*: London, Chapman & Hall, 570 p.
- Gutiérrez, F., Desir, G., Gutiérrez, M., 2003, Causes of the catastrophic failure of an earth dam built on gypsiferous alluvium and dispersive clays (Altorricón, Huesca Province, NE Spain): *Environmental Geology*, v. 43, p. 842–851. <https://doi.org/10.1007/978-94-011-7778-8>.
- Gutiérrez, F., Parise, M., De Waele, J., Jourde, H., 2014, A review on natural and human-induced geohazards and impacts in karst: *Earth-Science Reviews*, v. 138, p. 61–88. <https://doi.org/10.1016/j.earscirev.2014.08.002>.
- Gutiérrez, F., Mozafari, M., Carbonel, D., Gómez, R., Raeisi, E., 2015, Leakage problems in dams built on evaporites. The case of La Loteta Dam (NE Spain), a reservoir in a large karstic depression generated by interstratal salt dissolution: *Engineering Geology*, v. 185, p. 139–154.
- Houlsby, A.C., 1976, Routine interpretation of the Lugeon water-test: *Quarterly Journal of Engineering Geology and Hydrogeology*, v. 9, 303–313. <https://doi.org/10.1144/GSL.QJEG.1976.009.04.03>.
- James, AN., 1992, *Soluble material in civil engineering*: Chichester, U.K., Ellis Horwood, 300 p.
- Johnson, K.S., 2008, Gypsum-karst problems in constructing dams in the USA: *Environmental Geology*, v. 53, p. 945–950. <https://doi.org/10.1007/s00254-007-0720-z>.
- Karimi, H., Raeisi, E., Zare, M., 2005, Physicochemical time series of karst springs as a tool to differentiate the source of spring water: *Carbonates and Evaporites*, v. 20, no. 2, p. 138–147. <https://doi.org/10.1007/BF03175457>.
- Kiraly, L., 1975, Rapport sur l'état actual des connaissances dans le domaine des caractères physiques des roches karstiques, *in* Bueger and Dubertret, eds., *International Union of Geological Sciences, Series B*, 3, p.53–67.
- Lowe, D.J., 1992, The origin of limestone caverns: an inception horizon hypothesis, [Ph.D. Dissertation]: Manchester, U.K., Manchester Metropolitan University, 511 p.
- Milanović, P.T., 2000, *Geological Engineering in Karst: Dams, Reservoirs, Grouting, Groundwater Protection, Water Tapping, Tunneling*: Belgrade, Zebra, 347 p.
- Milanović, P.T., 2002, The environmental impacts of human activities and engineering constructions in karst regions: *Episodes*, v. 25, p. 13–21.
- Milanović, P.T., 2004, *Water Resources Engineering in Karst*: Boca Raton, Fla., CRC Press, 328 p. <https://doi.org/10.1201/9780203499443>.
- Milanović, P., 2011, Dams and Reservoirs in Karst, *in* van Beynen, P., eds., *Karst Management*: Dordrecht, Springer. https://doi.org/10.1007/978-94-007-1207-2_3.
- Palmer, A.N., 1975, The origin of maze caves: *Bulletin of the National Speleological Society*, v. 37, p. 57–76.
- Palmer, A.N., 1991, The origin and morphology of limestone caves: *Geological Society of America Bulletin*, v. 103, p. 1–21. [https://doi.org/10.1130/0016-7606\(1991\)103<0001:OAMOLC>2.3.CO;2](https://doi.org/10.1130/0016-7606(1991)103<0001:OAMOLC>2.3.CO;2).
- Palmer, A.N., 2007, *Cave Geology*: Trenton, N.J., Cave Books, National Speleological Society, 454 p.
- Parise, M. and Gunn, J., 2007, *Natural and anthropogenic hazards in karst areas: Recognition, Analysis and Mitigation*, Geological Society of London, Special Publication 279.
- Parise, M. and Lollino, P., 2011, A preliminary analysis of failure mechanisms in karst and man-made underground caves in Southern Italy: *Geomorphology*, v. 134, nos. 1–2, p. 132–143. <https://doi.org/10.1016/j.geomorph.2011.06.008>.
- Parise, M., Closson, D., Gutiérrez, F., Stevanović, Z., 2015, Anticipating and managing engineering problems in the complex karst environment: *Environmental Earth Sciences*, v. 74, p. 7823–7835. <https://doi.org/10.1007/s12665-015-4647-5>.
- Rahanjam, M., 2009, Modeling of water loss potential in future of Tang Douk Dam due to dissolution [M.Sc. Thesis]: Tehran, Iran, Tehran University. [Persian]
- Romanov, D., Gabrovšek, F., Dreybrodt, W., 2003, Dam sites in soluble rocks: a model of increasing leakage by dissolutional widening of fractures beneath a dam: *Engineering Geology*, v. 70, P. 17–35.

- Shabab-Boroujeni, B., 2012, Determination of effective factors on permeability in karstic dams in west of Zagros [M.Sc. Thesis]: Tehran, Iran, Tehran University. [Persian]
- Stevanović, Z., 2015, Karst Aquifers — Characterization and Engineering: Cham, Switzerland, Springer, 692 p. <https://doi.org/10.1007/978-3-319-12850-4>.
- Stocklin, J., Setudehnia, A., 1971, Stratigraphic Lexicon of Iran: Geological Survey of Iran Report 18-1971.
- Water Research Centre of Iran, 1997, Tracing studies of Kowsar (Tang e Douk) Dam Site: Behbahan, p. 35–37. [Persian]
- White, W.B., 1988, Geomorphology and Hydrology of Karst Terrains: New York, Oxford University Press, 464 p.
- Wright, V.P. (1991) Paleokarst types, recognition, controls and associations: In: Wright, V.P., ed., Paleokarsts and Paleokarstic Research Institute of Sedimentology, Occasional Publication Series, v. 2, p. 56–88.
- Zhou, W., and Beck, B.F., 2011, Engineering issues on karst, *in* Van Baynen, P.E., ed., Karst Management. Springer, Dordrecht, p. 9–45. https://doi.org/10.1007/978-94-007-1207-2_2.

CAVES IN SPACE

John Mylroie

Abstract

The definition of a cave has centered on its accessibility to humans, an understandable, but arbitrary, approach. Caves without humanly accessible entrances are still caves. As we reach out to the moons and planets of our solar system, and eventually the stars, we need to evaluate caves as possible reservoirs of extraterrestrial life and as potential human habitats. If humanly passable caves are a subset of all caves, then caves can exist from the tiny, subatomic dimension up to and including the entire universe. They can form and exist for only milliseconds or for billions of years. What's more, they can form in almost any solid material, and perhaps even in liquids, and contain within them vacuum, gases, liquids or solids. Caves can be initially classified as natural and artificial. Natural caves form either by constructive processes that build a boundary, which contains the void, or by destructional processes that remove or shift material to create a void, where none existed before. Caves are defined by answering five questions: 1. How did the void form? 2. How big is it? 3. How long has it lasted? 4. What does it contain? 5. How does it connect to exterior space? As humans move from a geocentric view of natural features to a more universal view, we need to see caves across a broader continuum of possibilities.

Introduction

At the National Speleological Society annual convention, on July 18–22, 2016, in Ely, Nevada, Dr. Penny Boston, who had recently been appointed Director of the NASA Exobiology Institute, convened a special session, entitled The Future of Cave and Karst Science and Exploration. The session had four presentations by: George Veni; John Mylroie and Joan Mylroie; Michael Spilde, Jason Kimble and Diana Northup; and Penny Boston. Dr. Boston's presentation was titled "Extraterrestrial Caves: Advanced Technologies in the Search" (Boston, 2016). After the four presentations were completed, there was a panel discussion composed of the four presenters with the audience. This discussion eventually began to contemplate how to view caves from an extraterrestrial perspective. One big question, from NASA's viewpoint, was what was a cave, and, perhaps more importantly, would extraterrestrial caves be the refugium for life on other moons and planets? The interactions between the panel and the audience were wide-ranging and, at times, innovative. Also, they were possibly controversial, as when George Veni suggested that the largest cave in the solar system was the underground ocean on Europa, a moon of Jupiter. Then, this author countered that the largest cave was the liquid outer core of the Earth, both being subsurface, fluid-filled chambers. An important point made by Penny Boston was how to present caves to other NASA scientists and administrators. As many cavers and cave scientists have long known, people not associated with caves commonly do not understand them, and have many misconceptions about caves in general. How do we, as cavers and cave scientists, present caves to NASA? Discussions continued informally after the session ended.

After the convention, this author began to contemplate the problem of defining caves from a solar system or, perchance, an entire universe perspective. After some initial ideas were placed on paper, the author eventually prepared a PowerPoint presentation. At the 17th International Congress of Speleology in Penrith, Australia on July 25, 2017 (almost a year to the day from the NSS session in 2016), the author gave the presentation in the Extraterrestrial Caves session (Meredith and Moore, 2017). Ironically, the presentation was a substitute for a talk originally submitted by Drs. Penny Boston and Diana Northrup, cancelled because Penny Boston could not attend. The presentation generated a great deal of spirited discussion, and it was proposed that the ideas presented should end up in the cave and karst literature. Hence the origin of this paper.

To make a clean break from an Earth-centered and human bias, it was decided to start from an especially simple and basic first principles approach. To avoid preconceptions, this discussion will depart from many of the standard terms used by cavers and cave scientists, and address a few important themes. The first is, obviously, what is a cave? From that beginning, further questions center on the nature of the void, essentially, what is inside the void—vacuum, a gas, a fluid? What are the spatial and temporal aspects of a void, the sense of scale in time and space? Finally, how would we define such voids, or arrange them in a hierarchy? The author, as a life-long science fiction reader, has encountered numerous examples of fictional extraterrestrial caves, where the story characters are called spelunkers more often than not. The book, *Caves of Karst* (Hoffman, 1969), is a good example of science fiction and caving not mixing well. These stories helped document how unrealistically caves are viewed by non-cavers, while at the same time provided novel insights into other ways of thinking about caves (e.g., Wikipedia, 2018). It is time, as cavers, to step back and view caves from an extraterrestrial viewpoint with new eyes.

What is a Cave?

The definition of a cave by cave scientists has almost always centered on the ability of humans to enter and explore an underground void, as presented by White (1988), Klimchouk (2004), Neuendorf et al. (2005), White and Culver (2005), Ford and Williams (2007), and Palmer (2007), among others. Portions of caves too small to admit humans are not caves according to Davies (1960). The single best treatment of what defines a cave is the classic article by Rane Curl (1964), "On the Definition of a Cave." Rane Curl recognized, as had many authors, the relative arbitrariness of using human beings as the dimensional frame of reference, perhaps best illustrated by Figure 1. A cave that humans can fit into was labeled by Curl (1964, p. 2) as a "proper cave," stating that such caves were a subset "of all subterranean cavities," in contrast to the limitations set by Davies (1960). Most importantly, he noted that, "A cave is a space rather than an object and consequently its definition involves the specification of its boundaries." (Curl, 1964, p. 1). Howard (1960) argued, "An opening is any volume surrounded by solid rock, but not filled by solid rock ... (it) may be filled with air, water, loose rock, mineral, clay or other debris" Use of humans to define caves will not work as we move into outer space, and possibly find life in underground voids.

Many of the authors above also wrestle with whether or not a cave must have a humanly accessible opening to the outside. It would seem ludicrous to characterize an underground void as not a cave because humans could not enter it.

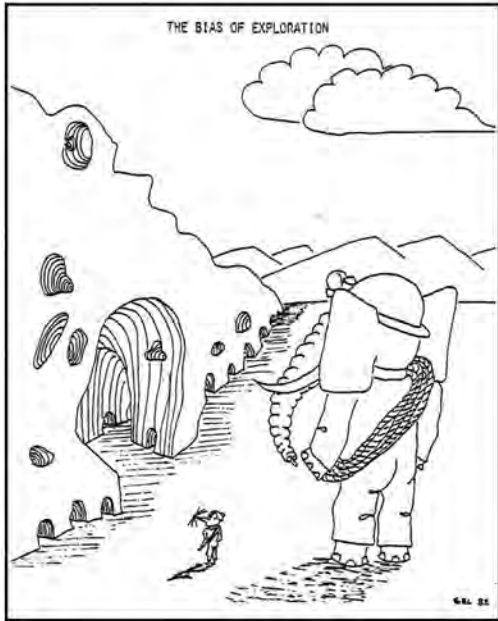


Figure 1. *The Bias of Exploration*, a cartoon by Dr. Stein-Erik Lauritzen, a Norwegian cave scientist, displays the problems when using an organism as the frame of reference for defining a cave. From Lauritzen (1983).

Is a cave, suddenly opened by a quarry, not a cave prior to the blast that opens it? If we ignore, for the moment, the human-sized issue, a cave can be defined as an interior space isolated from an exterior space (Fig. 2A). If an entrance connects the interior space to an exterior space, even if that connection is small, relative to the size of the interior space, the interior space is, topologically, just an extension of the exterior space (Fig. 2B). Again, Curl (1964) explored this matter, defining a cave entrance as "...another form of boundary to the cave space." It is conceivable that a cave, such as a lava bubble, could have life evolve inside it, from purely inorganic material, utilizing chemosynthesis for an energy source, without the void ever having had any connection to the outside space. Earlier, Curl (1958) had investigated the statistics of cave entrances, predicting that a large number of entrance-less caves existed. Varnedoe (1973) and White, (1988) demonstrated that thousands of entrance-less caves existed in Alabama, and were actually the most abundant cave type (Fig. 3).

What is in and Around the Cave?

A key question is what is in the cave? Howard (1960) stated that a cave could contain air, water, or various sediments. A lava tube on the Moon would contain a vacuum. Is a lava tube still full of magma a cave? If a cave can be filled with water and visited by cave divers, a lava tube, filled with molten rock, must also still be a cave, although exploration with current technology would be a problem (Fig. 4). On other bodies in the solar system or elsewhere in the universe, the cave could contain a variety of gases from hydrogen to chlorine, fluids from liquid methane to liquid mercury,

or solids from water ice to hydrocarbons. If a pre-existing cave is infilled completely by another solid material, be it ice or clay, as occurs on the Earth, is it still a cave? It was certainly a cave at one time. As demonstrated by Figure 4, cave

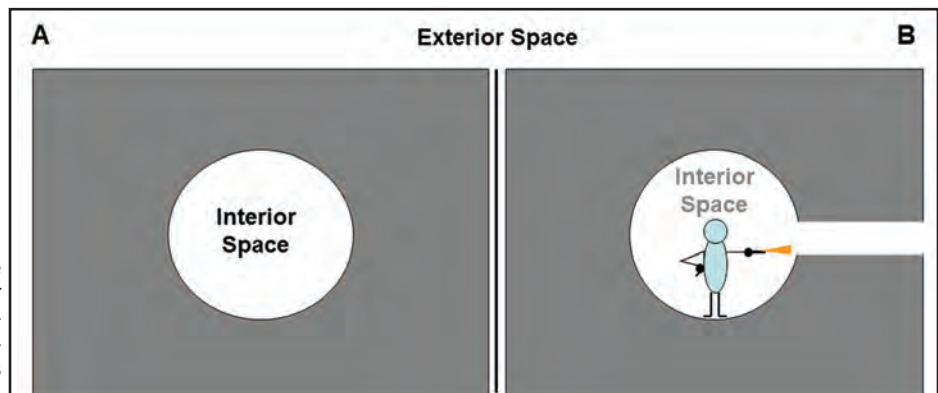


Figure 2. Caves as "interior space:" A) The interior space is isolated from the exterior space. B) The interior space has a connection to the exterior space, allowing direct exploration. Topologically, the interior space is now an extension of the exterior space.

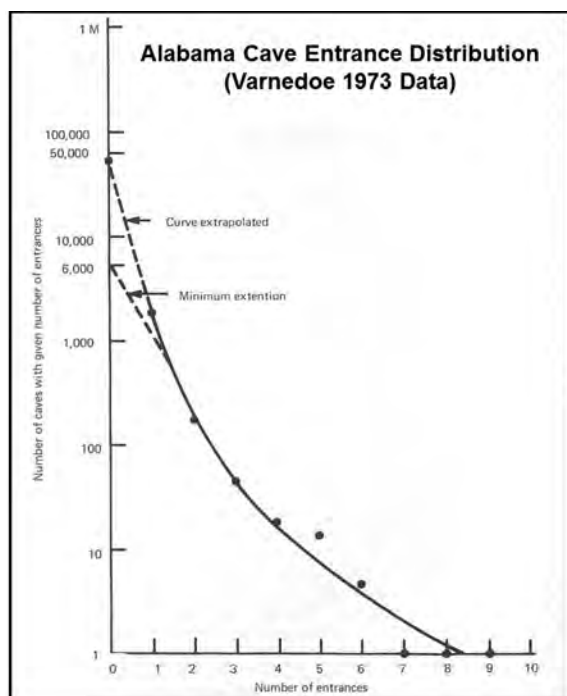


Figure 3. Plot of cave entrance number versus cave abundance data for Alabama (1973 data). The plot shows that the entrance number is inversely proportional to the number of caves, and that extending the plot to zero entrances demonstrates a minimum of 6,000 entrance-less caves, with perhaps as many as almost 50,000. The plot assumes the proper caves of Curl (1964). From White (1988).

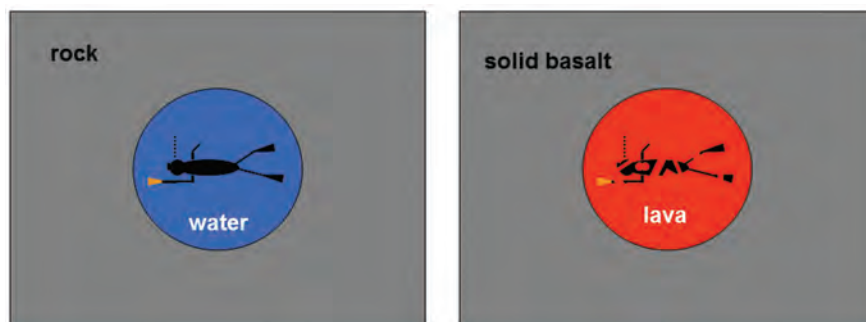


Figure 4. Examples of fluid-filled caves: A) Water-filled, a common type of cave subject to exploration with current technology. B) Lava-filled, also common, but not subject to exploration with current technology (at least, not for long).

“empty space” does not mean a vacuum. The void as a concept should be considered non-dimensional. Underground voids are sought by geophysicists, who specifically name them “subsurface voids” (e.g., Keary et al., 2002, Burger et al., 2006). Those voids do not contain a vacuum or simply air; they may also contain water, sediment or other deposits. These voids are detectable by geophysical techniques, precisely because the void is different in physical character from its surrounding material. For this discussion, a void is a region different from that which surrounds it.

Spatial and Temporal Aspects of a Cave

If we accept for the moment that a cave is a void with boundaries, then we are faced with two questions. What is the possible size range of the void, and what is the duration of the void’s existence? How small can a void be, and how large? From a purely theoretical point of view, the smallest measured objects in the universe are the building blocks of subatomic particles, quarks, at $\sim 0.43 \times 10^{-16}$ cm (ZEUS Collaboration, 2016). Depending on how the quarks were arranged to form a void boundary, the “cave,” so enclosed, could be smaller than the quarks themselves, or exceedingly small. Considering such a tiny void as a cave is a bit far-fetched, but viruses can be as small as 100 nanometers (Harris,

exploration on other planets and moons may require technology not available at the present. The exploration of active lava tubes, for example, could be tested on Earth. This would be technology above and beyond that needed to simply reach the target planet. Cavers like Bill Stone are already deep into developing the technology to explore the ice-covered, ocean caves of places like Europa, a moon of Jupiter (Vlahos, 2007).

Just as important as what is inside the cave is the nature of the material containing the cave. Many authors (e.g., Howard, 1960) have assumed the cave is in rock. This works well on Earth if glacial ice is considered a rock (ice is a rock to planetary scientists). Some asteroids may be iron-nickel alloys; caves in them would not be in rock as classically defined (e.g., Neuendorf, 2005), but in a metal. Consider an air bubble in water. It is a void with boundaries, as defined by Curl (1964); if fluid viscosity were sufficient to keep the bubble in one place, then it would be spatially constrained. But need it be? Is a moving bubble any different in its internal conditions than a bubble that stays in one place? While most caves on Earth stay in one place, some do move, such as voids in a moving glacier, or ones in diapiric salt. Plate tectonics moves caves around. Of course, all caves in the Earth move as the Earth moves through space, so it matters what frame of reference is selected. A spaceship is an artificial cave moving through a vacuum; an airplane is an artificial cave moving through the air; a submarine is an artificial cave moving through a liquid. Perhaps, the simplest definition is: a cave is a void with boundaries. To make this definition, we have to consider the meaning of the word “void.” The Cambridge Dictionary defines a void as: “a space with nothing in it,” giving as an example: “Some

parents use television to fill the void they have created by not spending enough time with their kids, he said.” A definition regarding gaps in time, even though time did not stop for the children; they merely did something else. Alternatively, the Cambridge Dictionary also defines void as: “a large hole or empty space,” giving as an example: “She stood at the edge of the chasm and stared into the void.” This definition regards dimensional space. Note that, despite the implication that a void has nothing in it, the chasm is air filled. The Cambridge Dictionary use of “large” is relative, and anthropogenic;

2006), so life, both on Earth and elsewhere, can be in exceptionally tiny voids. The other extreme measure of size would be the entire universe, which has a radius of 92 billion light-years (Redd, 2017). As nothing is known to exist beyond that scale dimension, the universe acts as a boundary to all it encloses, in the sense of Curl (1964), and we are all in an enormously big cave. On the Earth, cave size is determined by the structural nature of the enclosing material (usually rock) and the stresses that are placed on that rock, as explained by White (1988) in his discussion of the processes of cave breakdown. A cave on Earth can only be so big before the cave boundary (roof) fails. Not only are the materials in extraterrestrial conditions likely to be different than rocks in the Earth, the stresses under which those materials exist will also be very different than on Earth: gravity, rotational forces, temperature regime (including fluctuations and the timing of those fluctuations), photochemical and radiation effects, shock waves from impacts and *in situ* quakes, and tidal stresses. Lava tubes on the Moon are reported to be far bigger than any known on the Earth (Kaku et al., 2017), most likely as a result of the lower gravitational stresses. Otherwise, the Moon is a very Earth-like body in terms of composition, solar loading (albeit on a different time scale given the lunar day), and orbital characteristics. Lunar lava tubes indicate that the lack of an atmosphere is no impediment to cave formation. Moons like Io, which have erupting sulfur volcanoes, indicating a tube delivery system (caves) in the subsurface, are heated by tidal forces not experienced on Earth, to create a speleogenetic environment. In this case, the stresses help to make the cave, not destroy it.

Cave size has been the single most important characteristic of a cave for cavers on Earth. We want to know how big the cave is, both in terms of length, and in terms of passage size. Terms like “walking passage,” “stoop-walk,” and “crawlway” carry information on cave size, as does “dome,” “pit” and “hand-climb” in terms of vertical dimensions. Cave size depends on the specific conditions in existence at the time of cave formation, and on the history of the cave since its genesis. Furthermore, cave size will be relevant in extraterrestrial situations, only as it relates to the purpose of the mission at the time and the technology available. Missions to outer space with humans aboard are less likely than robotic missions, as the recent Mars rover work has demonstrated (Mann, 2012). The efforts of people like Bill Stone to develop technology to penetrate underground oceans on Europa are a similar robotic application. Recent work to develop probes that can penetrate the rubble of collapsed buildings for rescue purposes (e.g., Guizzo, 2011) have utilized robots of less than human size. If we are looking for life on other planets and moons, then we must be prepared to look for caves of all sizes. As well, if we are merely looking for a cave habitat that we can exist in, then the human dimension (proper caves) again becomes important, and the existence of large lava tubes on the Moon and Mars will become a focus of attention.

The dimension of size is not the only question. We are also interested in the dimension of time. When did the cave form, and how long will it last? Age and duration are, therefore, important. As with spatial dimensions, chronological dimensions also have extreme end members. How long must a cave exist to be thought a cave? Consider a bullet fired into water (Fig. 5A), the passage of the bullet into the fluid creates a void that exists for milliseconds to seconds of time. Is this void a cave? On Earth, we have caves that can form and disappear within human memory, such as caves in glacial ice, or caves in salt (Figs. 5B and C). Both ice and halite are rheids, deformable solids. Compared to caves that are millions of years old, such as Mammoth Cave, Kentucky (Palmer, 2007), ice and salt caves exist, but form and disappear in a blink of geologic time. In high altitude and high latitude regions of the earth, caves form in snow each year, and disappear each summer. If a snow cave forms and disappears in the same place each year, is it the same cave every time? Then, if a bear hibernates in it every year, is the bear in a cave? Do voids form in the frozen CO₂ polar caps on Mars; could they harbor life in frozen suspension? We keep track of many short duration events. The transuranium elements commonly have half-lives measured in seconds to milliseconds; they are formed in the laboratory. Thus, they exist and then they are gone. Transient as they are, we document them precisely. As presented earlier, if bubbles in water are caves, then they form and perhaps disappear in greater numbers and in shorter time spans than any other cave type on Earth. Bubbles in lava can be larger and exist far longer; being a bubble does not mean any obligatory size or temporal persistence. Caves are transient features; how transient depends on the scale of interest to the observer. How long can caves exist? Some of the oldest caves on Earth are in Australia, with ages going back more than 300 million years (Osborne, 2014). Lava tubes on the Moon may well be billions of

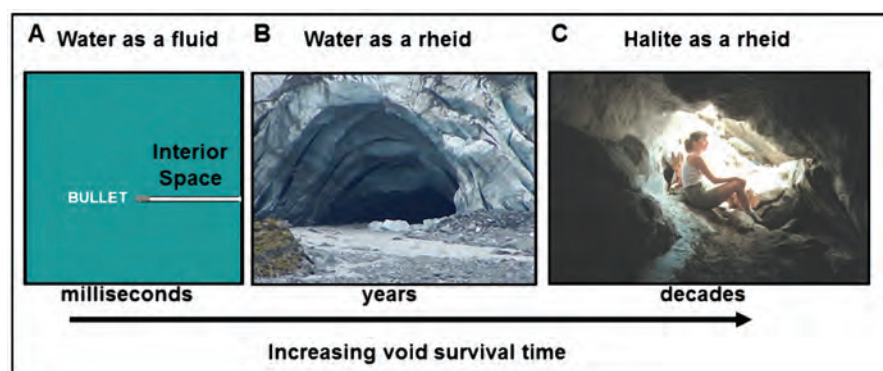


Figure 5. Examples of cave duration much shorter than average: A) A bullet fired into water creates a void that lasts milliseconds to seconds. B) Water ice is a rheid, a deformable solid, and ice caves can squeeze shut in a matter of years. C) Halite is also a rheid, and caves can squeeze shut in a matter of decades.

years old (Kaku, et al., 2017). On the scale of most major geologic processes, such as plate tectonics and evolution, caves can span the duration of those events. Planets and moons evolve through time. Some not very much, such as the Earth's moon, which displays landforms that appeared billions of years ago. Others, such as Io, are actively resurfacing. Mars in particular has undergone an aging process that resulted in cooling of the planetary interior, with loss of much of its original magnetic field and loss of much of its atmosphere. While life may not be able to exist on the surface of Mars today, it may have in the past, and caves could be a refugium for some of those organisms. That action can only occur if the caves have survived for the long transition of Mars from its original state to the conditions of today.

Cave Classification

Almost every cave scientist has tried to come up with a classification of caves. For examples, see the authors associated with the definition of a cave in the Introduction section above. This author has also played with the topic (e.g. Myloie, 1984; Myloie and White, 1992), using, in the first case, solely caves in soluble rock, and in the second case, including pseudokarst caves. Classifying caves needs to be re-thought in terms of our extraterrestrial interests. Figure 6 is such an attempt. First of all, underground voids need to be separated into natural and artificial (e.g., Parise et al., 2013). Maybe the author has read too much science fiction, but we may encounter voids on planets or moons that were created by other life forms, either as burrows by non-sentient organisms, or as purposed structures built by sentient ones (e.g., *Caves of Steel*, Asimov, 1953; this book won the 1954 Hugo Award as best book of the year, a science fiction "Oscar"). News media commonly conflates artificial and natural caves (Parise, et al., 2013). Out in space, the scientist will need to discern clearly between the two. Natural voids form in two ways. Either the void was already there, and the boundaries were placed around it, a constructional cave (Myloie and Myloie, 2013; Gradziński et al., 2018; White et al., 2018), as in a talus cave, or the boundary was already there and the void created within it; a destructional cave, as in a dissolutional cave. Figure 7 (Sweet, 1966) is a lighthearted approach to the constructional cave idea; note, it was published prior to the Apollo Moon landings. Figure 8 details the development of constructional caves in an idealized manner, subdividing the process into disordered or ordered (Figs. 8B and C, respectively). Destructional caves form by either moving the boundary material, as in fracture caves (Fig. 9A), or removing a material from within the boundary structure (Fig. 9B), by physical mass transport (e.g., suffosion caves), phase change (e.g., ice caves) or chemical processes (e.g., dissolutional caves). In all three cases, a pathway must be present to allow the material to exit to the exterior space, even if that pathway, as for dissolved material, is only a pore system millimeters in size. There are interesting extrapolations of this approach. If a gas evolves in a liquid, such as CO₂ bubbles in a carbonated beverage, the original material (the soda) has been displaced, as opposed to being removed by the gas, to create the void, analogous to the boundary movement that makes fracture caves. Are bubbles, therefore, destructional caves? While ice caves form by a phase change from solid to

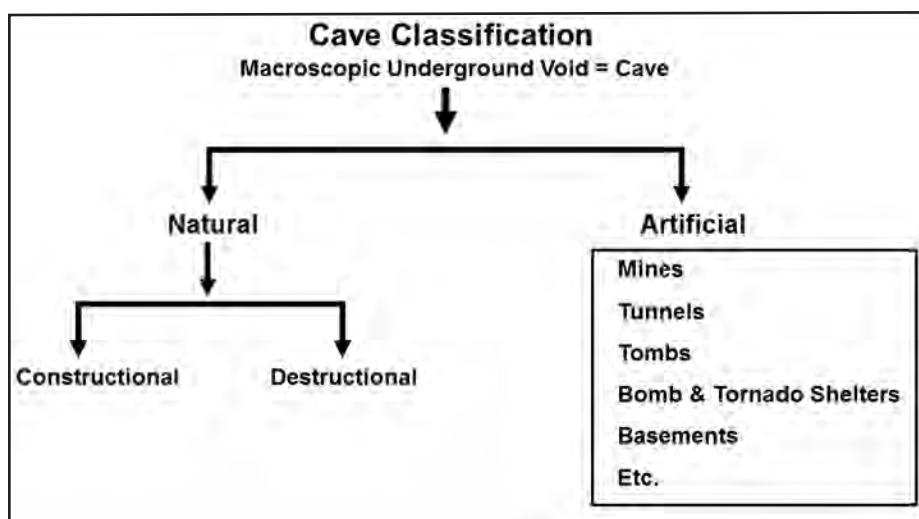


Figure 6. Simple classification of caves. In this case, a macroscopic underground void is assumed (the proper cave of Curl, 1964), such that human exploration is possible. Artificial caves smaller than humans exist, such as water pipes delivering water from the water main to a house. (See text for an explanation of constructional and destructional caves, or examine Figs. 8 and 9.)

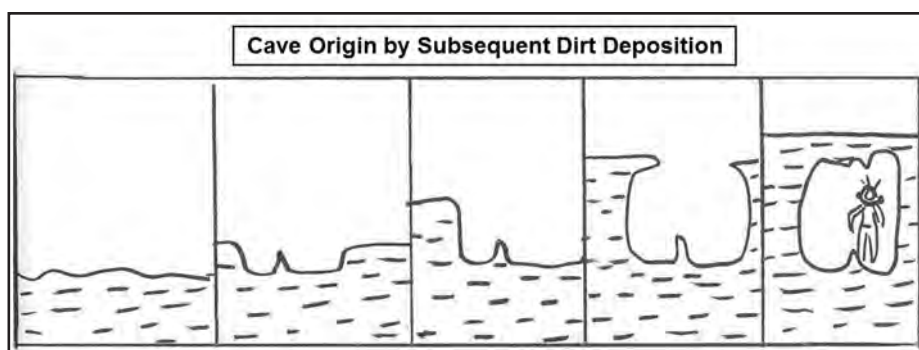


Figure 7. Cartoon of a caver's idea that a cave could be formed by building the void boundary around it, a constructional cave scenario. The cartoon was published prior to the Apollo Moon landings (Sweet, 1966).

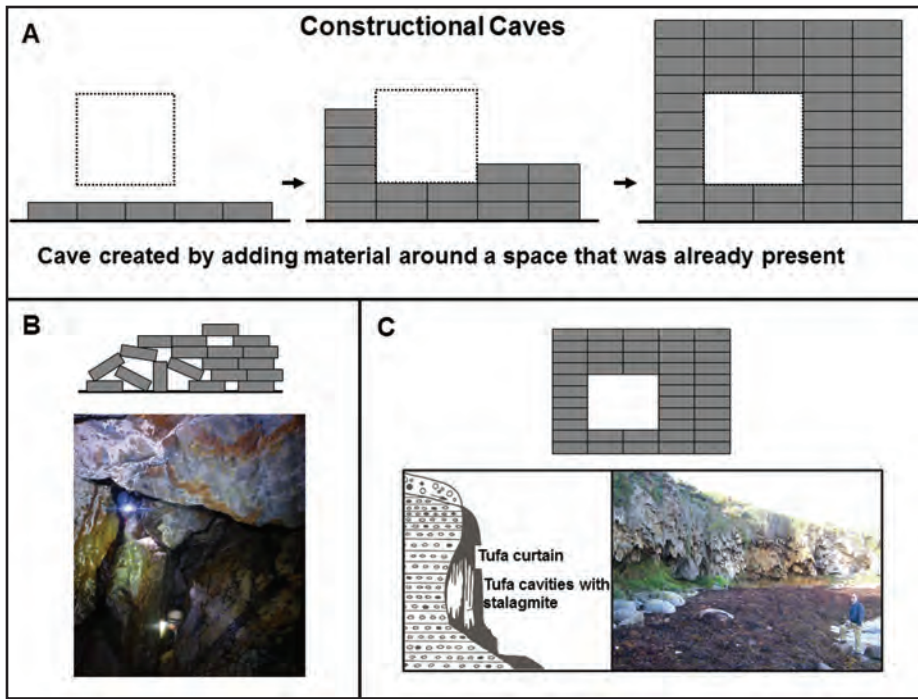


Figure 8. Constructional caves: A) Constructional caves form by building boundaries around a “pre-existing” void. In this diagram, the void is not symmetrically placed within the block to indicate that symmetry is not a requirement. B) An example of making a constructional cave by disordered application of the boundary, as in a talus cave (photo of Pittsford Cave, Vermont, courtesy of John Dunham). C) An example of making a constructional cave by ordered application of the boundary, as in a tufa cave. Diagram on the left was re-drawn from Bögli, 1980; photo on the right is a tufa curtain from the Margaret River coastal region, Western Australia.

liquid, lava tubes form in the reverse, by solidifying the boundary, while the void remains in the fluid state, and then, mass transport evacuates the fluid. Technically, the molten lava does not have to depart, the void in that case is merely fluid filled. The departure of the fluid makes exploration by humans more feasible (e.g., Fig. 4). A tectonic fissure is an example of a destructional cave; but if breakdown blocks help to roof it over, then both destructional and constructional processes have helped to make the cave (Fig. 10). Figure 10 also demonstrates some of the bias among observers. Figure 10B would be considered a cave by most cavers, but Figure 10A perhaps not, until at least the roofing stage had occurred, as seen in Figure 10C.

The point of offering this simple classification is to remind the observer that, while there are many processes that make caves, be it dissolution or pseudokarst, etc., there are only two ways to make a void: constructional and destructional. This approach makes it easier to assess voids found on other planets and moons. How

voids are made is a key step in determining the role those voids play in the landscape (or spacescape), and, perhaps if we are lucky, the local ecology.

Is it a Cave?

There are lots of arguments about what is a cave and what is not. Curl (1964) felt any underground void was a cave in a continuum of void sizes, but if humans can enter, it was a proper cave. Davies (1960) felt that if humans could not enter, it was not a cave, hence, the dilemma of Figure 1. For extraterrestrial exploration, by human or robot, the “Curl Continuum” is best to use. We cannot pick and

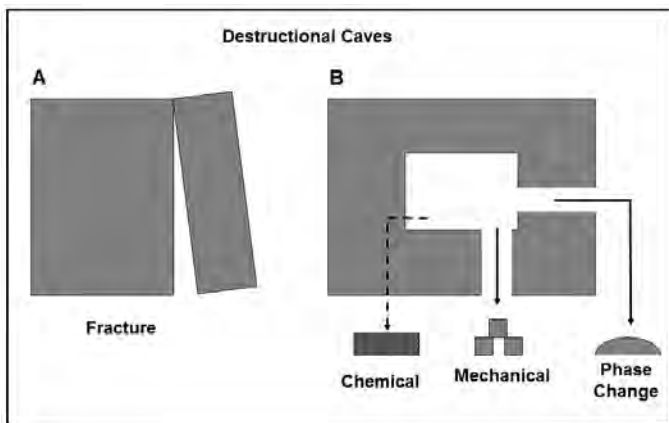


Figure 9. Destructional caves: A) Fracture of the boundary material, which requires movement or displacement to create the void (assuming we accept the Curl (1964) definition of a cave entrance as a boundary). B) Removal of boundary material by chemical mass transport, physical mass transport, or phase-change mass transport. Note that chemical diffusion of boundary material to the exterior space may utilize many especially small entrances. In both the A and B cases, the space that became the cave was not present prior to the destructional action.

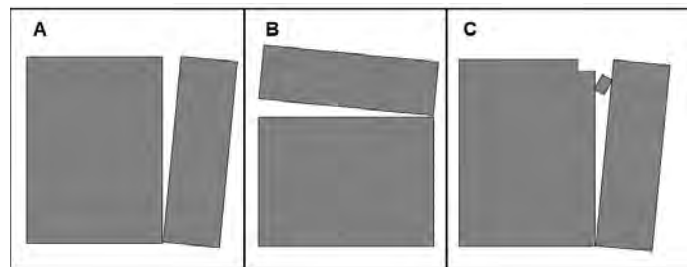


Figure 10. Three fracture cave situations: A) A vertically open fracture would be considered by many observers to lack a roof and, therefore, was not a cave. B) A 90° change in orientation creates a roof, and many would now consider the fracture to be a cave; topologically A and B are the same. C) The fracture, a destructional cave, has had a roof added by a constructional process, talus generation. Most observers who considered A not a cave would consider C to be a cave.

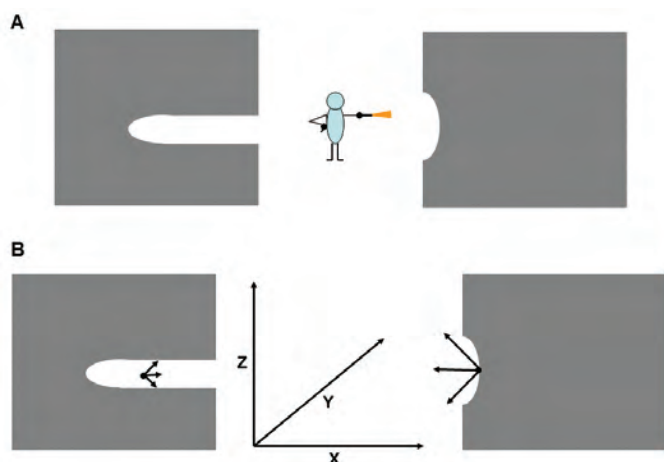


Figure 11. When is an indentation in a boundary material a cave? A) Two examples of indentations: The one on the left would be called a cave by most observers; the one on the right, is not a cave. Can this be qualified? B) Consider three axis that are mutually perpendicular. The shape of the right-hand indentation cannot keep any of the three vectors from directly reaching exterior space; however, the left-hand indentation cannot reach exterior space with any of the three vectors (the middle vector hits the cave wall between the vector and the viewer).

able to decide, at any dimensional scale? Consider Figure 11B, with three vectors at right angles to each other. If the indentation is deep enough to accept the tri-axial figure, with its origin on the centerline of the cave, and block all three axes, then it is a cave; if not, then it is not a cave. For the special case of an indentation, that is circular with a radius of unity, the point at which the axes can no longer reach the surface is also unity. This means that any dimensional scale, be it nanometers, centimeters, meters or kilometers, will work if it is the unity radius of the indentation (Fig. 12). For other geometries, such as a wide slot, it may be sufficient to say only two vectors need to be blocked from exterior space. Figure 10 is an example where both A and B are caves by the tri-axial test, utilizing only two vectors. This treatment is presented just as an example to show that we can make decisions that, while arbitrary, are still based in geometry and not human dimension.

Summary

If we consider caves to be voids within a material, then whether the void is humanly enterable is a secondary condition; dimensional scale is not the issue. Dimensional scale is important to us, and it may also be important for life forms other than on Earth, but at dimensional conditions far different than what we expect. (That could be microbial life at the small scale, yet think of the large monster in the asteroid in the Star Wars movie, *The Empire Strikes Back* at the big scale). Chronological scale is a more difficult issue; how long must a void survive to be a cave? Technically, any time at all, from milliseconds to eons. However, voids with durations approaching human life spans are best for recreational caving. In the search for extraterrestrial life, the older the cave, the better. As in some cases, the cave may be the last refuge for life if the surface above has become inhospitable. If the cave itself has also become inhospitable, it may contain evidence of past life that has been erased from the surface above. Alternatively, if life currently exists in Europa's underground oceans, then the most recent water geysers and feeder pipes (caves) would be most likely to contain active life from below; very young caves could be important.

The question of extraterrestrial caves can be broken down into five subparts:

1. How did the void form?
2. How big is it?
3. How long has it lasted?
4. What does it contain?
5. How does it connect to exterior space?

If we can answer these five questions, we may be able to assess how that cave functions as a part of an extraterrestrial landscape, and how life may have utilized the cave in the past, or still utilizes it today.

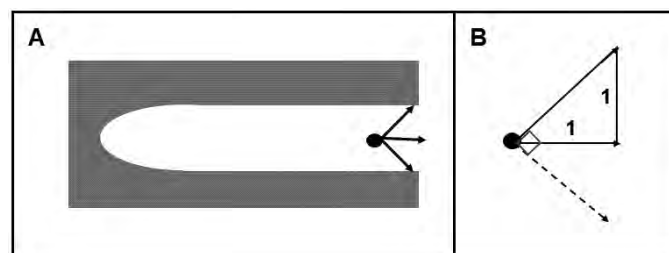


Figure 12. Quantification of cave vectors. Assume a circular cave, as in A. If the cave, which meets the vector requirement, has a radius of unity (1), then the indentation need only be as deep as that radius, as in B.

choose where life will be and how it will be. As actor Jeff Goldblum said in the movie *Jurassic Park*, "Life will find a way."

Still, it might be useful in some cases to decide about what is a cave. Many cavers have done long hikes to find a cave that the farmer says "it is back in the woods," only to find it is a shelter cave. Is it really underground? Furthermore, is it really a cave? Figure 11A offers a cave-or-not-cave situation as an example. Topologically, both openings are the same, an indentation into the side of a solid material. How can we quantify this situation to be

Acknowledgements

Many thanks to Penny Boston for getting this ball rolling, and to Diana Northup for arranging to have my PowerPoint be presented in the Extraterrestrial Caves session at the 17th ICS. The single reviewer and the editor improved the manuscript. Much gratitude to the many cavers and cave scientists who have shared ideas with me for almost five decades.

References

- Asimov, I., 1953, *Caves of Steel*: New York, Pyramid Books, 189 p.
- Bögli, A., 1980, *Karst Hydrology and Physical Speleology*: New York, Springer-Verlag, 284 p. <https://doi.org/10.1007/978-3-642-67669-7>.
- Boston, P., 2016, Extraterrestrial caves: Advanced technologies in the search, 2016 National Speleological Society Convention Program Guide, Ely Nevada, Abstracts, p. 85.
- Burger, H.R., Sheehan, A. F., Jones, C.H., 2006, *Introduction to Applied Geophysics*: New York, Norton, 600 p. Cambridge Dictionary, <https://dictionary.cambridge.org/us/dictionary/english/void>.
- Curl, R. L., 1958, A statistical theory of cave entrance evolution: *Bulletin of National Speleological Society*, v. 20, p. 9–22.
- Curl, R. L., 1964, On the definition of a cave: *Bulletin of National Speleological Society*, v. 26, no. 1, p. 1–6.
- Davies, W. E., 1960, Origin of caves in folded limestones: *Bulletin of the National Speleological Society*, v. 22, Part 1, p. 5–18.
- Ford, D.C. and Williams, P., 2007, *Karst Hydrology and Geomorphology*: Chichester, Wiley, 562 p. <https://doi.org/10.1002/9781118684986>.
- Gradziński, M., Bella, P., and Holübek, P., 2018, Constructional caves in freshwater limestone: A review of their origin, classification, significance and global occurrence: *Earth-Science Reviews*, v. 185, p. 179–201. <https://doi.org/10.1016/j.earscirev.2018.05.018>.
- Guizzo, E., 2011, Japan earthquake: More robots to the rescue: *IEEE Spectrum*. <https://spectrum.ieee.org/automaton/robotics/industrial-robots/japan-earthquake-more-robots-to-the-rescue>.
- Harris, A. 2006, Influenza virus pleiomorphy characterized by cryoelectron tomography: *Proceedings of the National Academy of Sciences*, v. 103, p. 19123–19127. <https://doi.org/10.1073/pnas.0607614103> [accessed December 20, 2017].
- Hoffman, L., 1969, *Caves of Karst*: New York, Ballantine Publishing, 224 p.
- Howard, A. D., 1960, Geology and origin of the crevice caves of the Iowa, Illinois and Wisconsin lead-zinc district: *Journal of the Yale Speleological Society*, v. 2, n. 4, Part I, p. 63.
- Kaku, T. Haruyama, J., Miyake, W., Kumamoto, A., Ishiyama, K., Nishibori, T., Yamamoto, K., Crites, S.T., Michikami, T., Yokota, Y., Sood, R., Melosh, H.J., Chappaz, L. and Howell, K.C., 2017, Detection of intact lava tubes at Marius Hills on the Moon by SELENE (Kaguya) Lunar Radar Sounder: *Geophysical Research Letters*, v. 44, no 20, p. 10,155–10,161. <https://doi.org/10.1002/2017GL074998>.
- Keary, P., Brooks, M., Hill, I., 2002, *An Introduction to Geophysical Exploration*: Oxford, Blackwell Science, 262 p.
- Klimchouk, A., 2004, Caves, in Gunn, J., ed., *Encyclopedia of Cave and Karst Science*: New York, Fitzroy Dearborn, p. 203–205.
- Lauritzen, S-E., 1983, *Arctic and Alpine Karst Symposium*: Oslo, Norway, University of Oslo, 89 p.
- Mann, A., 2012, Humans vs. robots: Who should dominate space exploration? <https://www.wired.com/2012/04/space-humans-vs-robots/>.
- Meredith, A-M and Moore, K., 2017, Conference Handbook, in *Proceedings, 17th of the International Congress of Speleology*: Penrith, Au., Australian Speleological Federation, p. 110–111.
- Mylroie, J. E., 1984, Hydrologic classification of karst landforms, in LaFleur, R., ed., *Groundwater as a Geomorphic Agent*: Boston, Allen and Unwin, p. 157–172.
- Mylroie, J. E. and White, W. B., 1992, Cave Geology. in Rea, G. T., ed., *Caving Basics*: Huntsville, Ala, National Speleological Society, p. 123–139.
- Mylroie, J.E. and Mylroie, J.R., 2013, Pseudokarst caves in the littoral environment, in Lace, M. J., and Mylroie, J. E., eds., *Coastal Karst Landforms*, Coastal Research Library 5: Dordrecht, Springer, p. 3–14.
- Neuendorf, K.K.E., Mehl, J.P., and Jackson, J.A., 2005, *Glossary of Geology*, 5th Edition: Alexandria, Va., American Geological Institute, p. 102.
- Osborne, R.A.L., 2014, Understanding the origin and evolution of Jenolan caves: The next steps, in *Proceedings of the Linnean Society of New South Wales*: Kingsford, N.S.W., Au., v. 136, p. 77–97. <https://www.biodiversitylibrary.org/item/206950#page/80/mode/1up>
- Palmer, A.N., 2007, *Cave Geology*: Dayton, Ohio, Cave Books, 454 p.
- Parise, M., Galeazzi, C., Bixio, R. and Dixon, M., 2013, Classification of artificial cavities: A first contribution by the UIS Commission, in *Proceedings of the 16th International Congress of Speleology*: Czech Republic, Brno, v 2, p. 230–235. https://artificialcavities.files.wordpress.com/2013/09/contributo-brno2013_classification.pdf
- Redd, N.T., 2017, How Big is the Universe? <https://www.space.com/24073-how-big-is-the-universe.html>.
- Sweet, K., 1966, Cave origin by subsequent dirt deposition: *MSM Spelunker*, v. 10, no. 1, p. 17. in Plummer, W.T., ed., 1966 *Speleodigest*: Vienna, Va., National Speleological Society, section. 4, p. 5.
- Varnedoe, W.W., 1973, *Alabama Caves and Caverns*: Huntsville, Ala., Privately published.
- Vlahos, J., 2007, Robot subs in space, *Popular Science*, February 2007. <https://www.popsci.com/military-aviation-space/article/2007-02/robot-subspace>. [accessed December 20, 2017]
- White, W.B., 1988, *Geomorphology and Hydrology of Limestone Terrains*: New York, Oxford, 464 p.
- White, W.B., and Culver, D.C., 2005, Cave, definition of in Culver, D.C. and White, W.B., eds., *Encyclopedia of Caves*: Burlington, Elsevier, p. 81–85.
- White, S.Q., Grimes, K.G., Mylroie, J.E., and Mylroie, J.R., 2018, The earliest time of karst cave formation: *Cave and Karst Science*, v. 45, no.1, p. 15–18.
- Wikipedia, Subterranean Fiction. https://en.wikipedia.org/wiki/Subterranean_fiction.
- ZEUS Collaboration, 2016, Limits on the effective quark radius from inclusive *ep* scattering at HERA: *Physics Letters B*, v. 757, p. 468–472. https://ac.els-cdn.com/S0370269316300776/1-s2.0-S0370269316300776-main.pdf?_tid=4bc73369-159d-4be3-aacd-0a428bd8c153&acdnat=1539695138_f0d6e06c2a9f00a3e1618989df75eb33 [accessed December 20, 2017]

RELICT DRAINAGE EFFECTS ON DISTRIBUTION AND MORPHOMETRY OF KARST DEPRESSIONS: A CASE STUDY FROM CENTRAL TAURUS (TURKEY)

Mehmet Furkan Şener¹, Muhammed Zeynel Öztürk^{1*}

Abstract

Karst depressions and relict valleys, formed as a result of the combination of karst and fluvial processes, are characteristic landforms of the Taurus karst region in Turkey. Development of these two landforms is interrelated, and the main aim of this study is to explain the role of paleovalley networks on morphometric properties of the depressions. For this purpose, in this study, spatial distribution of karst depressions and relict valleys, and morphometric properties of depressions are investigated on the Ermenek Plateau based on 1:25,000-scaled, topographic maps. About 10,000 karst depressions are mapped, 49.5 % and 50.5 % of them being located in and out of relict valleys, respectively. According to morphometric calculations, there are significant differences in dimensional properties of the two groups of depressions. Mean area, perimeter, short and long axes of relict valley depressions are 2.6, 1.6, 1.6 and 1.4 times larger, respectively, than plateau depressions. Relict valley depressions and plateau depressions are elliptical- and circular-shaped, respectively. Relict valley density has positive effect, while non-relict valley density has negative effect (limiting factor) on spatial distribution of depression density.

Introduction

Karst terrains, in which dissolution by water is the dominant geomorphic process, have distinctive hydrology, surface and subsurface landforms. Large areas of the ice-free continental area of the Earth, especially in the Northern Hemisphere and Mediterranean region, are underlain by karst (Ford and Williams, 2007; De Waele et al., 2009, 2011). Karst terrains cover about 40 % of Turkey, and the largest, most important karst terrain is the Taurus Mountains (Nazik and Poyraz, 2017). Gentle slopes of high karst plateaus are significant morphological units of the Taurus karst region, and these plateaus are highly karstified, also due to effects produced by tectonics (Klimchouk et al., 2006; Monod et al., 2006; Doğan et al., 2017; Doğan and Koçyiğit, 2018). This plateau includes many landforms such as caves, gorges, dry valleys, depressions, ponors and springs, and most of these karst landforms follow structural and orographic lineaments (Elhatip, 1997; Gunn and Günay, 2004; Öztürk et al., 2018b).

Karst depressions (doline, uvala or natural, enclosed depressions) are characteristic landforms of high, karst plateaus in the mid-latitudes and the Taurus karst region in Turkey (Gams, 2000; Öztürk et al., 2018b). Within the neritic limestones, above 2,000 m a.s.l. and low-angle plateaus create appropriate topographic conditions for formation of karst depressions (Gams, 2000; Plan and Decker, 2006; Faivre and Pahernik, 2007; Daura et al., 2014; Öztürk et al., 2015). Dry valleys without surface streams are another characteristic landform of mid-latitude high karst terrains (Warwick, 1964; Parise, 2011; Bočić et al., 2015) and Taurus karst plateaus (Nazik, 1992; Monod et al., 2006; Doğan et al., 2017). Karst valleys are called as dry valley, relict valley, ancient valley, fossil valley, solution valley, paleovalley, paleokarst valley in different studies (Fermor, 1972; Day, 1983; Doğan and Özel, 2005; Sauro, 2013). Originally, these valleys have evolved as normal valleys due to fluvial erosion in the “pre-karst phase” of surface development (Dreybrodt and Gabrovšek, 2003; Košutnik, 2007). Then, the surface drainage started to form an underground drainage network due to joints and fractures, as a result of tectonic uplift (Monod et al., 2006; Bočić et al., 2015). Therefore, the surface drainage network on the karst plateau disappeared and turned into a network of dry valleys (Bočić, 2003). Later on, it was gradually replaced by solution depressions as a result of karstification (Doğan and Özel, 2005; Bočić et al., 2015; Petrovic et al., 2016). The bottoms of these valleys are covered with elongated depressions and conical, residual hills (Monod et al., 2006; Ford and Williams, 2007; Radulović, 2013). The depressions form the most important connections between surface and underground drainage systems (Sauro, 2012). Besides, underground channels and speleological objects can be present under dry valleys (Bočić, 2003). These processes were called “reorganization of drainage by karstification” by Williams (1982).

Although karst plateaus are a variant of the fluvial, geomorphological system (Ford et al., 1988), these plateaus are characterized by a lack of surface drainage. As a result, solution depressions and relict valleys have been formed by a combination of karst and fluvial processes (Košutnik, 2007; Sauro, 2013); the development of these two landforms is strictly related (Day, 1983; Segura et al., 2007). In this study, the spatial distribution of karst depressions and relict valleys, and the effects of relict valleys on depression morphometry are investigated on the Ermenek Plateau, based on GIS tools. The main aims of this study are: (1) to determine the spatial distribution of karst depressions with respect

¹Department of Geography, Faculty of Arts and Sciences, Niğde Ömer Halisdemir University, Niğde, Turkey

*Corresponding Author: muhammed.zeynel@gmail.com

to relict and non-relict valleys; (2) to explain the relationships between spatial distributions of these; and (3) to explain the effects of a relict valley on morphometric properties of depressions.

Study Area

The Ermenek Plateau is one of the most characteristic plateaus of the Taurus Mountains, which form a continuous karst belt across the southern part of Turkey; the study area covers 1,584 km² of the plateau surface (Fig. 1). Mean elevation of study area is 1,707 m a.s.l., and there are many summits over 2,000 m a.s.l. at the northern part of the area. The plateau surface is eroded by many rivers (Oğuzun, Balkusan, Akerik and Gündür rivers), which run in a NW-SE direction, therefore, parallel to the Göksu River (Fig. 1c). These rivers have incised more than 100 m and the slopes are more than 30° steep. For example, the Balkusan River, located on the southern part of the plateau, incised ca. 300

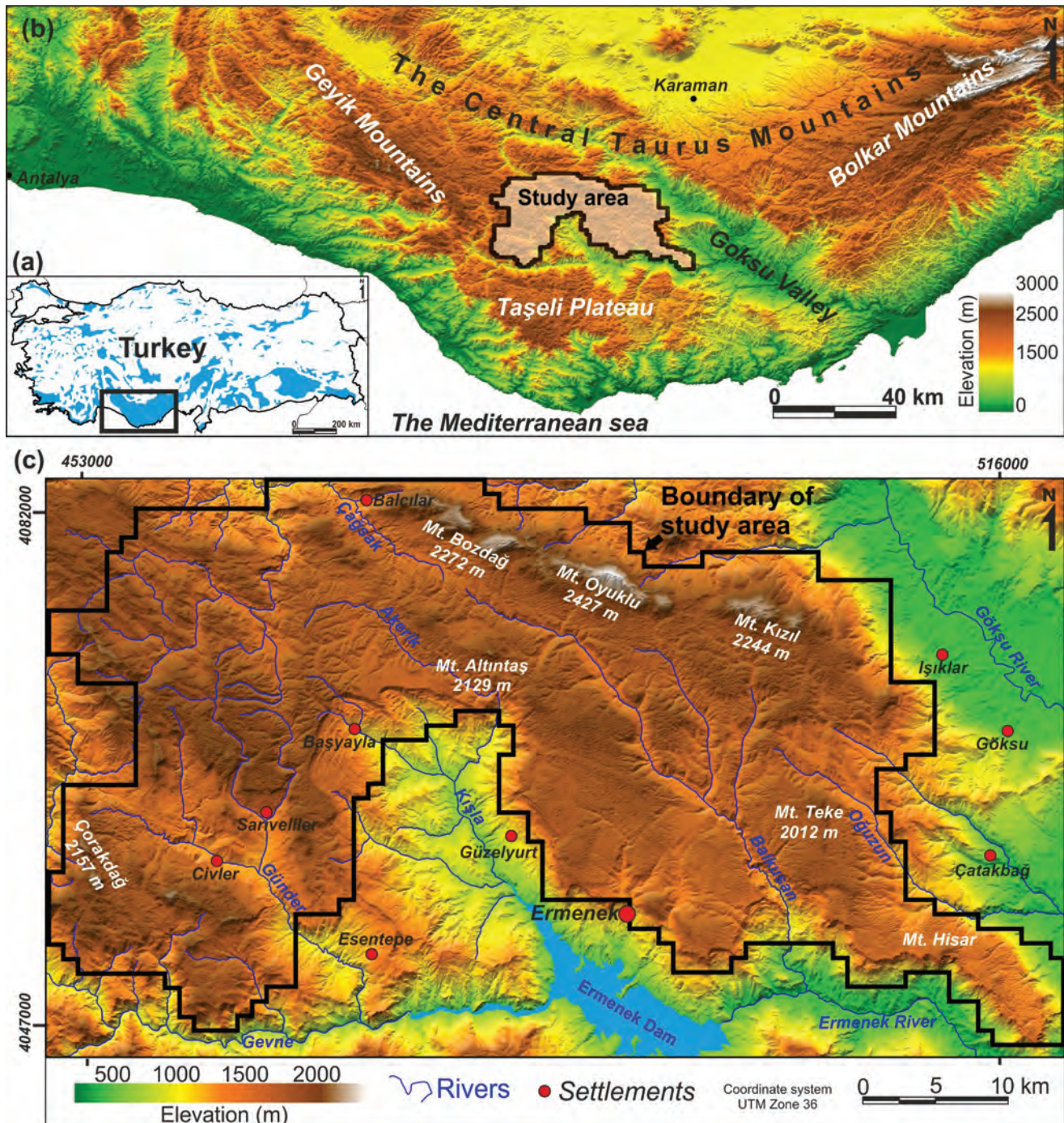


Figure 1. (a) Outcrops of carbonate rocks in Turkey (Nazik and Tuncer, 2010), (b) the Central Taurus Mountains and location of the study area, (c) digital elevation model of study area (black line shows boundary of study area).

m and the river side slopes are up to 50° steep. The eastern and southern boundaries of plateaus are limited by steep slopes (Fig. 3a). According to the Ermenek Meteorology Station (at 1,267 m a.s.l.), the mean annual temperature is 11.6 °C, and mean annual precipitation is 667 mm.

The study area mostly consists of neritic limestones, carbonates, and clastic rocks that were deposited in Mut-Ermenek Basin (Fig. 2, 3). This basin is one of several, small Cenozoic basins in the southern part of Turkey (Şafak et al., 2005; Janson et al., 2010). The basin was formed as a result of orogeny collapse in the extensional back arc regime of the Cyprus arc to the south (Robertson, 2000). The basin was inundated by the sea in the Early Miocene, and jointly covered with an extensive, thick succession of late Burdigalian to Serravalian carbonates, including reef and platform limestones. The NW-SE, NE-SW, and E-W directed fault systems developed in basins that are related to the orogenic collapse (Esirtgen et al., 2016). The study area is mainly comprised of the Burdigalian-Serravalian limestones in the Ermenek Basin, represented by the Mut Formation (Gedik et al., 1979). This consists of limestones, but also contains sandstone, conglomerate, and marl bands. The white, cream-colored limestones contain micro and macro fossils, such as algae, foraminifera, echinid, lamellibranch, gastropod and coral (Özkale et al., 2007). The reef limestones are characterized by organisms of warm, clear and shallow marine environments. Besides, NW-SE, NE-SW, and E-W-directed fault systems cut the Miocene marine sequences, as well (Esirtgen et al., 2016).

Method

Morphometric analysis of karst landforms is a useful tool for evaluation of karst areas (Jennings, 1975; Day, 1983; Bondesan et al., 1992; Bruno et al., 2008; Basso et al., 2013; Öztürk et al., 2017, 2018a). These morphometric analyses enable us to develop a hypotheses on the evolution and dynamics of karst systems (Jeanpert et al., 2016), and to classify karst landforms (Aguilar et al., 2016). In this study, morphometric properties of karst depressions in relict valleys and on the pla-

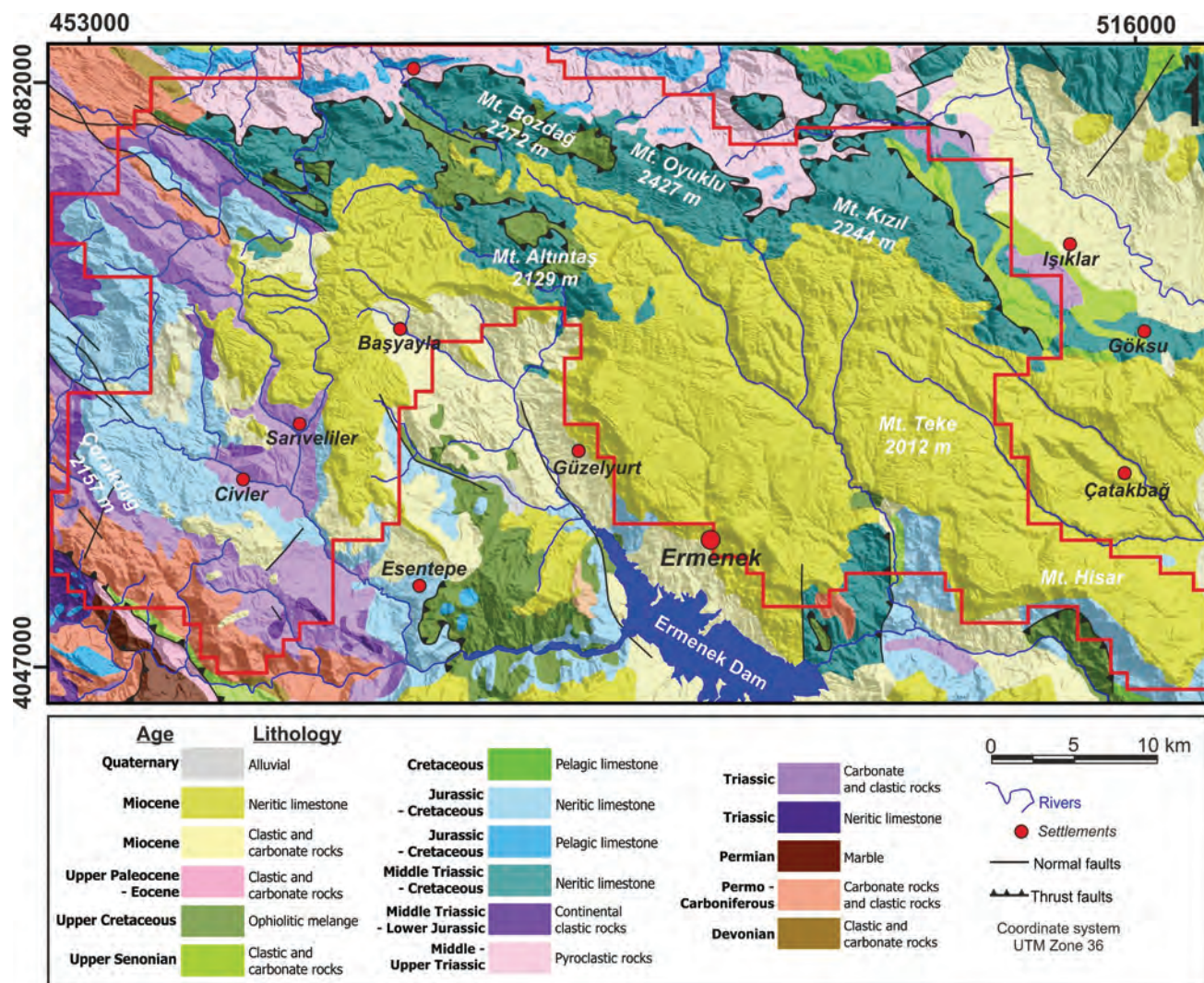


Figure 2. Geological map of study area (arranged from Şener, 2002a, 2002b. Red line shows boundary of study area).

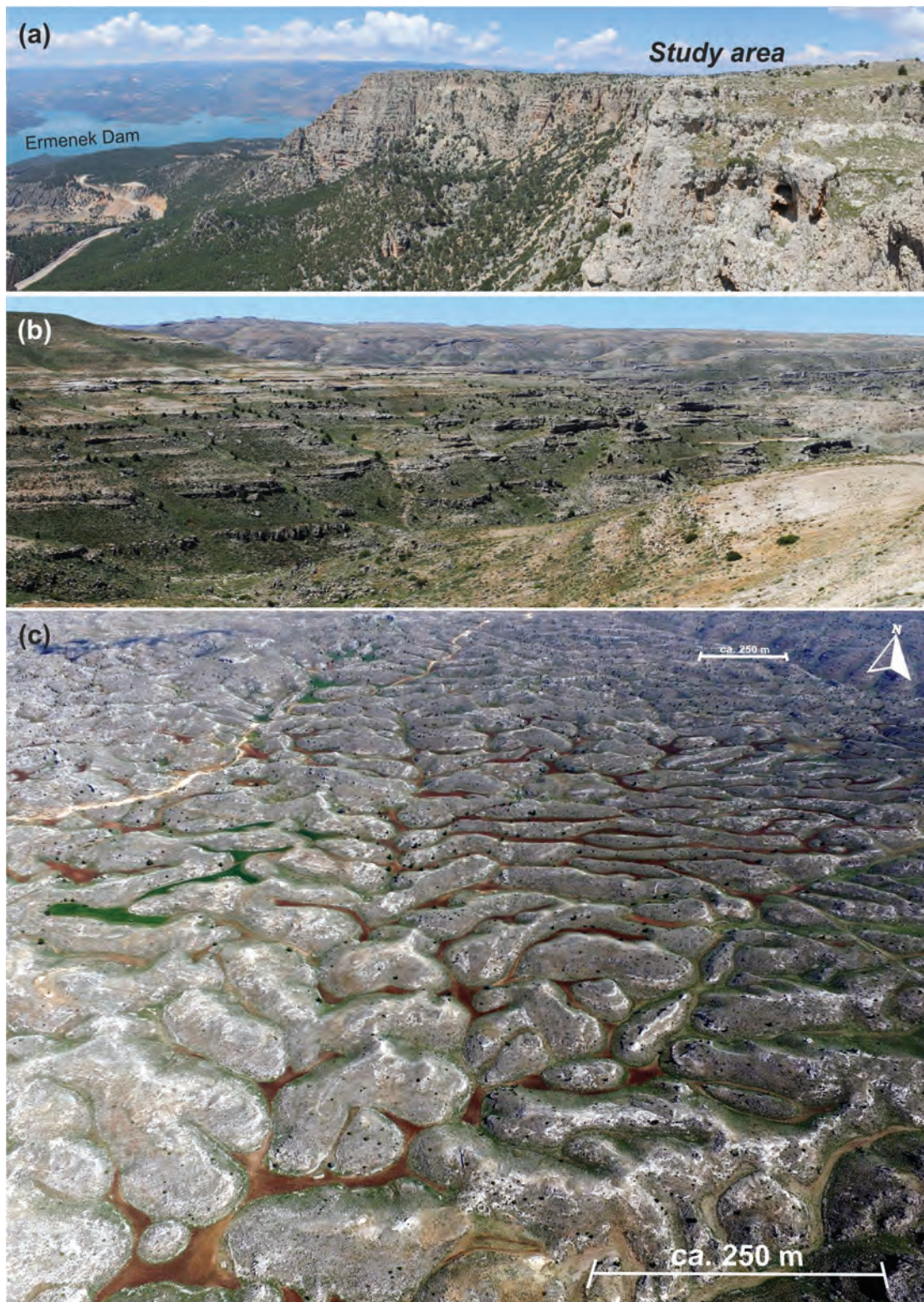


Figure 3. (a) Steep slopes at the southern parts of the plateaus, (b) the Miocene neritic limestone layers and (c) drone image of plateau surface.

depressions were drawn manually. Depressions are used as a sensitive indicator for tectonic activity in a karst region, and azimuth orientation of the doline long axes provides important clues about their joint systems (Day, 1983; Nazik, 1986; Pardo-Igúzquiza et al., 2013; Pepe and Parise, 2014; Jeanpert et al., 2016; Öztürk et al., 2017, 2018a). Therefore, the orientation angles of depressions were calculated as an azimuth of the long axis within the depression, and rose diagrams were created for the two depression groups.

teau surface (outside of relict valleys) are investigated. Topographic maps (UTM zone 36), 1:25,000-scale, produced by The General Command of Mapping (Turkey), were used to determine the distribution of karst depressions, relict and non-relict valleys on the plateau (Day, 1983; Denizman, 2003; Applegate, 2003; Angel et al., 2004; Florea, 2005; Faivre and Pahernik, 2007; Telbisz et al., 2009; Benac et al., 2013; Bočić et al., 2015; Keskin and Yılmaz, 2016; Iovine et al., 2016; Margiotta et al., 2016; Parise et al., 2018). The uppermost, closed-contour lines of karst depressions on topographic maps (classical method) were delineated as polygons in a GIS, and basic morphometric properties (area, perimeter, long axis, short axis, elongation ratio and circularity index) were calculated. Elevation values of the depression were determined from topographic maps, with reference to uppermost, closed-counter values.

The long axis (a line connecting the two farthest points) and short axis of depressions

The drainage network was divided into two categories: relict and non-relict valleys. Relict valleys developed due to karst denudation processes from the primary valley morphology (Bočić et al., 2015). Other valleys are recognized as non-relict valleys. In other words, if the valleys have depressions at their thalwegs, they are classified as relict, otherwise as non-relict valleys. Relict and non-relict valleys were determined by vectorization of the theoretical thalwegs (Bočić et al., 2015). Then, the depressions, which are located in and outside of relict valleys, were determined using GIS analyses (Fig. 4). The data sets were examined in 1 km × 1 km quadrants to determine spatial densities of depression, relict and non-relict valleys, and the relationships between them (Pahernik, 2012; Bočić et al., 2015). Besides, minimum, 5 %, 25 %, average, 75 %, 95 % and maximum values are calculated for evaluation of morphometric elevation characteristics of depressions (Öztürk et al., 2018b).

Results

The uppermost, closed-contour lines of 9,934 depressions were digitized as polygons in a GIS framework, and the areal properties of the polygons were calculated. In a 1,584 km² area, 9,934 depressions were mapped between 1,215 and 2,375 m a.s.l. The morphometric parameters are presented in Table 1. The highest percent of depressions is observed between 1,850 and 1,950 m a.s.l. (~40 %), with maximum depression density of 75

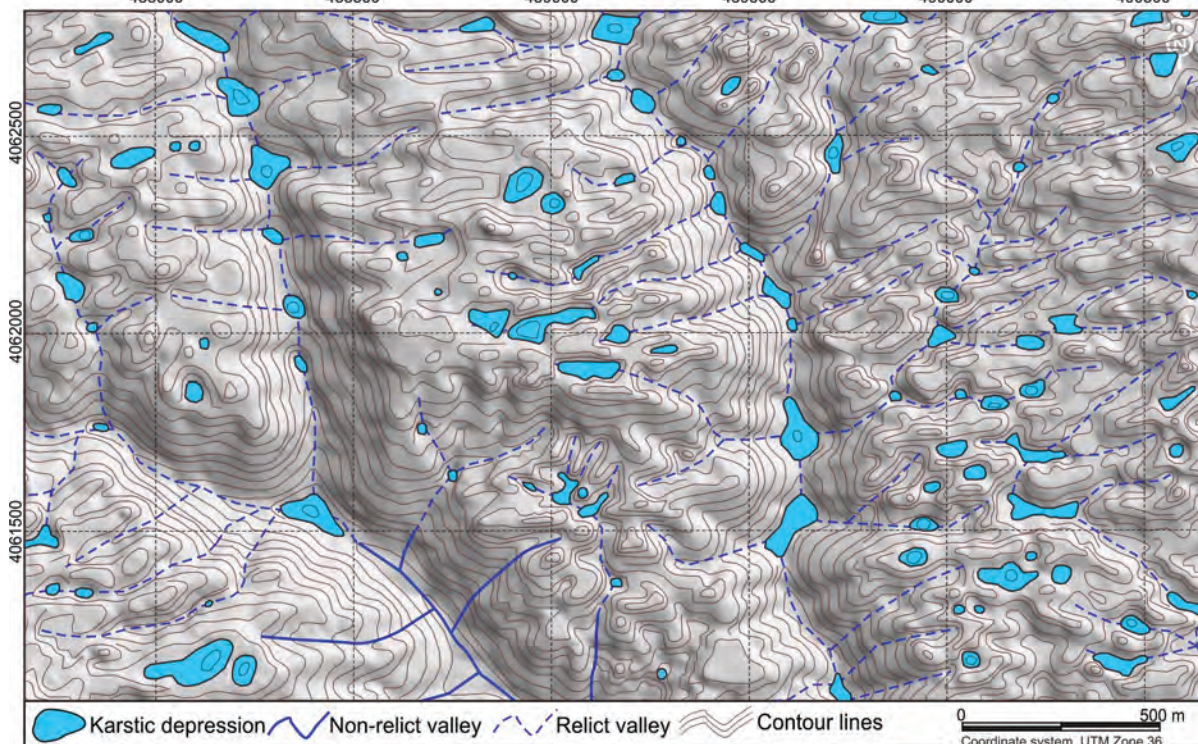


Figure 4. Examples of relict and non-relict valleys (contour interval is 10 m).

depressions/km² between these elevations. According to classification of depression density by Faivre and Pahernik (2007), 65.1 % of the study area is characterized by low density (<10 depressions/km²), 33.4 % with moderate density (10–40 depressions/km²), 0.34 % with high density (40–70 depressions/km²) and only 0.03 % with very high density (>70 depressions/km²; Fig. 5). Spatial distribution of depression density is parallel to the main river direction, due to plateau surface being eroded by rivers in the NW-SE direction. Depression density increases with distance from the main rivers (Fig. 5).

Relict valley density increases at the central parts of the plateau. It is greater than three km/km² over 1,150 m a.s.l., with maximum density (8.5 km/km²) between 1,750 and 1,900 m a.s.l. Non-relict valley density reaches 11 km/km² on the plateau surface, and a negative correlation is observed between the distribution of relict and non-relict valley densities ($r = -65$; Fig. 6a, c).

Relict and non-relict drainage density has two effects on the distribution of depression density: While relict drainage density has a positive effect, non-relict drainage density has a negative effect (limiting factor) on the spatial distribution of depression density. A positive correlation is observed between depression density and relict drainage density ($r = 0.6$), while a negative correlation ($r = -0.5$) is observed between depression density and non-relict drainage density (Fig. 6b, d).

Solution depressions can be found both on the plateau surface (or on interfluvium) and in the relict valleys. Thus, depressions are divided into two groups: (1) relict valley depressions and (2) plateau surface depression in this study. Inside and outside of relict valleys, 4,917 (49.5 %) and 5,017 (50.5 %) depressions are located, respectively. These per-

Table 1. Basic statistics of relict valley and plateau depressions.

Statistical Measure	Relict valley depressions (5,017)					Plateau depressions (4,917)									
	Elevation (m)	Area (m ²)	Perimeter (m)	Short axis (m)	Long axis (m)	Elongation ratio	Circularity index	Statistical Measure	Elevation (m)	Area (m ²)	Perimeter (m)	Short axis (m)	Long axis (m)	Elongation ratio	Circularity index
Minimum	1,240	61	30	6	10	1.00	1.02	Minimum	1,215	44	27	6	9	1.00	1.01
5 %	1,700	213	55	14	19	1.05	1.06	5 %	1,680	152	47	13	16	1.04	1.06
25 %	1,790	507	85	21	31	1.25	1.11	25 %	1,800	319	68	18	24	1.18	1.09
Mean	1,856	4,027	210	42	78	1.75	1.38	Mean	1,873	1,547	129	31	48	1.51	1.21
Median	1,855	1,141	131	31	49	1.50	1.18	Median	1,880	605	93	24	34	1.35	1.14
75 %	1,920	3,109	232	49	90	1.97	1.39	75 %	1,940	1,473	149	36	56	1.67	1.22
95 %	2,020	14,551	629	108	234	3.24	2.38	95 %	2,050	5,866	333	71	128	2.50	1.65
Maximum	2,265	818,389	6,992	921	1,889	10.90	14.06	Maximum	2,375	64,069	1,306	281	441	6.75	4.06
Stand. dev.	107	17,314	284	40	90	0.8	0.6	Stand. dev.	120	3,040	108	21	41	0.5	0.2

centages provide perfect conditions for statistical analysis of the morphometric properties of the two depression groups.

There is no significant difference in the distribution, while there are significant differences in the dimensional properties of the two groups. The minimum values of the two groups are similar. Strong, positive correlations are observed between perimeter and area, short and long axes, elongation ratio and circularity index in the two groups. Generally, the values are larger for the relict valley depressions than for the plateau depressions: mean area by 2.6, perimeter by 1.6, short axes by 1.6 and long axes by 1.4 times. Standard deviations of the relict valley depressions are higher than for those of the plateau depressions (Table 1). As a result, relict valley depressions and plateau depressions are elliptical and circular-shaped, respectively (Fig. 8a and d). These differences resulted from the enlargements of the relict valley depressions. Besides, solution pits and conical or tower-shaped residual hills are observed in relict valley depressions (Figs. 8b and c).

The long axes orientations of the depression are used as an indicator for the direction of tectonic structures, and these orientations provide important clues about the fracture systems (Pepe and Parise). As shown in Figure 9, dominant directions are ENE-WSW and WNW-ESE for both depression types, which are in accordance with the tectonic evolution of the study area.

These results indicate that relict valley density is one of the most important factors to determine the spatial distribution of depression density on the Ermenek Plateau. Depression density reaches its maximum in a well-developed, relict-valley network on the neritic limestones. The relict valley depressions are more elongated, whilst the plateau depressions are more circular.

Discussion

Dry valley and karst depressions have been investigated for a long time (Reid, 1887; Warwick, 1964; Fermor, 1972; Day, 1983; Jennings, 1982), due to their important role in interpretation of morphotectonic development of karst surfaces, as well as their hydrological role in response to rainfall (Parise, 2003). Especially, relict and dry valleys are used for paleodrainage reconstructions (Bočić, 2003; Monod et al., 2006; Petrovic et al., 2016; Doğan et al., 2017), and a few studies explain the relationship between both (Williams, 1972; Jennings, 1975; Bočić et al., 2015).

In this study, the spatial distribution of karst depressions and relict valleys, and the effects of relict valley depression morphometry are investigated on the Ermenek Plateau. Non-relict valley density is a limiting factor for depression density. When non-relict valley density increases, depression densities decline (Fermor, 1972; Öztürk et al., 2017). Because of this correlation, depression density is greatest at maximum distances from non-relict valleys.

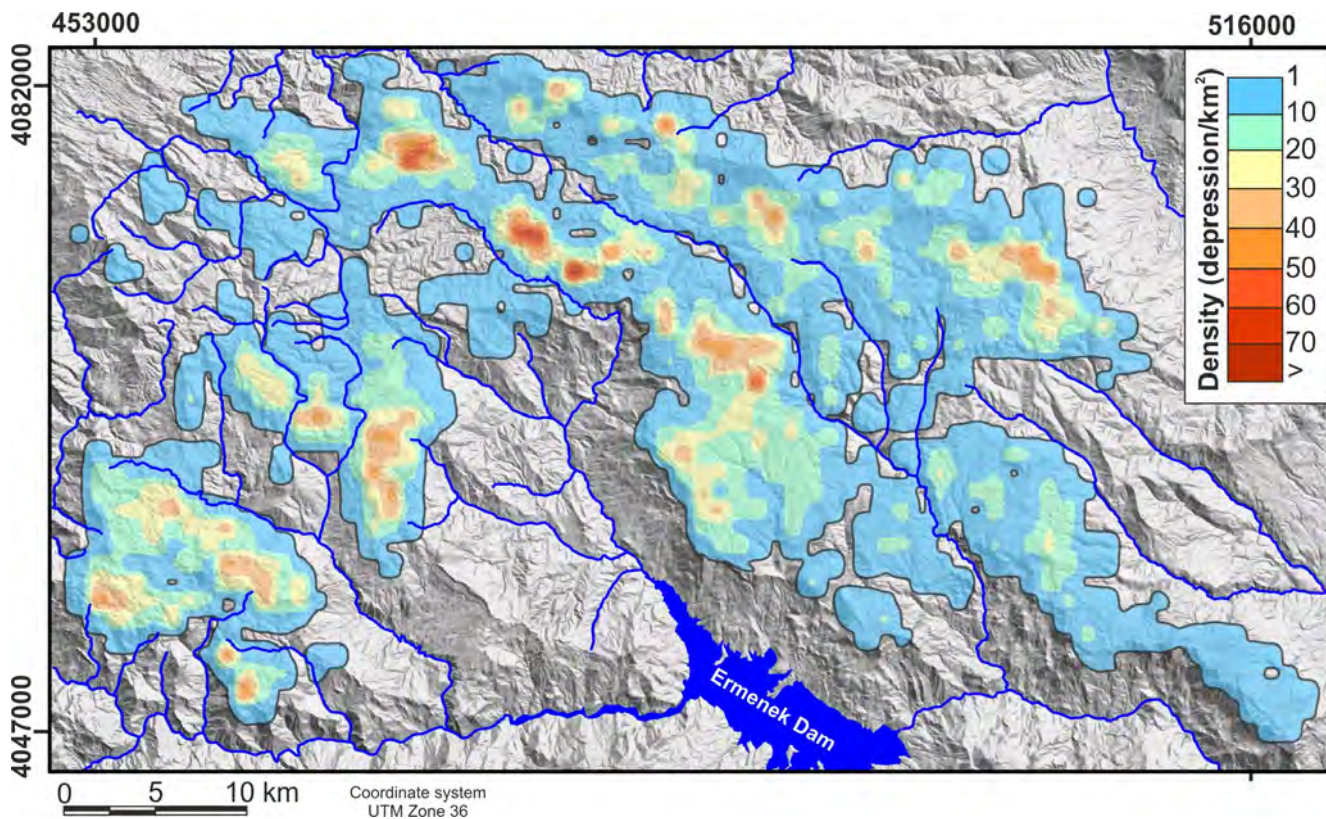


Figure 5. Spatial distribution of depression density.

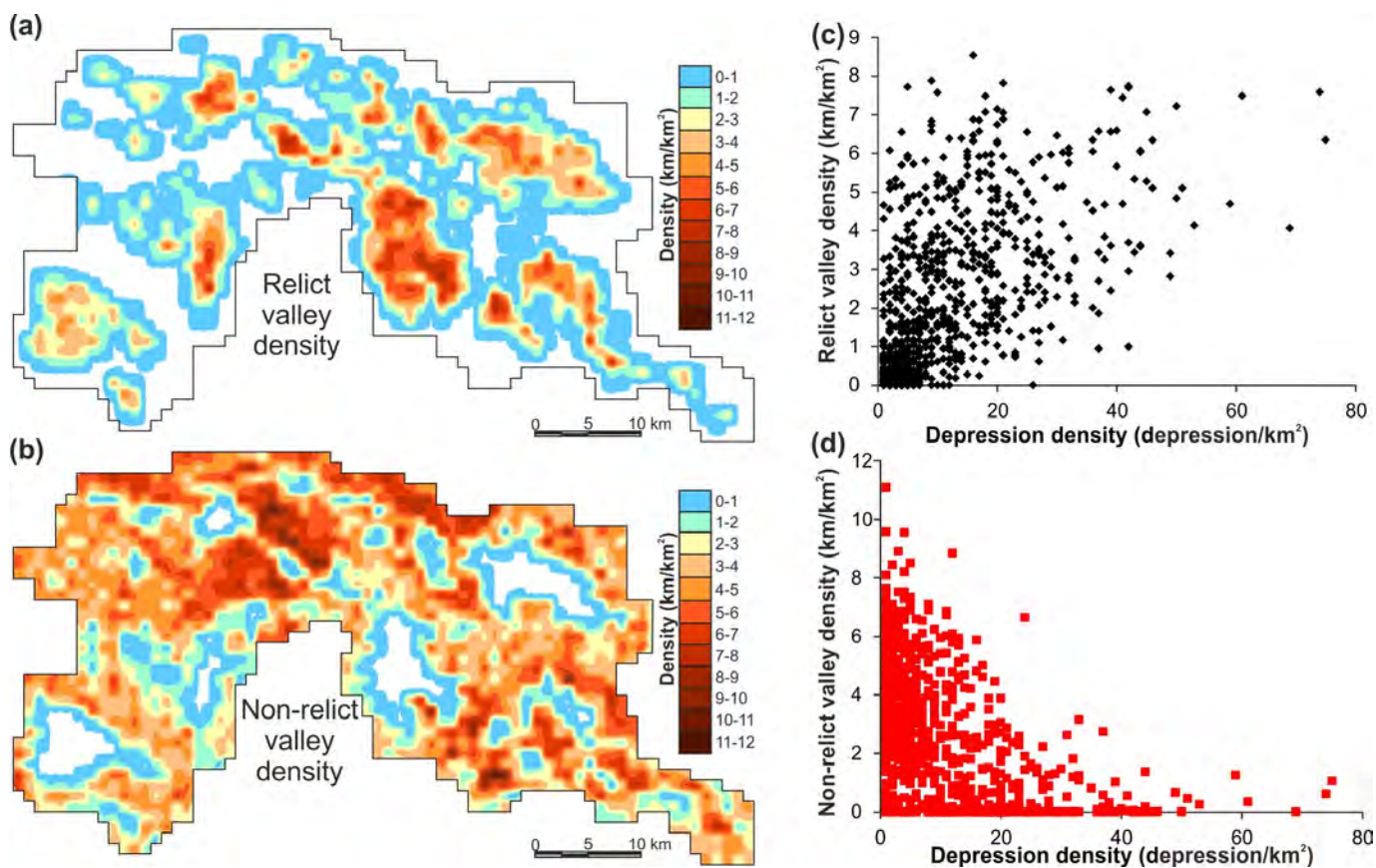


Figure 6. Spatial distribution of (a) relict valley density, (b) correlations between depression density and relict valley density, (c) non-relict valley density and (d) correlations between depression density and non-relict valley density.

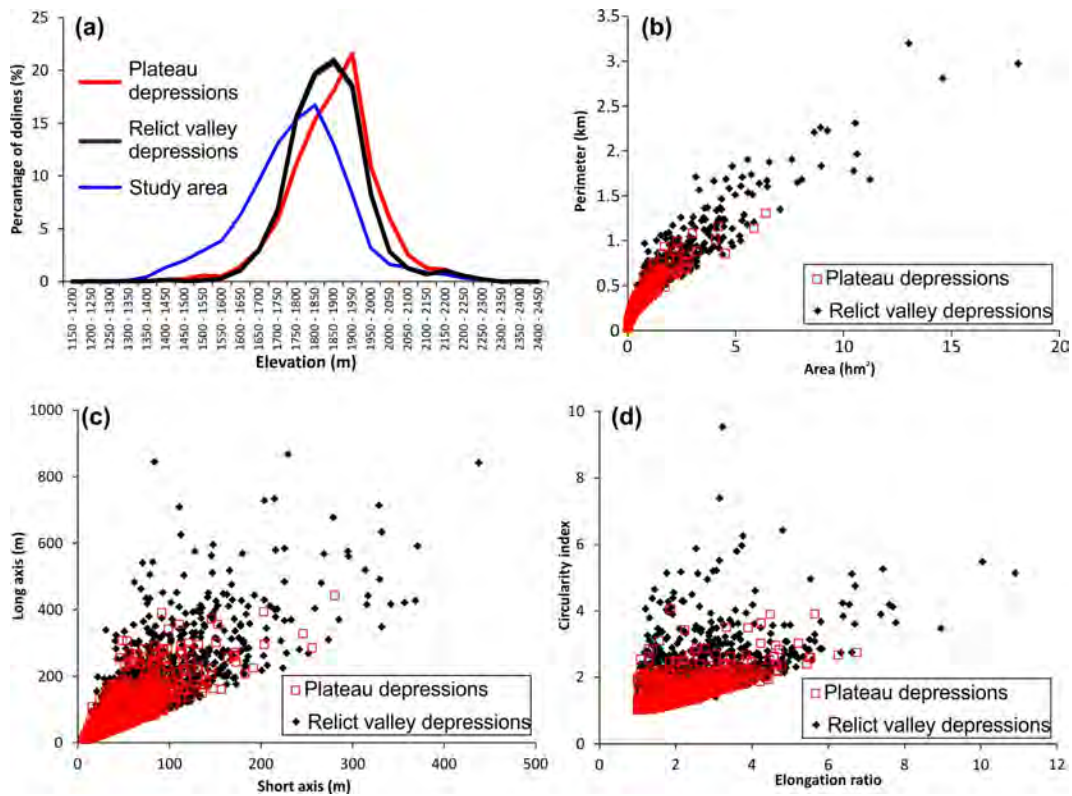


Figure 7. (a) Change of depression elevation and relationships between (b) perimeter and area, (c) long and short axis, (d) circularity index and elongation ratios (maximum values of relict valley depressions are not shown in figure 7b).

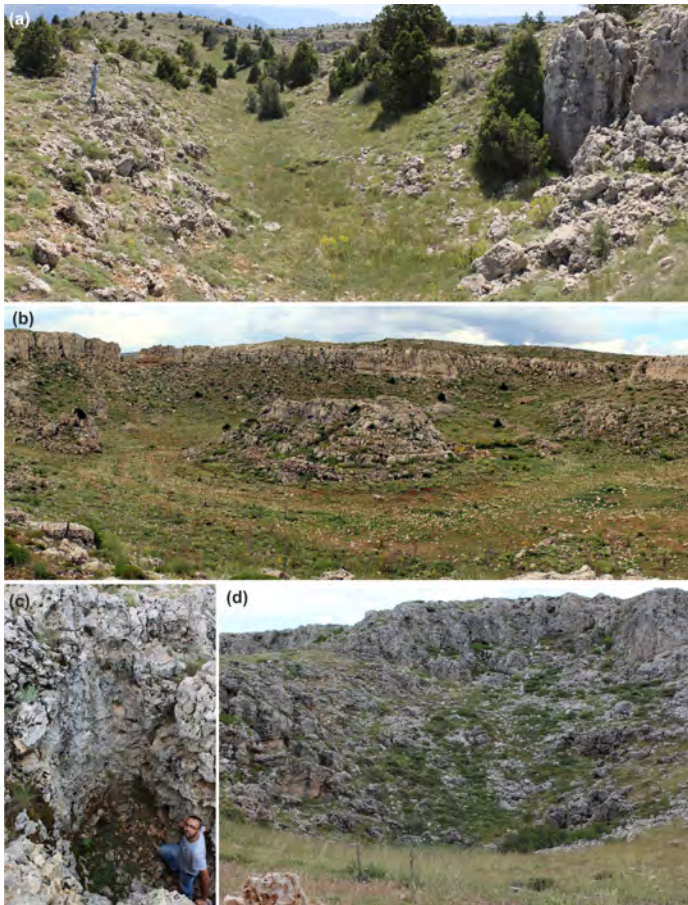


Figure 8. Depressions types on plateau: (a) elongated relict valley depression, (b) residual hill in relict valley depression, (c) solution pit in relict valley depression and (d) circular plateau depression.

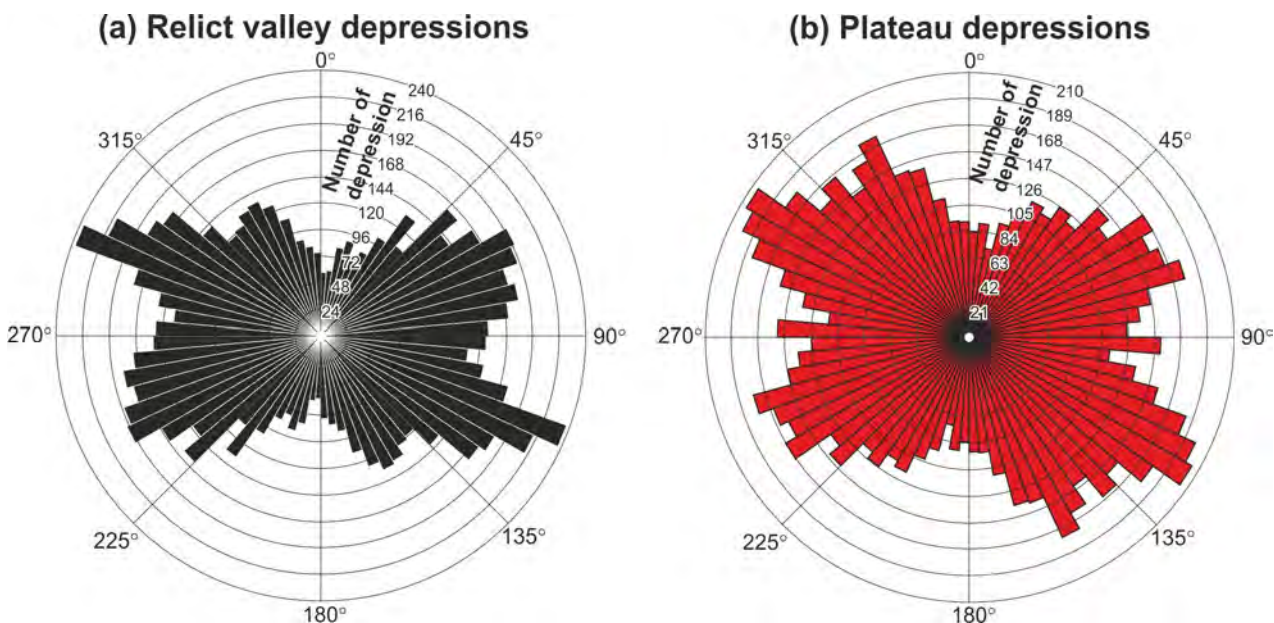


Figure 9. Rose diagrams for the long axis of (a) relict valley depressions and (b) plateau depression.

Statistically, relict valley depressions have complex shape and larger area than plateau depressions. Similarly, length, width and depth of valley depressions are greater than plateau depressions in New Zealand (Jennings, 1975). This situation results from hydrological properties of the two groups. Since karst depression is a hydrological form (Sauro, 2012) and each depression has its own catchment area (drainage basin) (Gunn, 1981; Ford and Williams, 2007). Thus, closed-solution depressions have the same function in karst landscapes as valley depressions in fluvial landscapes (Williams, 1972; Gutiérrez et al., 2014). While relict valley depressions have large basins, and they can be found to join points of more than one paleovalley tributary and joint system. Plateau depressions have small basins. In other words, while plateau depressions located at low paleovalley order (generally one), relict valley depressions have high paleovalley order (Day, 1983). Thus, valley depressions are exposed to accelerated solution. Most of the water of the valley slopes is conveyed in the lower part of the depression, in contrast to plateau depressions (Sauro, 2013). As a result, depressions in relict valleys start to enlarge and lose to circular shape (Doğan and Özel, 2005).

Conclusions

In this study, the spatial distribution of karst depressions and relict valleys, and relict valley effects on depression morphometry are investigated on the Ermenek Plateau, based on 1:25,000-scaled topographic maps. Depressions totaling 9,934 were mapped. Out of these, 4,917 and 5,017 depressions are located inside and outside of relict valleys, respectively. Mean area, perimeter, short and long axes of relict valley depressions are significantly larger than the plateau depressions. Besides, standard deviations of relict valley depressions are higher than plateau depressions. As a result, while relict valley depressions are elongated, plateau depressions are circular in shape. These situations result from hydrological differences between two depression groups. Relict drainage density has positive effects, while non-relict drainage density has negative effects (limiting factors) on spatial distribution of depression density. Dominant orientations of both depressions are ENE-WSW and WNW-ESE, and these orientations are in harmony with tectonic directions of the study area. According to these results, both landforms are impressed by the same tectonic evolution, and geomorphologic development of depressions are associated with paleodrainage patterns.

Acknowledgements

This study was supported by the Scientific and Technological Research Council of Turkey (TUBITAK) (Project no: 115Y580). We express our sincere thanks for their financial support. We also thank to Dr. Mesut Şimşek and Mustafa Utlu.

References

- Aguilar, Y., Bautista, F., Mendoza, M.E., Frausto, O., and Ihl, T., 2016. Density of karst depressions in Yucatán state, Mexico: *Journal of Cave and Karst Studies*, v. 78, p. 51–60. <https://doi.org/10.4311/2015ES0124>.
- Angel, J.C., Nelson, D.O., and Panno, S.V., 2004. Comparison of a new GIS-based technique and a manual method for determining sinkhole density: An example from Illinois' sinkhole plain: *Journal of Cave and Karst Studies*, v. 66, p. 9–17.

- Applegate, P., 2003, Detection of sinkholes developed on shaly Ordovician limestones, Hamilton County, Ohio, using digital topographic data: Dependence of topographic expression of sinkholes on scale, contour interval, and slope: *Journal of Cave and Karst Studies*, v. 65, p. 126–129. <https://caves.org/pub/journal/PDF/V65/v65n2-Applegate.pdf>.
- Basso, A., Bruno, E., Parise, M., and Pepe, M., 2013, Morphometric analysis of sinkholes in a karst coastal area of southern Apulia (Italy): *Environmental Earth Sciences*, v. 70, p. 2545–2559. <https://doi.org/10.1007/s12665-013-2297-z>.
- Benac, Č., Juračić, M., Matićec, D., Ružić, I., and Pikelj, K., 2013, Fluvio-karst and classical karst: Examples from the Dinarics (Krk Island, Northern Adriatic, Croatia): *Geomorphology*, v. 184, p. 64–73. <https://doi.org/10.1016/j.geomorph.2012.11.016>.
- Bočić, N., 2003, Relation between Karst and Fluvio-karst Relief on the Slunj Plateau (Croatia): *Acta Carsologica*, v. 32. <https://doi.org/10.3986/AC.V32I2.343>.
- Bočić, N., Pahernik, M., and Mihevc, A., 2015, Geomorphological significance of the palaeodrainage network on a karst plateau: The Una-Korana plateau, Dinaric karst, Croatia: *Geomorphology*, v. 247, p. 55–65. <https://doi.org/10.1016/j.geomorph.2015.01.028>.
- Bondesan, A., Meneghel, M., and Sauro, U., 1992, Morphometric analysis of dolines: *International Journal of Speleology*, v. 21.
- Bruno, E., Calcaterra, D., and Parise, M., 2008, Development and morphometry of sinkholes in coastal plains of Apulia, southern Italy. Preliminary sinkhole susceptibility assessment: *Engineering Geology*, v. 99, p. 198–209. <https://doi.org/10.1016/j.enggeo.2007.11.017>.
- Daura, J., Sanz, M., Josep Forn S.J., Asensio, A., and Julia, R., 2014, Karst evolution of the Garraf Massif (Barcelona, Spain): doline formation, chronology and archaeo-palaeontological archives: *Journal of Cave and Karst Studies*, v. 76, p. 69–87. <https://doi.org/10.4311/2011ES0254>.
- Day, M., 1983, Doline morphology and development in Barbados: *Annals of the Association of American Geographers*, v. 73, p. 206–219. <https://doi.org/10.1111/j.1467-8306.1983.tb01408.x>.
- De Waele, J., Gutiérrez, F., Parise, M., and Plan, L., 2011, Geomorphology and natural hazards in karst areas: A review: *Geomorphology*, v. 134, p. 1–8. <https://doi.org/10.1016/j.geomorph.2011.08.001>.
- De Waele, J., Plan, L., and Audra, P., 2009, Recent developments in surface and subsurface karst geomorphology: An introduction: *Geomorphology*, v. 106, p. 1–8. <https://doi.org/10.1016/j.geomorph.2008.09.023>.
- Denizman, C., 2003, Morphometric and spatial distribution parameters of karstic depressions, Lower Suwannee River Basin, Florida: *Journal of Cave and Karst Studies*, v. 65, p. 29–35.
- Doğan, U., and Koçyiğit, A., 2018, Morphotectonic evolution of Maviboğaz canyon and Suğla polje, SW central Anatolia, Turkey: *Geomorphology*, v. 306, p. 13–27. <https://doi.org/10.1016/j.geomorph.2018.01.001>.
- Doğan, U., Koçyiğit, A., and Gökkaya, E., 2017, Development of the Kembos and Eynif structural poljes: Morphotectonic evolution of the Upper Manavgat River basin, central Taurides, Turkey: *Geomorphology*, v. 278, p. 105–120. <https://doi.org/10.1016/j.geomorph.2016.10.030>.
- Doğan, U., and Özel, S., 2005, Gypsum karst and its evolution east of Hafik (Sivas, Turkey): *Geomorphology*, v. 71, p. 373–388. <https://doi.org/10.1016/j.geomorph.2005.04.009>.
- Dreybrodt, W., and Gabrovšek, F., 2003, Basic processes and mechanisms governing the evolution of karst: *Speleogenesis and Evolution of Karst Aquifers*, v. 1, p. 1–25.
- Elhatip, H., 1997, The influence of karst features on environmental studies in Turkey: *Environmental Geology*, v. 31, p. 27–33. <https://doi.org/10.1007/s002540050160>.
- Esirtgen, T., Ilgar, A., Bozkurt, B., and Demirkaya, S., 2016, Structural development of Oligo–Miocene basins in Central Taurides, in 69th Geological Congress of Turkey, Ankara, p. 8–9.
- Faivre, S., and Pahernik, M., 2007, Structural influences on the spatial distribution of dolines, Island of Brač, Croatia: *Zeitschrift für Geomorphologie*, v. 51, p. 487–503. <https://doi.org/10.1127/0372-8854/2007/0051-0487>.
- Fermor, J., 1972, The dry valleys of Barbados: A critical review of their pattern and origin: *Transactions of the Institute of British Geographers*, p. 153–165. <https://doi.org/10.2307/621559>.
- Florea, L., 2005, Using state-wide GIS data to identify the coincidence between sinkholes and geologic structure: *Journal of Cave and Karst Studies*, v. 67, p. 120–124.
- Ford, D.C., Palmer, A.N., and White, W.B., 1988, Landform development; karst, in Back, W., Rosenshein, J.S., and Seaber, P.R., eds., *Hydrogeology (The geology of North America)*, Geological Society of America, p. 401–412.
- Ford, D., and Williams, P., 2007, *Karst Hydrogeology and Geomorphology: West Sussex, England*, John Wiley & Sons Ltd. <https://doi.org/10.1002/9781118684986>.
- Gams, I., 2000, Doline morphogenetic processes from global and local viewpoints: *Acta Carsologica*, v. 29, p. 123–138.
- Gedik, A., Birgili, Ş., Yılmaz, H., and Yoldaş, R., 1979, Mut-Ermenek-Silifke yöresinin jeolojisi ve petrol olanakları: *Bulletin of the Geological Society of Turkey*, v. 22, p. 7–26.
- Gunn, J., 1981, Hydrological processes in karst depressions: *Z. Geomorph.*, (N. F.), v. 25, p. 313–331.
- Gunn, J., and Günay, G., 2004, Turkey, in Gunn, J., ed., *Encyclopedia of Caves and Karst Science*, Taylor and Francis Group, p. 1583–1589. <https://doi.org/10.4324/9780203483855>.
- Gutiérrez, F., Parise, M., De Waele, J., and Jourde, H., 2014, A review on natural and human-induced geohazards and impacts in karst: *Earth-Science Reviews*, v. 138, p. 61–88. <https://doi.org/10.1016/j.earscirev.2014.08.002>.
- Iovine, G., Vennari, C., Gariano, S.L., Caloiero, T., Lanza, G., Nicolino, N., Suriano, S., Ferraro, G., and Parise, M., 2016, The “Piano dell’Acqua” sinkholes (San Basile, Northern Calabria, Italy): *Bulletin of Engineering Geology and the Environment*, v. 75, p. 37–52. <https://doi.org/10.1007/s10064-015-0737-6>.
- Janson, X., Van Buchem, F.S.P., Dromart, G., Eichenseer, H.T., Dellamonica, X., Boichard, R., Bonnaffe, F., and Eberli, G., 2010, Architecture and facies differentiation within a Middle Miocene carbonate platform, Ermenek, Mut Basin, southern Turkey: *Geological Society, London, Special Publications*, v. 329, p. 265–290. <https://doi.org/10.1144/SP329.11>.
- Jeanperré, J., Genthon, P., Maurizot, P., Folio, J.-L., Vendé-Leclerc, M., Sérino, J., Join, J.-L., and Iseppi, M., 2016, Morphology and distribution of dolines on ultramafic rocks from airborne LiDAR data: the case of southern Grande Terre in New Caledonia (SW Pacific): *Earth Surface Processes and Landforms*, v. 41, p. 1854–1868. <https://doi.org/10.1002/esp.3952>.
- Jennings, J.N., 1975, Doline morphometry as a morphogenetic tool: New Zealand examples: *New Zealand Geographer*, v. 31, p. 6–28. <https://doi.org/10.1111/j.1745-7939.1975.tb00793.x>.
- Jennings, J.N., 1982, Quaternary complications in fluvio-karst at Coleman Plain, N.S.W.: *Australian Geographer*, v. 15, p. 137–147. <https://doi.org/10.1080/00049188208702809>.
- Keskin, İ., and Yılmaz, I., 2016, Morphometric and geological features of karstic depressions in gypsum (Sivas, Turkey): *Environmental Earth Sciences*, v. 75, p. 1040. <https://doi.org/10.1007/s12665-016-5845-5>.

- Klimchouk, A., Bayari, S., Nazik, L., and Törk, K., 2006, Glacial destruction of cave systems in high mountains, with a special reference to the Aladaglar massif, Central Taurus, Turkey: *Acta Carsologica*, v. 35, p. 111–121, <http://carsologica.zrc-sazu.si/downloads/352/klimchouk.pdf> (accessed September 2017).
- Košutnik, U.J., 2007, Questions of dry valleys in karst: Case study of Mali dol, Kras (Slovenia): *Acta Carsologica*, v. 36, p. 425–431. <https://doi.org/10.3986/ac.v36i3.176>.
- Margiotta, S., Negri, S., Parise, M., and Quarta, T.A.M., 2016, Karst geosites at risk of collapse: the sinkholes at Nociglia (Apulia, SE Italy): *Environmental Earth Sciences*, v. 75, p. 8. <https://doi.org/10.1007/s12665-015-4848-y>.
- Monod, O., Kuzucuoglu, C., and Okay, A., 2006, A Miocene palaeovalley network in the Western Taurus (Turkey): *Turkish Journal of Earth Sciences*, v. 15, p. 1–23.
- Nazik, L., 1992, Beyşehir Gölü Güneybatısı ile Kemboş Polyesi Arasının Karst Jeomorfolojisi: İstanbul Üniversitesi, 298 p.
- Nazik, L., 1986, Beyşehir Gölü yakın güneyi karst jeomorfolojisi ve karstik parametrelerin incelenmesi: *Jeomorfoloji Dergisi*, v. 14, p. 65–77.
- Nazik, L., and Poyraz, M., 2017, Türkiye karst jeomorfolojisi genelini karakterize eden bir bölge: Orta Anadolu Platoları karst kuşağı: *Türk Coğrafya Dergisi*, p. 43–43. <https://doi.org/10.17211/tcd.300414>.
- Nazik, L., and Tuncer, K., 2010, Türkiye karst morfolojisinin bölgesel özellikleri: *Türk Speleoloji Dergisi*, v. 1, p. 7–19.
- Özkale, O., Yetiş, C., and İbilioğlu, D., 2007, Stratigraphy of the Kozlar (Mut-Mersin) area: *Çukurova University Journal of the Faculty of Engineering and Architecture*, v. 22, p. 261–273.
- Öztürk, M.Z., Şener, M.F., Şener, M., and Şimşek, M., 2018, Structural controls on distribution of dolines on Mount Anamas (Taurus Mountains, Turkey): *Geomorphology*. <https://doi.org/10.1016/j.geomorph.2018.05.023>.
- Öztürk, M.Z., Şimşek, M., Şener, M.F., and Utlu, M., 2018, GIS based analysis of doline density on Taurus Mountains, Turkey: *Environmental Earth Sciences*. <https://doi.org/10.1007/s12665-018-7717-7>.
- Öztürk, M.Z., Şimşek, M., and Utlu, M., 2015, Tahtalı Dağları (Orta Toroslar) karst platosu üzerinde dolin ve uvala gelişiminin CBS tabanlı analizi: *Türk Coğrafya Dergisi*, v. 65, p. 59–68. <https://doi.org/10.17211/tcd.22648>.
- Öztürk, M.Z., Şimşek, M., Utlu, M., and Şener, M.F., 2017, Karstic depressions on Bolkar Mountain plateau, Central Taurus (Turkey): Distribution characteristics and tectonic effect on orientation: *Turkish Journal of Earth Sciences*, v. 26, p. 302–313. <https://doi.org/10.3906/yer-1702-3>.
- Pahernik, M., 2012, Spatial density of dolines in the Croatian Territory: *Croatian Geographical Bulletin*, v. 74, p. 5–26.
- Pardo-Igúzquiza, E., Durán, J.J., and Dowd, P.A., 2013, Automatic detection and delineation of karst terrain depressions and its application in geomorphological mapping and morphometric analysis: *Acta Carsologica*, v. 42, p. 17–24. <http://doi.org/10.3986/ac.v42i1.637>.
- Parise, M., 2003, Flood history in the karst environment of Castellana-Grotte (Apulia, southern Italy): *Natural Hazards and Earth System Science*, v. 3, p. 593–604. <https://doi.org/10.5194/nhess-3-593-2003>.
- Parise, M., 2011, Surface and subsurface karst geomorphology in the Murge (Apulia, Southern Italy): *Acta Carsologica*, v. 40, p. 79–93. <https://doi.org/10.3986/ac.v40i1.30>.
- Parise, M., Pisano, L., and Vennari, C., 2018, Sinkhole clusters after heavy rainstorms: *Journal of Cave and Karst Studies*, v. 80, p. 83–82. <https://doi.org/10.4311/2017ES0105>.
- Pepe, M., and Parise, M., 2014, Structural control on development of karst landscape in the Salento Peninsula (Apulia, SE Italy): *Acta Carsologica*, v. 43, p. 101–114. <https://doi.org/10.3986/ac.v43i1.643>.
- Petrovic, A.S., Calic, J., and Gajovic, V., 2016, Paleodrainage network reconstruction on Miroč Mt. (eastern Serbia): *Revista de Geomorfologie*, v. 18, p. 59–65.
- Plan, L., and Decker, K., 2006, Quantitative karst morphology of the Hochschwab plateau, Eastern Alps, Austria: *Zeitschrift für Geomorphologie Supplementband*, v. 147, p. 29–54.
- Radulović, M.M., 2013, A new view on karst genesis: Carbonates and evaporites, v. 28, p. 383–397.
- Reid, C., 1887, On the origin of dry Chalk Valleys and of Coombe Rock: *Quarterly Journal of the Geological Society*, v. 43, p. 364–373. <https://doi.org/10.1144/GSL.JGS.1887.043.01-04.29>.
- Robertson, A.H.F., 2000, Mesozoic-Tertiary Tectonic-Sedimentary Evolution of a South Tethyan oceanic basin and its margins in Southern Turkey: *Geological Society, London, Special Publications*, v. 173, p. 97–138. <https://doi.org/10.1144/GSL.SP.2000.173.01.05>.
- Şafak, Ü., Gökçen, N.S., and Gürbüz, K., 2005, The mid-Cenozoic succession and evolution of the Mut basin, southern Turkey, and its regional significance: *Sedimentary Geology*, v. 173, p. 121–150. <https://doi.org/10.1016/j.sedgeo.2004.03.012>.
- Sauro, U., 2012, Closed depression in karst area, in White, W. and Culver, D., eds., *Encyclopedia of Caves*, Academic Press, p. 140–155.
- Sauro, U., 2013, Landforms of mountainous karst in the middle latitudes: reflections, trends and research problems: *Acta Carsologica*, v. 42, p. 5–16. <https://doi.org/10.3986/ac.v42i1.629>.
- Segura, F.S., Pardo-Pascual, J.E., Rosselló, V.M., Fornós, J., and Gelabert, B., 2007, Morphometric indices as indicators of tectonic, fluvial and karst processes in calcareous drainage basins, South Menorca Island, Spain: *Earth Surface Processes and Landforms*, v. 32, p. 1928–1946. <https://doi.org/10.1002/esp.1506>.
- Şenel, M., 2002a, 1/500000 scaled geology map of Turkey, Adana sheet: General Directorate of Mineral Research and Exploration.
- Şenel, M., 2002b, 1/500000 scaled geology map of Turkey, Konya sheet: Ankara, Mineral Research and Exploration Institute.
- Telbisz, T., Dragušica, D., and Nagy, B., 2009, Doline morphometric analysis and karst morphology of Biokovo Mt (Croatia) based on field observations and digital terrain analysis: *Hrvatski Geografski Glasnik*, v. 71, p. 5–22.
- Warwick, T.G., 1964, Dry valleys of the Southern Pennines, England: *Erdkunde*, v. 18, p. 116–123. <https://doi.org/10.3112/erdkunde.1964.02.07>.
- Williams, P., 1982, Karst landforms in New Zealand, in Soons, J. and Selby, M.J., eds., *Landforms of New Zealand*, p. 187–209.
- Williams, P., 1972, Morphometric analysis of polygonal karst in New Guinea: *Geological Society of America Bulletin*, v. 83, p. 761–796. [https://doi.org/10.1130/0016-7606\(1972\)83\[761:MAOPKI\]2.0.CO;2](https://doi.org/10.1130/0016-7606(1972)83[761:MAOPKI]2.0.CO;2).

FORMATION MECHANISMS FOR THE LARGEST SANDSTONE SINKHOLE IN OHIO

Joshua A. Novello¹ and Ira D. Sasowsky²

Abstract

Sinkholes formed in sandstone are not common, but are known in locations worldwide. A mechanical origin (i.e. jointing/slumping) for such features is usually invoked and related to the development of crevice caves. Some researchers have inferred a contribution of dissolution processes to the formation of such caves. In northeast Ohio, there are Pennsylvanian age sandstone/conglomerate-capped hills containing small cave systems; sinkholes serve as entrances in some of these. This study investigates the origin of the largest known of these sinkholes—an eight-meter deep, near-vertical pit on the east flank of Little Mountain (Geauga County, Ohio). Structure-From-Motion photogrammetry models the feature for morphometric analysis, using computer and 3-D printed models. Rock and sediment samples were collected to evaluate disaggregation of the bedrock. Adjoining blocks and joints were mapped to place geometric constraints on potential formation mechanisms. The surface opening is a rough, irregular quadrilateral, about 3.8 m by 6.2 m, and is overhung on three sides. The walls are roughly coincident with joints without distinct fracture surfaces. The floor is sandy and has a few large sandstone boulders apparently emplaced by collapse. At several locations, the walls are spalling off in 3 to 10 centimeter-thick sheets or blocks. Joint-controlled cave passages, some with flowing water, lead into and out of the sinkhole. There is significant variability of induration between samples collected from the host rock. Some samples were poorly indurated, indicating ongoing weathering. The geometry of the sinkhole and adjacent blocks, both in map and vertical perspective, shows that the feature could not have formed solely by simple translation (sliding) of blocks. The overhanging, upper portions do not fit back together if opposite walls of the sinkhole are brought together. Additionally, the major joint to the east of the sinkhole is continuously aligned, which is inconsistent with major motion of the eastern sinkhole wall mass. This sinkhole likely formed and continues to grow through a variety of processes including mechanical joint widening, fluvial erosion, and arenization—cement dissolution, granular disintegration of bedrock and grain transport. Such processes should be considered when evaluating creation of sinkholes in a variety of settings.

Introduction

Sinkholes are common landforms in karst terrains developed on limestone or evaporites, often in association with extensive cave and subterranean drainage systems. Dissolution of soluble bedrock in the presence of undersaturated water is the major cause of sinkhole formation (Gutiérrez et al., 2014). The growth of such features in sandstone is much rarer and has been attributed to the mechanical processes of jointing and slumping, where block displacement produces gaps in the bedrock. Although jointing and slumping are common in northeastern Ohio, several features observed at the sinkhole in this study seem inconsistent with a wholly mechanical genesis via this mechanism. Cement dissolution and granular disintegration of the bedrock may contribute to sinkhole formation; these are explored as possible mechanisms.

Little Mountain, 39 km northeast of Cleveland in Lake and Geauga Counties, Ohio, is a knob, ranging in elevation from 365 m to 385 m above sea level (Fig. 1). To the northwest, a plain grades lakeward to an elevation of 174 m, where it meets Lake Erie (USGS-NGTOC, 2016). Dissected by streams, the region was glaciated by the Wisconsinan, Illinoian and an unknown number of previous ice sheets (Fig. 1 and Ohio Division of Geological Survey, 2005). The knob is composed of Pennsylvanian Sharon Conglomerate, the basal formation of the Pottsville Group, which unconformably overlies the Mississippian Cuyahoga Formation (Stout, 1944). Little Mountain was formerly developed as a resort with hotels, cottages and club houses (Pierson, 1892). The property is currently owned by The Holden Arboretum, as well as some private landowners.

Geomorphology of Little Mountain is similar to “rock cities” described in many localities. Joints, widened into crevices, separate rock blocks resembling streets and buildings in urban settings (Migoñ et al., 2017). One such set of crevices in Geauga County is accompanied by a cave system (Fig. 2), Little Mountain Caverns, with a number of sinkholes serving as entrances. The largest of these sinkholes (Figs. 3-A, 3-B, and 3-D) is about 6.2 m long, 3.8 m wide, 8 m deep, tapers to the north, and is the focus of this study. An uneven sinkhole floor is covered in breakdown and sand. Trees at the surface contribute significant leaf litter, and the canopy is visible from the sinkhole floor. The curved walls are covered in thick moss, through which white quartz pebbles and cross stratification remain visible in the bedrock. At the surface, the

¹Dept. of Geosciences, University of Akron, Akron, Ohio 44325-4101 USA, Jan90@zips.uakron.edu

²Dept. of Geosciences & Center for Environmental Studies, University of Akron, Akron, Ohio 44325-4101 USA, ids@uakron.edu

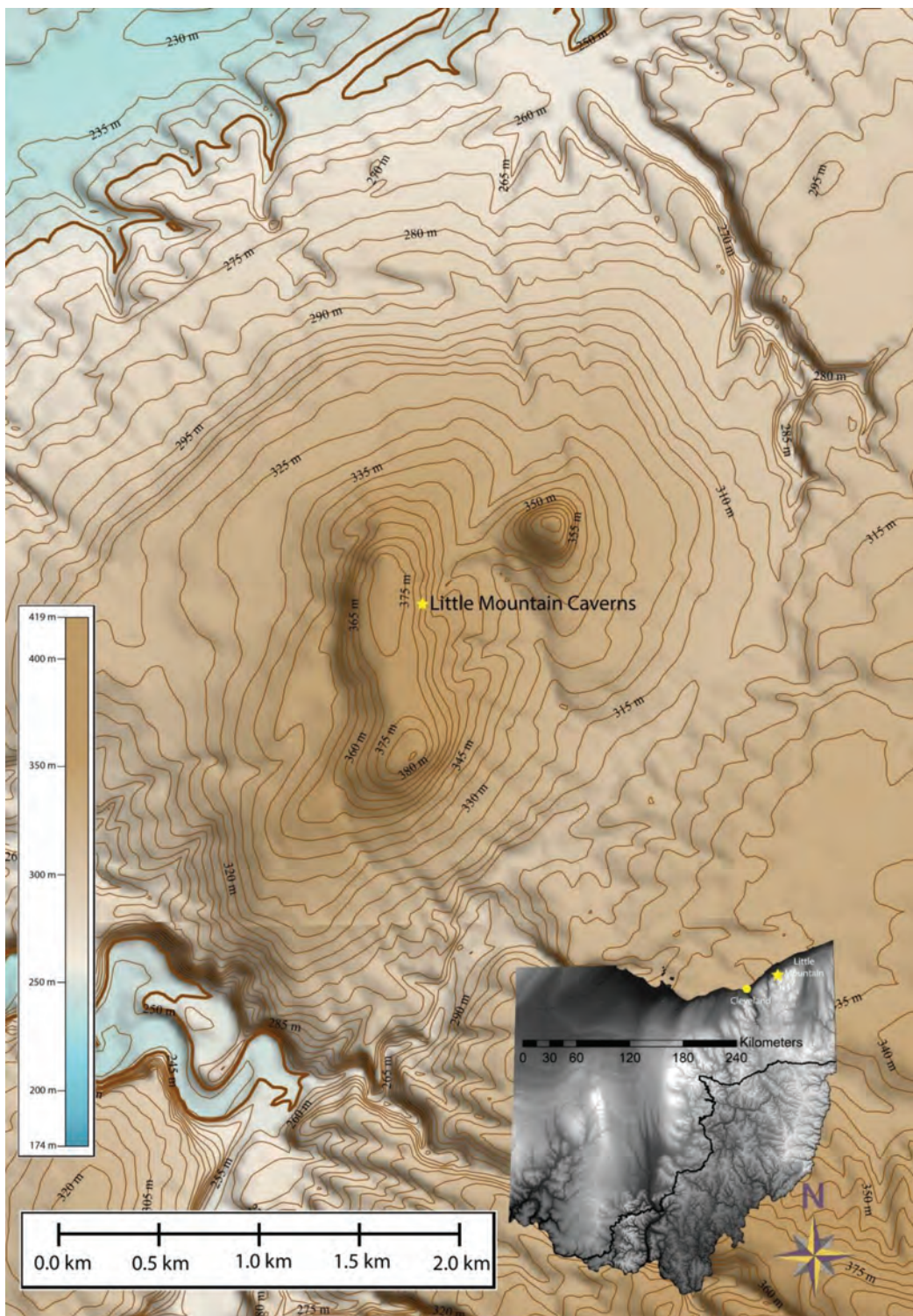


Figure 1. Topographic map of Little Mountain. Base data from Chardon, Chesterland, Mentor and Painesville USGS quadrangles (Ohio Geographically Referenced Information System). Inset map depicting farthest advance of multiple glaciations, modified from Powers et al. (2002) and Ohio Division of Geological Survey (2005).

These fluctuations would have initiated fractures and drained substantial quantities of meltwater through the Sharon Conglomerate on multiple occasions. Pre-Illinoian and Illinoian glaciations may have also contributed to joint formation and propagation as their ice margins advanced or retreated. Cave and sinkhole formation may have initiated as early as pre-Illinoian glaciations.

sinkhole is a rough quadrilateral whose curvilinear edges drop off steeply into the pit. Without a ladder, the sinkhole can be accessed only through a 0.75 m wide cave passage (Figs. 4-A and 4-B), which intersects its southern end. A cave passage at its northern end terminates against a bedrock wall.

Fyodorova (1998) documented three types of caves in sandstones and conglomerates of north-eastern Ohio: fracture caves formed by mechanical processes, true caves, and seepage caves. Dissolution controls the formation of the latter two. Filiano (2014) recognized valley stress relief, exposure to weathering, and dissolution as contributing factors in joint propagation and enlargement, as well as cave formation in this region. Ohio's glacial history may also play a role. The overburden of 1.6 km thick glaciers (Ohio Division of Geological Survey, 2005) would have depressed the land surface and possibly initiated joints. As the glaciers receded, relieving the overburden, joints and fractures in the Sharon Conglomerate may have propagated due to isostatic rebound. Copious amounts of glacial meltwater would also have passed through the system over a period of years. During the 10,000 years the Wisconsin ice sheet occupied Ohio, its margin fluctuated significantly (Hansen, 2017).

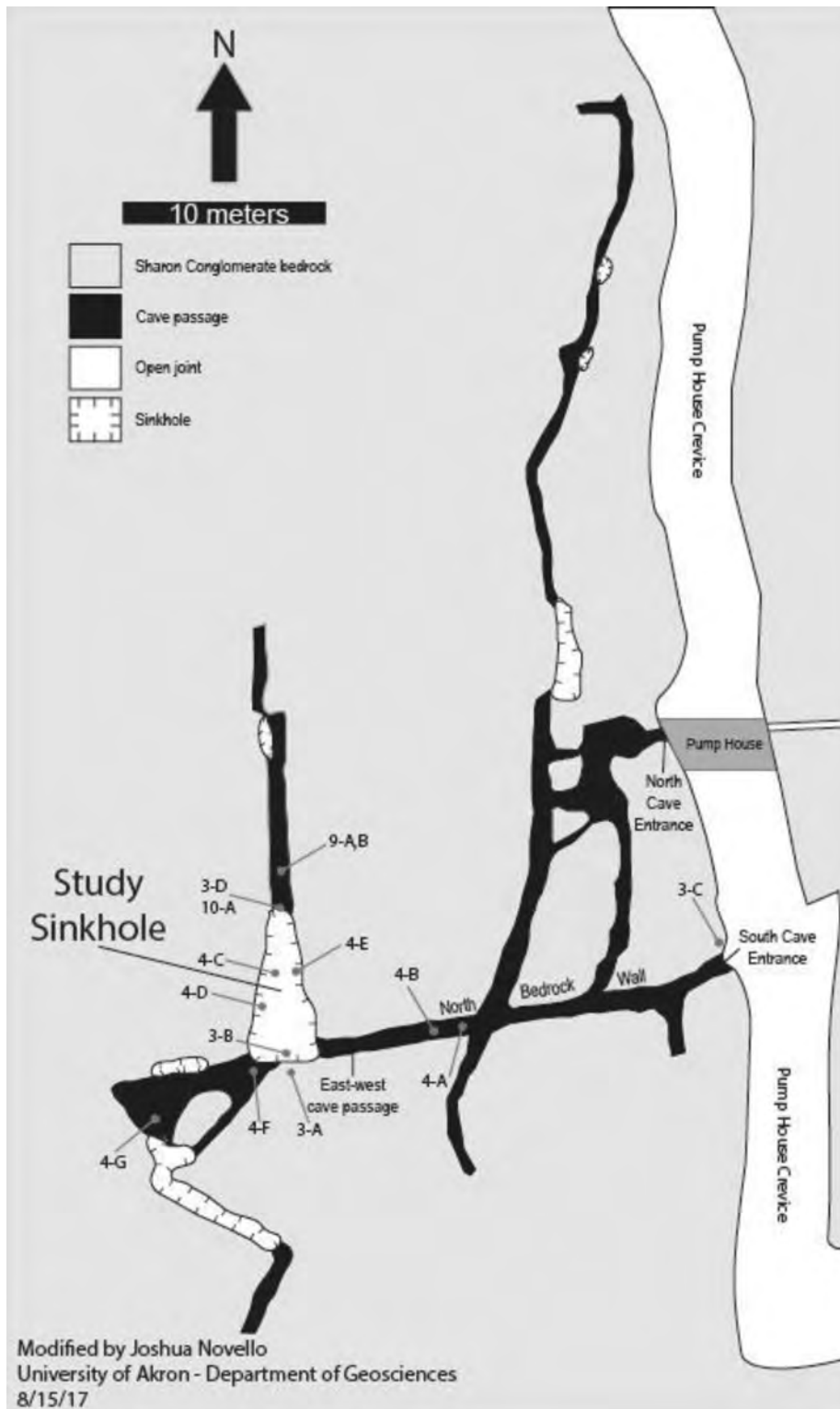


Figure 2. Map of Little Mountain Caverns showing sinkholes, pump house crevice and cave passages. Numbers correspond to figures referenced in text and show the location from which each photo was taken. Cliff face alignment of open joints is approximate. Modified from cave map provided by Ohio Cave Survey, undated.

al Oceanic and Atmospheric Administration, 2016).

Observations of bedrock jointing, fracturing, weathering, and disintegration were recorded. Correlative sedimentary structures and joint patterns were noted and described. Stratigraphic and morphologic features of the sinkhole walls were recorded to determine whether opposing sides fit together. Rock and sediment samples were collected, photographed

Jointing is an important factor in the weathering and erosion of sandstones. Sauro (2014) describes a process whereby arenization is initiated along conjugate joints, and loose sand is then piped or mechanically eroded, resulting in anastomosing pillars. Wray and Sauro (2017) note that arenization—the dissolution of a relatively small fraction of silica cement, followed by fluvial transport of loose sediment—is most effective along existing fractures. Due to the slow reaction rate of silica dissolution, water can remain aggressive for a long time as it travels through strata with high silica content (Martini, 2000). If joints were indeed propagated as glaciers advanced and retreated, subglacial meltwater may have taken advantage of these pathways, initiating arenization and subsequent cave and sinkhole formation processes. The massive volumes of water and amount of time it would have taken to drain make plausible the initiation of karst features via the aforementioned process (Young and Young, 1992). Arenization may continue today with meteoric and seepage water driving dissolution.

The generally-accepted mechanism of sinkhole and cave formation in sandstones of northeastern Ohio is mechanical jointing and slumping. The authors considered that alternative mechanisms could play a significant role in formation as well. This study aimed to investigate the processes that formed what is thought to be the largest sandstone sinkhole in Ohio.

Procedures

Little Mountain was visited 11 times from September 2016 to March 2017 for data collection. Sinkhole dimensions were mapped using a DistoX survey device (Heeb, 2009). Displacement across a large crevice to the east, in which an abandoned pump house lies, was also measured. Magnetic declination in the study area was 8.66° W throughout this study (National



Figure 3. Photographs of sinkhole and surroundings. A) View into the sinkhole from the surface. View is to the north. Depth is 8 meters in the tapered, northern end of the sinkhole. Note crescent-shaped cutout (highlighted in yellow) on eastern edge. Photo courtesy of Noah B. Novello. B) View towards the surface from within the sinkhole. Aperture tapers to the north. C) Pump house crevice, three meters wide. View to the north. Cliff face on the left is roughly parallel to the east wall of the sinkhole. Note relative alignment of crevice faces. Photo courtesy of Noah B. Novello. D) View (southward) from within the sinkhole.

and described using a 10x hand lens for color, weathering, induration, mineral composition, grain size, sorting and rounding. Rock samples were designated as LMRC-# (Little Mountain Rock Chip) and sediment samples as LMSD-# (Little Mountain Sediment Deposit).

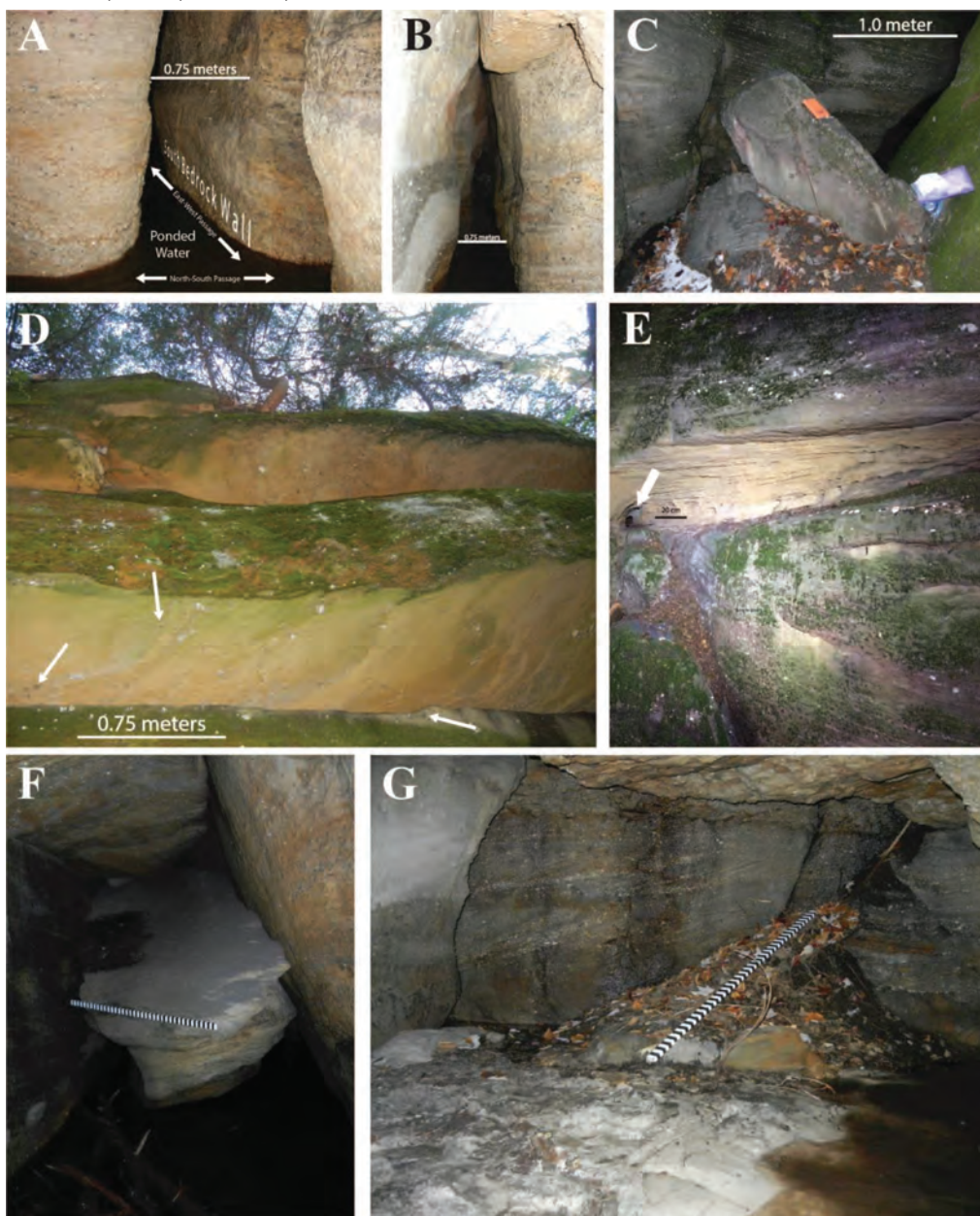


Figure 4. Photographs of interior of sinkhole and cave passages. A) Cross-cutting north-south and east-west-trending cave passages. View is to the east. Floor is submerged in water. B) View westward in the east-west cave passage. Note undercut ceiling and lack of collapse boulder. Passage terminates at sinkhole. C) Sandstone collapse boulders in the center of the sinkhole. View is to the south. D) View upward from interior of sinkhole showing west wall overhanging beds. Moss covered surfaces are vertical in contrast to tan, undercut bedding planes. White arrows indicate manganese-oxide coating present on some pebbles but absent on sand. E) Mid-level conduit in friable sandstone bed, east wall of sinkhole. View is to the northeast. F) Large collapse boulder in a room with significant material missing. G) Accumulation of fine quartz sand in room with low ceiling southwest of sinkhole. A sand cone emanates from the crevice in the upper right. Emery stick is 150 cm long. View is to the northwest. LMSD-1 collected here.

Samples were collected in an effort to compare induration between locations in the sinkhole, cave passage and surrounding areas. Location and presence of sediment was noted to determine its origin and transport pathway.

A digital model of the sinkhole was constructed using Structure-From-Motion photogrammetry. A 12.1-megapixel Nikon Coolpix S8100 digital camera was used to take photographs from floor to surface in 360° with approximately 80 % overlap between consecutive images. A large photoset with significant overlap is required to produce an accurate model (Westoby et al., 2012). Images were imported into Agisoft Photoscan Professional (Agisoft Photoscan Professional, 2016) for photogrammetric processing. A 3-D point cloud was generated by matching key points in each photograph. Imagery was overlain on this 3-D point cloud. The model was then exported as a Stereolithography file (.STL), a format which stores information about the surface geometry of 3-D objects (Chakravorty, 2017). The .STL file was exported to Tinkercad (Autodesk, 2018), a web browser-based, 3-D design tool, where it was further processed and analyzed by the authors. Two printed scale models (Model A, a cast of the sinkhole, and Model B, a mold of the sinkhole) were produced. Both models were used to gain different perspectives of the morphology and geometry of the feature. Model scales are the ratio of length in the model to the length in real space.

Sinkhole volume was determined via a water displacement test using Model A. The model was placed in a thin, plastic bag and submerged in a water-filled beaker. Overflow was poured into two 100 mL graduated cylinders and volume was recorded. Ten trials were performed and averaged.

Model B was prepared with removal of the upper ~0.5 m of material in order to simultaneously show the interior morphology and near-surface expression of the sinkhole from map view. Doing so facilitates comparison of the concavity of the model walls and the near-surface expression of the sinkhole.

Results

Morphology and Modeling

Depths of the southeastern and northeastern corners of the sinkhole are approximately 8 m and 6.5 m, respectively. The sinkhole tapers from a width of 3.8 m at the south end to approximately 0.5 m at its north end. The long axis of the sinkhole measures 6.2 m and trends roughly northwest. At the south end, the sinkhole intersects a cave passage trending east-west (Fig. 2). The east wall of the sinkhole and west wall of the pump house crevice are roughly parallel to one another and constitute opposite sides of the same block of rock.

Digital photographs, totaling 857, were processed as described above and were used to generate 3-D PDFs (Fig. 5). Cross-stratification, weathering, vegetation and other features can be easily observed.

Model A (Fig. 6), 1/85 scale, and Model B (Fig. 7), 1/51 scale, were exported to Tinkercad. The volume of Model A, averaged over 10 trials, is 108.5 cm³ (Table 1); hence, the volume of material missing from the sinkhole was determined to be 66.6 m³. Model B shows the morphology of the bedrock walls of the sinkhole.

Bedrock and Sediment

Six rock samples were collected and are composed overwhelmingly of detrital quartz. Samples LMRC-3, LMRC-6, and LMRC-7 contained approximately 1% mica flakes. Samples varied from fine to medium sandstone with quartz-pebble inclusions. Bedrock cement is silica, although hematite is also present. Significant differences of induration exist between samples collected from the host rock, with some disintegrating completely upon collection. Liesegang banding

Table 1. Sinkhole volume derived from water displacement trials using model A, 1/85 scale.

Trial	Volume of Water Displaced, cm ³	Scaled Sinkhole Volume, cm ³	Scaled Sinkhole Volume, m ³
1	108.0	66,325,500.0	66.3
2	111.5	68,474,937.5	68.5
3	111.0	68,167,875.0	68.2
4	108.0	66,325,500.0	66.3
5	111.5	68,474,937.5	68.5
6	104.0	63,869,000.0	63.9
7	104.5	64,176,062.5	64.2
8	109.0	66,939,625.0	66.9
9	108.5	66,632,562.5	66.6
10	109.0	66,939,625.0	66.9
Average	108.5	66,632,562.5	66.6 ± 1.6

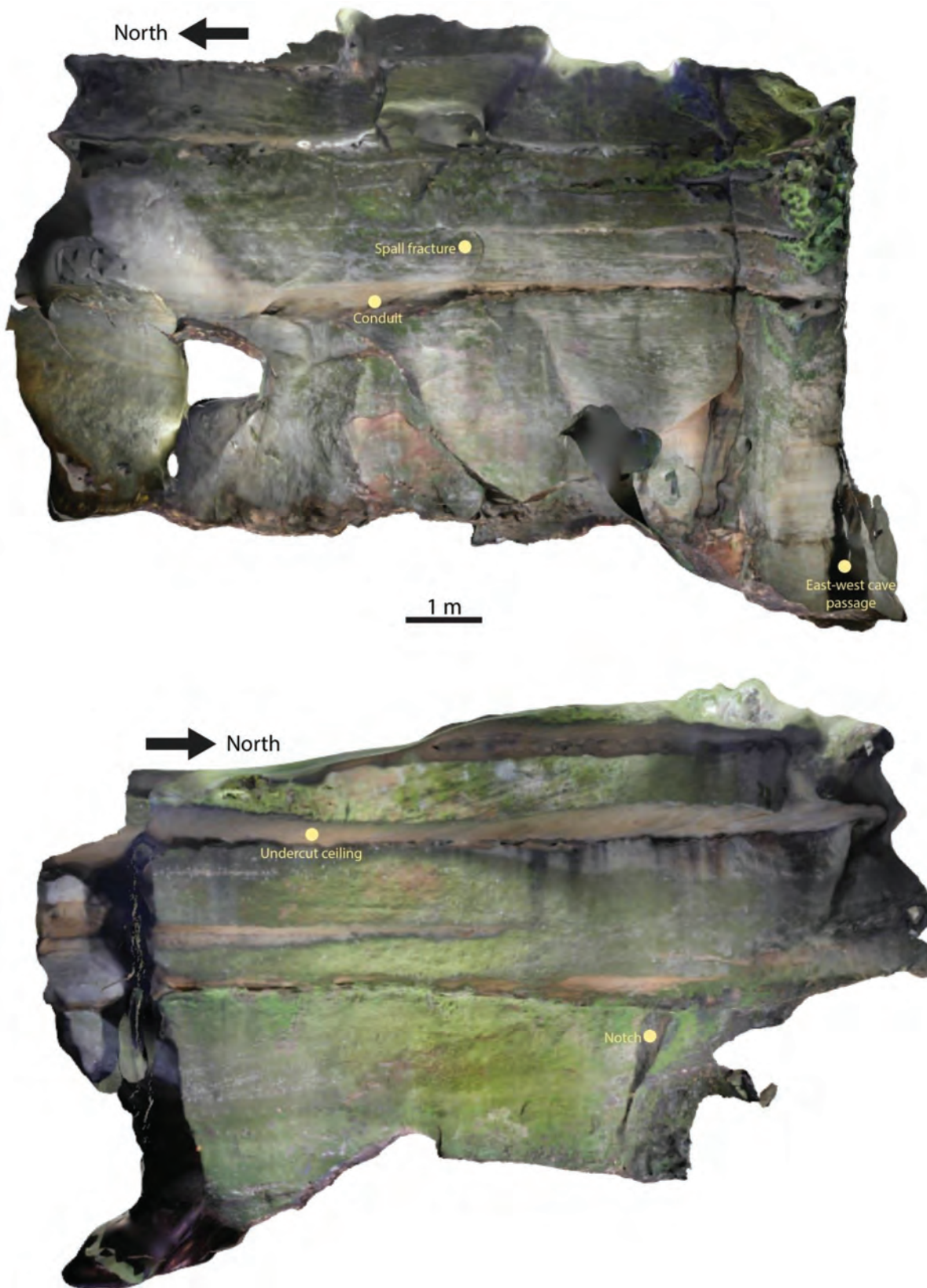


Figure 5. Structure-From-Motion model of the east (top) and west (bottom) walls of the sinkhole.

was observed in samples and throughout cave passages. Aligned, sedimentary structures and crosscutting, perpendicularly-aligned joints were observed in the cave. Sinkhole walls are concave and conglomeratic, especially near the base. Six sediment samples were collected. All samples taken from within the sinkhole and cave passages were com-

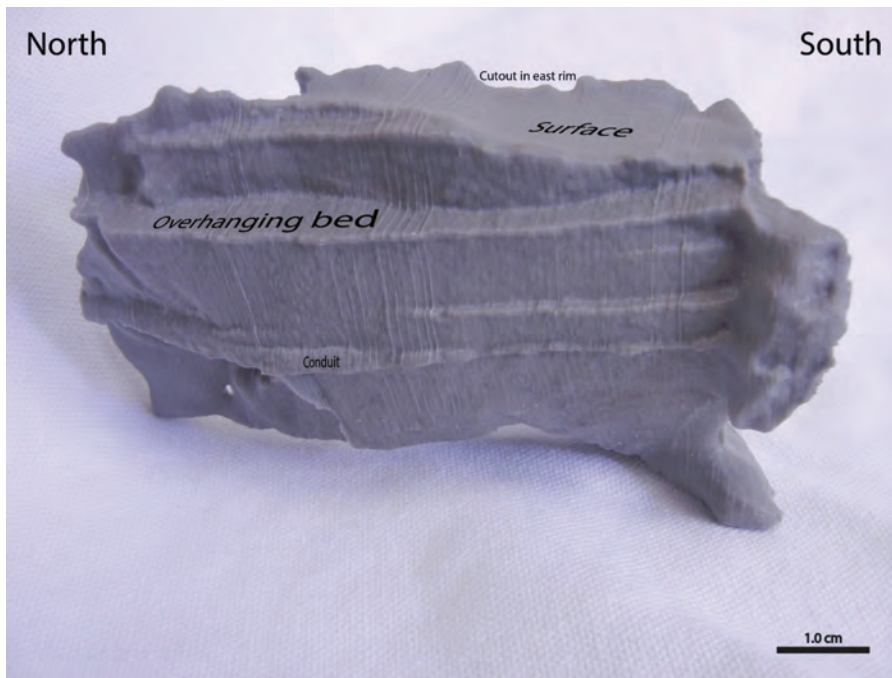


Figure 6. 3-D printed Model A showing the west wall of the sinkhole. Scale is 1:85. Parallel, vertical lines are printing artifacts.

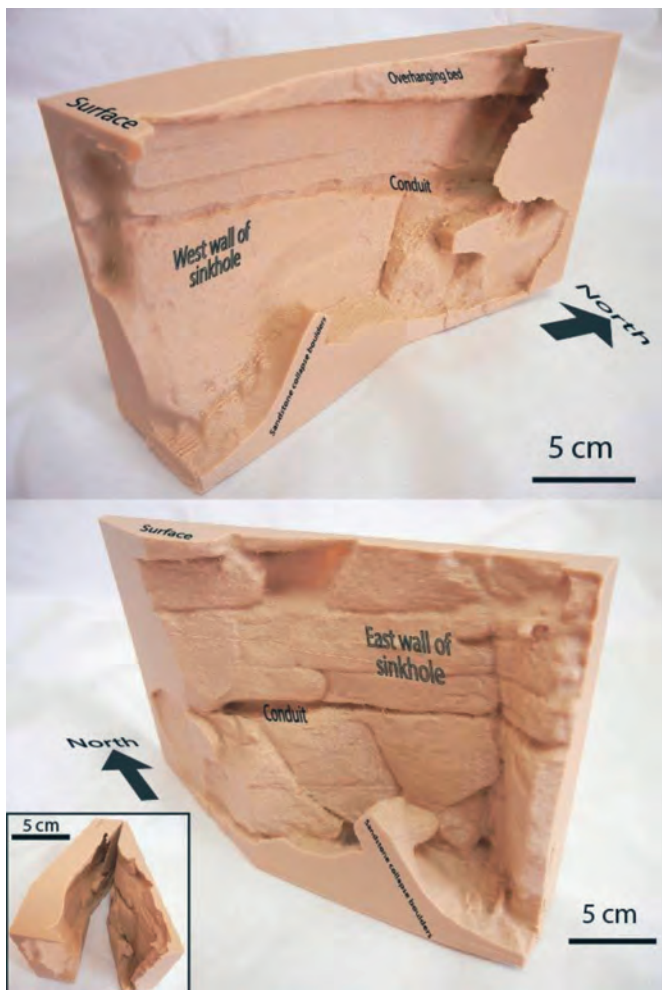


Figure 7. 3-D printed Model B showing walls of the sinkhole. Inset shows model from the surface looking inward. Scale is 1:51. The upper half meter of the sinkhole was excluded from the model to show the surface morphology.

posed primarily of quartz sand, with a small fraction of quartz pebbles. Samples collected outside the sinkhole and cave system contained quartz sand and pebbles and varying amounts of organic material. Organic content increased with distance from the sandstone knob.

Several sandstone boulders lie on the sinkhole floor (Fig. 4-C). Along the east rim of the sinkhole, there is a crescent-shaped cutout directly above one of the largest boulders (Fig. 3-A).

Sinkhole walls are overhung on all sides, except the south. The undersides of overhanging beds (Fig. 4-D) are actively weathering. Freshly-weathered surfaces were commonly punctuated by quartz pebbles, covered in manganese oxides. No collapse correlating to the flat underside of these overhanging beds was observed within the sinkhole. Similar overhanging or freshly weathered features were observed on the walls of cave passages, with no associated breakdown (Figs. 4-A and 4-B).

Connecting to the southwest end of the sinkhole, a large room contains a collapse boulder approximately 4 m long, 1 m tall, and 2 m wide (Fig. 4-F). A significant amount of bedrock is missing from this room. Continuing west past this boulder, a low-ceilinged room about 5 m long, 5 m wide, and 1.5 m tall is reached (Fig. 4-G). Bedrock has also been removed from within this room. A sand cone composed of fine quartz sand (LMSD-1) emerges from a crevice in the north wall, fanning out into the room, following the form described by Duszyński et al. (2016).

Several spall fractures were observed within the sinkhole and cave passages (Figs. 5 and 8). A small, poorly cemented spall in the northwest corner of the sinkhole disinte-

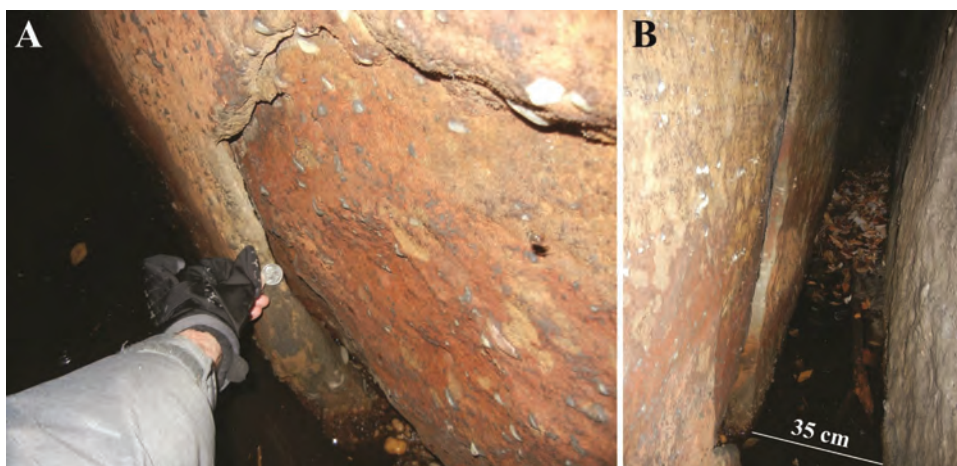


Figure 8. Spall fracture in cave passage north of sinkhole. A) View northeast. B) View south. Note red staining and separation of outer spall from inner wall. LMRC-4 collected at this location.

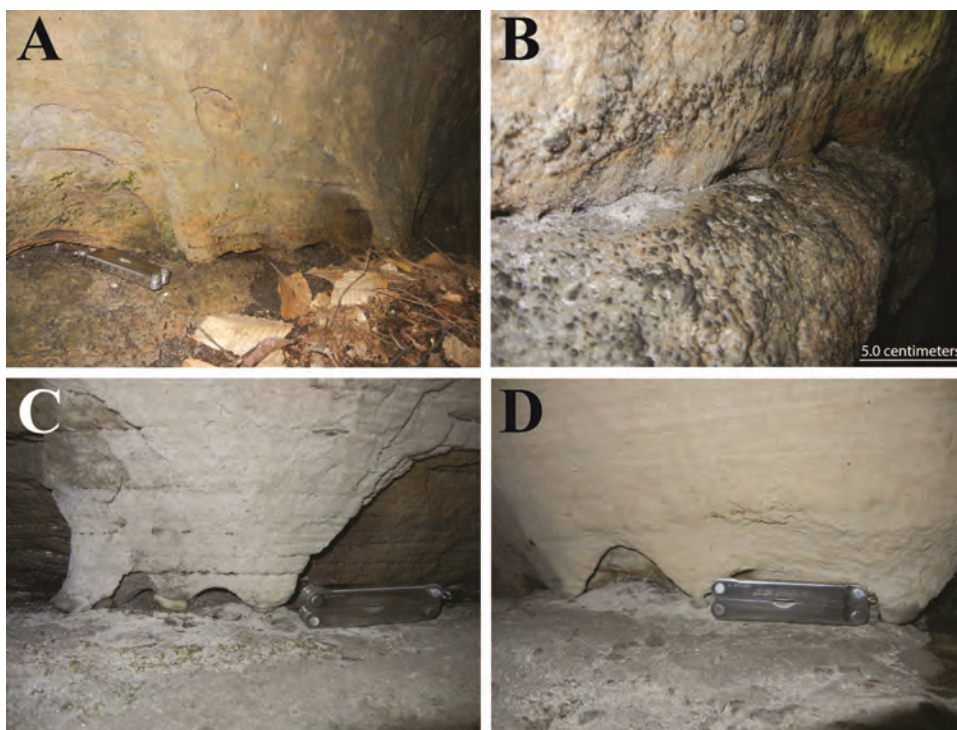


Figure 9. Anastomosing pillars throughout the study area. Note freshly weathered surfaces and loose sand. Multitool (10 cm long) for scale. A) Within the sinkhole. B) Within the east-west cave passage. C and D) Within a joint to the north of the sinkhole. Note quartz pebble bases.

base of the same cone, is composed of 5% medium, quartz sand and 95% organic material. Significant quantities of sand were also found in soil on the slopes of Little Mountain.

Discussion

The results and their implications for understanding the processes are summarized in Table 2 with associated figures and references.

Morphology and Modeling—Evidence not explained by translation

If the sinkhole walls were brought together, the top edges would meet before the interior walls touched, due to their concavity. The walls would not fit like puzzle pieces; a gap would continue to exist between the east and west walls of the sinkhole. The concavity is most readily observed when looking up from within the sinkhole (Fig. 3-B) and along its long axis (Fig. 3-D). Since the gap would not close if the walls were brought together, the sinkhole cannot be the result of simple mechanical separation.

grated completely upon collection. In the north cave passage, a large spall fracture was observed (Fig. 8). The outer wall appears to be parting from the inner, and a small gap has formed between the two. LMRC-4, collected here, is friable but better cemented than the small spall in the sinkhole. The two are separated by roughly four or five meters. Two spall fractures were also observed in the low-ceilinged room southwest of the sinkhole.

Small-scale, anastomosing pillars were observed in a mid-level, friable bed within the sinkhole and in other places throughout Little Mountain (Figs. 9 A-D). These pillars are usually bounded above and below by bedding planes. Frequently, a quartz pebble forms the base of a pillar. Pillars and bounding beds exhibited freshly weathered surfaces. Loose sand was observed in conjunction with these structures.

Loose sand was also observed on the floor of several cave passages, the southern sinkhole entrance and the room southwest of the sinkhole (Fig. 4-F). Sand in the latter was probed to a depth of over 15 cm, indicating a substantial accumulation. Sand at the south end of the sinkhole was estimated to be from 3 to 8 cm deep.

Sand cones emerging from joints and crevices were observed around the margins of the Little Mountain (Fig. 10). Collected near the apex of one cone, LMSD-5 is composed of 60 % medium, quartz sand and about 40% organic material. LMSD-4, collected from the

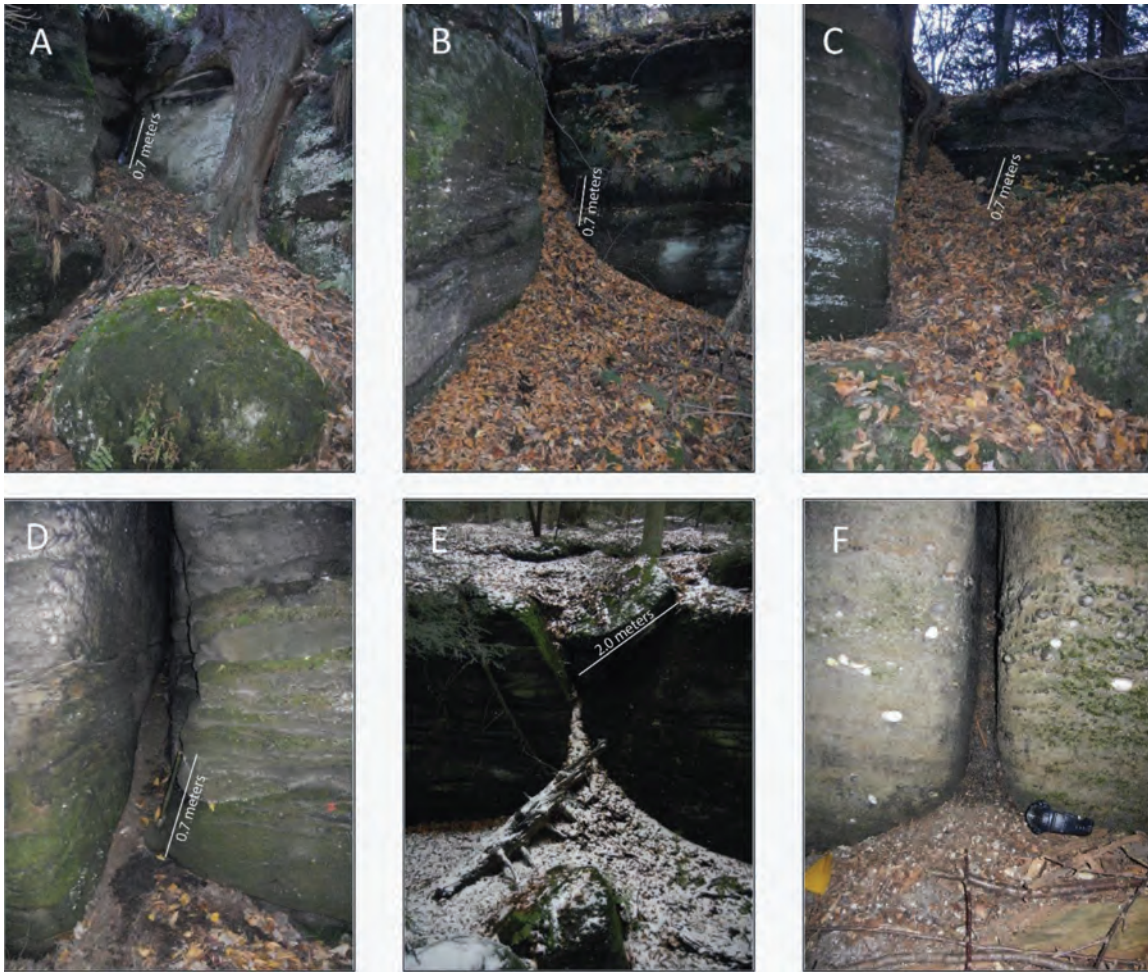


Figure 10. Photographs of sand cones on Little Mountain. A) Southeast of sinkhole in pump house joint (LMSD-4 and LMSD-5 collected here). B) South of pump house stream, east of pump house joint. C) Immediately east of southern cave entrance. D) North of pump house. E) North within pump house joint, note collapsed surface block and spreading of cone. F) North of sinkhole, note joint full of sand behind cone. Wristwatch for scale.



Figure 11. LMRC-1 collected from collapse boulder in sinkhole. Note iron oxide staining.

The east wall of the sinkhole and the west wall of the pump house crevice are roughly parallel to one another (Fig. 2). Bedrock between these walls comprises the north bedrock wall of the southern cave entrance. If jointing and slumping were solely responsible for producing the sinkhole, the north bedrock wall would have advanced downhill farther east than the south block. This block would protrude into the pump house crevice, resulting in a narrower passage. The result would not be the continuously-aligned, evenly-spaced crevice in which the pump house lies (Figs. 2 and 3-C). The southern and northern block crevice faces are relatively aligned. The north crevice face does not reflect the greater eastward advance which would be expected if the sinkhole was the result of block movement.

On opposite walls of the east-west-trending cave passage, planar tabular cross-stratification was observed and appears to have been part of the same dune. Additionally, a north-south-trending cave passage cross cuts the east-west-trending cave passage (Fig. 4-A). This implies alignment of the north and south blocks prior to and after propagation of both joints while the sinkhole may have continued to widen. If the north block had slumped eastward to produce the sinkhole, the northern section of the north-south cave passage would have widened or migrated eastward, relative to the southern section, which is not the case. The north block, therefore, is unlikely to have slumped far enough to the east to produce the sinkhole.

Table 2. Sinkhole formation mechanisms observed on Little Mountain.

Mechanism	Figure	Source
<u>Arenization/granular disintegration</u>		
Loose sand throughout sinkhole and cave passages	4-G, 9-A, 9-B	Present study
Sinkhole concavity	3-A, 3-B, 3-D, 12	Present study
Freshly weathered surfaces punctuated by manganese oxide coated quartz pebbles	4-A, 4-B, 4-D, 4-E, 5, 8A, 9-A, 9-B, 9-C, 9-D	Present study
Overhanging beds	3-B, 3-D, 4-D, 5, 6, 7	Present study
Evacuation of bedrock from confined spaces	3-A, 3-D, 4-F, 4-G	Present study
Anastomosing arches with quartz pebble bases, loose sand	4-E, 9-A, 9-B, 9-C, 9-D	Fyodorova (1998), present study
Dissolution pits in thin section - evidence of occurrence in NE Ohio	...	Fyodorova (1998)
Continuously aligned walls of pump house crevice	2, 3-C	Present study
Aligned joints of the east-west and north-south trending cave passages	2, 4-A	Present study
<u>Underground erosion and fluvial grain transport</u>		
Sand Cones	4-G, 10-A, 10-B, 10-C, 10-D, 10-E, 10-F	Duszyński et al. (2016), present study
Conduits	4-E, 5	Duszyński et al. (2016), present study
<u>Undercutting and collapse</u>		
Boulders within sinkhole	3-D, 4-C, 12	Present study

Structure-From-Motion photogrammetry was successful in generating accurate 3-D models. Viewing Models A and B as 3-D-printed hand samples provided different perspectives for analysis and feature observation. The actual depth of the south end of the sinkhole was measured to be approximately eight meters, though Mmodel A indicates a depth of 6.3 m, due to absence of the uppermost data. Therefore, the calculated volume of 66.6 m³ is conservative, and the sinkhole is actually greater in volume. This is the largest sandstone sinkhole in Ohio to our knowledge.

Bedrock and Sediments—Evidence for removal of material and undercutting

Sandstone collapse boulders lie on the floor of the sinkhole (Fig. 4-C). LMRC-1 collected from one of the boulders was friable and disintegrated significantly upon collection, indicating weak cementation (Fig. 11). At the land surface, a crescent-shaped cutout on the eastern rim of the sinkhole may correspond to the rounded edge of the upper boulder (Fig. 3-B). These boulders may have been emplaced via joint propagation, expansion via arenization or fluvial erosion, and subsequent collapse as the void neared the surface (Fig. 12).

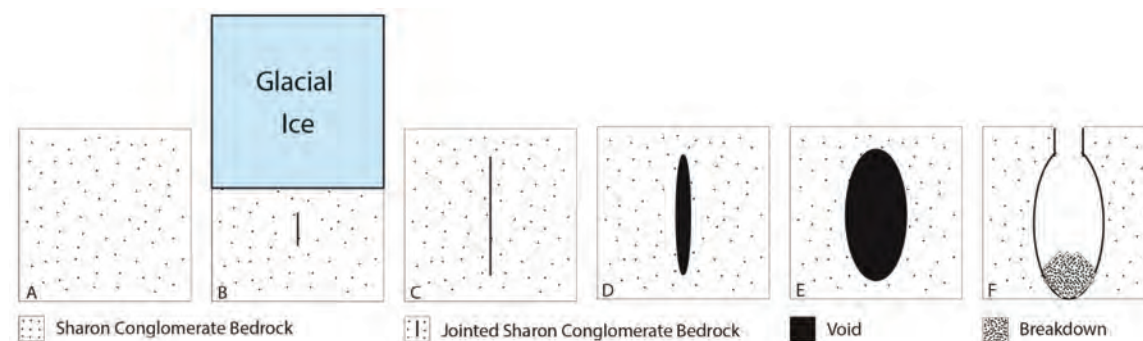


Figure 12. Schematic model showing one possible formation process for the sinkhole. A) Unjointed Sharon Conglomerate. B) Glacial advance exerts tremendous downward force on the bedrock, initiating fractures. C) During and after glacial retreat, glacio-isostatic rebound propagates existing fractures and initiates new fractures. D) Existing joints widen via the arenization process as significant volumes of glacial meltwater, meteoric, and seepage water pass through the conglomerate. E) The void widens significantly, stretching toward the surface as arenization and granular disintegration continue. F) The thin bridge spanning the void collapses into the sinkhole as arenization progresses further toward the surface, resulting in present-day conditions.

subsequent collapse as the void neared the surface (Fig. 12).

No corresponding breakdown underlies overhanging beds in the sinkhole (Fig. 4-D), suggesting granular disintegration and transport of grains. The tan undersides of overhanging beds appear fresh in

contrast with gray, weathered, vertical surfaces in the sinkhole, indicating active removal of grains. Similarly, undercutting was observed in cave passages without associated breakdown (Fig. 4-B). In the sinkhole and cave passages, black deposits on the walls, likely manganese oxide, are observed primarily on pebbles in a matrix of uncoated sand. Loose quartz sand, deposited on narrow ledges throughout the cave, may have disaggregated from the bedrock prior to deposition of such oxides (Fig. 9-B), indicating ongoing granular disintegration. Sand on the ledges may also be attributed to incipient anastomosing pillars in the passage. Deposition of this sand by transport from the land surface is not suspected as the deposits are partially recessed into the wall between pillars and also because a true ceiling exists. Sand is also present in the recesses of other pillars (Figs. 9-C and 9-D). Loose sand, observed on the floor of the sinkhole and cave passages, further indicates granular disintegration and subsequent transport from a nearby location.

Two other features in the cave system connected to the sinkhole appear to have formed via bedrock disintegration. The room with the large collapse boulder (Fig. 4-F) and the low-ceilinged room (Fig. 4-G) could not have formed by movement of consolidated bedrock. In both cases, the volumes of bedrock missing are too large to have been removed via the 0.75 m cave passages as large, indurated masses. Bedrock must have been removed from these confined spaces via granular disintegration and subsequent transport. The low-ceilinged room is now an area of deposition, as a large cone of moderately rounded, well-sorted, 100% fine quartz sand is present. Similar sand cones have been observed elsewhere on Little Mountain and are discussed below.

Many small-scale, anastomosing pillars were observed in the walls of the sinkhole and surrounding area, usually bounded by bedding planes (Fig. 9). Pillar bases composed of quartz pebbles may be the result of the increased efficacy of arenization on cement between grain boundaries rather than on clasts themselves. Cement dissolution would allow for erosion of individual grains while leaving intact the larger pebble at the base. Freshly weathered surfaces and an abundance of loose sand indicate that these structures represent an active weathering process in the Sharon Conglomerate. If pillars were generated solely by mechanical action of flowing water, the sand grains would have been immediately carried away. Instead, small piles of sand are observed in conjunction with anastomosing pillars. Fyodorova (1998) documented anastomosing pillars in Patterson Farm caves, which are also in the Sharon Conglomerate of Geauga County, Ohio. Other authors have described large-scale, well-developed, anastomosing pillars in Venezuela (Sauro, 2014). Samples collected from the Venezuelan pillars, and examined with a petrographic microscope and SEM, revealed a range of dissolution features indicative of the arenization process, including minor pitting as well as v-shaped dissolution features (Sauro, 2014). Venezuelan pillar formation was attributed to expansion of strata-bound fractures via arenization. Although no petrographic or SEM work was conducted during the current study, Fyodorova (1998) documented pitting, v-shaped notches, and other dissolution features in samples taken from the Sharon Conglomerate and Berea Sandstone in neighboring Cuyahoga, Portage, and Summit counties. While dissolution features are direct evidence of arenization elsewhere in Northeast Ohio, the presence of pillars alone may provide indirect evidence of the arenization process on Little Mountain.

Several sand cones emanate from the cliff faces of Little Mountain in the vicinity of the sinkhole and cave system (Fig. 10). The deposits document processes operating in the area which are also at work in the sinkhole. At the apex of the sand cone in Fig. 10-A, sediment is composed of medium quartz sand and organic debris. Sand fraction decreases significantly near the base of the cone. This may be due to the episodic nature of deposition during periods of high precipitation, while organic material accumulates consistently throughout the year. Sections nearer the apex are generally less exposed to the elements and falling organic debris. Those sections nearer the base are open to the surrounding area, and more frequently receive debris from other sources. The pattern of greater sand fraction near the apex and lower fractions at the base was observed for all sand cones inspected. Cones demonstrate that significant volumes of sediment, matching that which composes the Sharon Conglomerate, have accumulated outside the bounds of the bedrock knob at Little Mountain. A shallow hole was dug downhill to the east, where bedrock is the underlying Cuyahoga Formation. Below the surface, significant quantities of sand, mixed with organic material, indicate that sand from the Sharon Conglomerate is washing downslope. The source of these sheet deposits is likely the sand cones uphill and blocks of Sharon Conglomerate, which have broken from the bedrock cap. Disaggregated bedrock is actively being transmitted outside the knob via joints and crevices.

In the sinkhole, there are a number of possible outlets for disintegrated sand. All cave passageways contain ponded or slowly flowing water. Water originating in a southwest passage flows throughout the cave, exiting through the pump house and draining downhill through a narrow, adjacent joint. Sediment could have been carried into the east-west cave passage during periods of high precipitation. There are also two potential conduits, whose terminations are unknown. The first lies at the contact between the Sharon Conglomerate and the Cuyahoga Formation on the east side of the sinkhole. It presents as a triangular opening, trending northeast. This fracture may intersect an adjacent cave passage, which could drain through the pump house. A second conduit in the mid-level, friable bed may have played an earlier role in sand removal (Fig. 4-E). LMRC-3 disintegrated completely upon collection from this bed.

Several spall fractures were observed in the sinkhole and cave passages, which also seem to contribute to formation of the sinkhole. Two spalls observed in the room southwest of the sinkhole are larger and analogous to another spall observed in the sinkhole (Fig. 5). The concave morphology of the fractures is consistent with that observed in the sinkhole.

Conclusion

Numerous lines of evidence (Table 2) point to a complex history for the growth of this sinkhole. If the sinkhole had opened as the result of mechanical movement of the bounding blocks, the western face of the pump house crevice would be displaced eastward. Displacement was not observed in the pump house crevice (Figs. 2 and 3-C).

Simple jointing and slumping are not adequate mechanisms to explain all gaps and voids observed on Little Mountain, and cannot explain formation of the sinkhole. Multiple examples within the sinkhole, cave passages, and surrounding area demonstrate that large volumes of bedrock must have been evacuated from confined spaces as individual sand grains. Variations in induration can be found within as little as 0.5 m. Jointing clearly initiates formation of gaps on Little Mountain. However, other processes must be at work to create the sinkhole and possibly other large openings. Therefore, the hypothesis of jointing and slumping as the sole genetic mechanism is rejected. Arenization is suggested and supported by our data as a plausible mechanism for sinkhole growth (Wray and Sauro, 2017). Silica saturation indices of -1.137 for the spring flowing from the pump house indicate that water flowing at Little Mountain is capable of dissolving silica (Fyodorova, 1998).

This study demonstrates that the largest sandstone sinkhole in Ohio could not have formed solely by mechanical/translational processes. Continuous alignment of the pump house crevice, as well as those within the cave system, precludes sinkhole genesis via jointing and translation. Multiple glacial advances and retreats, over at least the last 300,000 years, provided ample opportunity for joint propagation, as well as copious volumes of silica-undersaturated water. Joint widening, via arenization, provides a mechanism for loosening of sand while the cave system and crevices act as transport conduits. Enlarged joints could easily result in collapse as they extend toward the surface.

Concave sinkhole wall morphology and anastomosing pillars are analogous to pillars described by Sauro (2014), with meteoric and seepage water likely driving arenization and transport. Conduit flow in non-carbonate rocks at Little Mountain appears to play a significant role in groundwater movement as well as cave and sinkhole development. Although direct evidence of silica dissolution was not evaluated in the present study, several features consistent with arenization have been documented and recognized elsewhere in Northeast Ohio and Venezuela.

A future study could examine individual quartz sand grains for features indicating dissolution of silica cement, such as pitting and formation of v-shaped notches. Additional supporting evidence may be derived from porosity determination within the sinkhole and cave system. Wray and Sauro (2017) suggested that post-arenization porosity of 20% may result in ready disintegration and transport of quartz grains from a bedrock mass. Evidence from these methods may help determine the degree to which silica dissolution plays a role in sinkhole formation at Little Mountain.

This sinkhole likely formed as flowing water dissolved silica cement in the Sharon Conglomerate and eroded poorly-cemented grains from otherwise confined spaces, resulting in eventual ceiling collapse (Fig. 12). Sand was then transported via the cave system or conduits to cones around the margins of the knob. Grains were further transported downhill via surface runoff and slope transport processes, covering the slopes of Little Mountain in sandy sheet deposits.

Acknowledgements

We would like to thank Mike Watson and The Holden Arboretum for granting permission and access to conduct this study on Little Mountain. The contributions of the following people in conducting field work were greatly appreciated: Caryn Schuster, Eric, Noah, Roy, and Ronna Novello, RJ McGinnis, Hunter Campbell, Joe Millard and Connor Estes. At the University of Akron, Dr. John Peck, Dr. Shanon Donnelly, Dr. Linda Barrett, Dr. Hazel Barton, Elaine Butcher, Tom Quick and Maria Hawkins provided invaluable assistance and insight. We are grateful to Kathy Sasowsky for reviewing the manuscript and providing thoughtful recommendations. John Harman generously provided the DistoX used for the project. We would also like to thank Dr. Malcom Field, Dr. Benjamin Schwartz, and the three anonymous reviewers who provided valuable recommendations on improvements to this manuscript. Sincere thanks to all who contributed to this project!

References

- Agisoft PhotoScan Professional, 2016, (Version 1.2.6 Software) retrieved from: <http://www.agisoft.com/downloads/installer/>.
Autodesk, 2018, Tinkercad: Tinkercad is a simple, online 3D design and 3D printing app for everyone, <https://www.tinkercad.com/>.
Chakravorty, D., 2017, STL File Format for 3D Printing—Simply Explained: <https://all3dp.com/what-is-stl-file-format-extension-3d-printing/> (accessed May 2018).

- Duszyński, F., Migoń, P., and Kasprzak, M., 2016, Underground erosion and sand removal from a sandstone tableland, Stołowe Mountains, SW Poland: *Catena*, v. 147, p. 1–15. <https://doi.org/10.1016/j.catena.2016.06.032>.
- Filiano, G.L., 2014, Role of joints and rock stresses in the formation of sandstone caves in northeastern Ohio [M.S. thesis]: University of Akron, 200 p.
- Fyodorova, A.I., 1998, Hydrogeochemical study of cave systems in the Berea sandstone and Sharon sandstone/conglomerate of northeastern Ohio [M.S. thesis]: University of Akron, 121 p.
- Gutiérrez, F., Parise, M., De Waele, J., Jourde, H., 2014, A review on natural and human-induced geohazards and impacts in karst: *Earth-Science Reviews*, v. 138, p. 61–88. <https://doi.org/10.1016/j.earscirev.2014.08.002>.
- Hansen, M.C., 2017, The Ice Age in Ohio: Ohio Division of Geological Survey, Educational Leaflet No. 7, Revised Edition.
- Heeb, B., 2009, Paperless Cave Surveying, document available at: <http://paperless.bheeb.ch/download/DistoX.pdf> (accessed October 2016).
- Martini, J.E.J., 2000, Dissolution of quartz and silicate minerals. *in*: Klimchouk, A.B., Ford, D.C., Palmer, A.N., Dreybrodt, W. (eds.), *Speleogenesis: Evolution of Karst Aquifers*. National Speleological Society, Huntsville, pp. 452–457.
- Migoń, P., Duszyński, F., and Goudie, A., 2017, Rock cities and ruiniform relief: Forms–processes–terminology: *Earth-Science Reviews*, v. 171, p.78–104. <https://doi.org/10.1016/j.earscirev.2017.05.012>.
- National Oceanic and Atmospheric Administration, 2016, Magnetic Field Calculators: <https://www.ngdc.noaa.gov/geomag-web/#declination> (accessed November 2016).
- Ohio Cave Survey, author and date unknown, Sketch Map of Little Mountain Caverns.
- Ohio Division of Geological Survey, 2005, Glacial map of Ohio: Ohio Department of Natural Resources, Division of Geological Survey, page-size map with text, 2 p., scale 1:2,000,000.
- Pierson, I.K., 1892, Plan of the Little Mountain Club property, Little Mountain, Geauga County, Ohio.
- Powers, D.M., Laine, J.F., and Pavey, R.R., 2002, Shaded elevation map of Ohio: Ohio Division of Geological Survey Map MG-1, 1:500,000 scale.
- Sauro, F., 2014, Structural and lithological guidance on speleogenesis in quartz-sandstone: Evidence of the arenization process: *Geomorphology*, v. 226, p. 106–123. <https://doi.org/10.1016/j.geomorph.2014.07.033>.
- Stout, W., 1944, Sandstones and conglomerates in Ohio: *The Ohio Journal of Science*, v. 44, no. 2, p. 75–88.
- USGS US Topo 7.5-minute map for Mentor, OH 2016: USGS–National Geospatial Technical Operations Center (NGTOC), scale 1:24,000.
- Westoby, M.J., Brasington, J., Glasser, N.F., Hambrey, M.J., and Reynolds, J.M., 2012, ‘Structure-from-Motion’ photogrammetry: A low-cost, effective tool for geoscience applications: *Geomorphology*, v. 179, p. 300–314. <https://doi.org/10.1016/j.geomorph.2012.08.021>.
- Wray, R. A. L. and Sauro, F., 2017, An updated global review of solutional weathering processes and forms in quartz sandstones and quartzites: *Earth-Science Reviews*, v. 171, p. 520–557. <https://doi.org/10.1016/j.earscirev.2017.06.008>.
- Young, R. and Young, A., 1992, *Sandstone Landforms*: Springer-Verlag, Berlin Heidelberg, Germany, 304 p. <https://doi.org/10.1007/978-3-642-76588-9>.

THE RELATIONSHIP BETWEEN PRESENCE OF BROWN BEAR (*URSUS ARCTOS*) AND DIVERSITY OF AIRBORNE ALGAE AND CYANOBACTERIA IN THE GŁÓWNIOWA NYŻA CAVE, TARTRA MOUNTAINS, POLAND

Joanna Czerwik-Marcinkowska^{1,C}, Tomasz Zwijacz-Kozica², Wojciech Pusz³, and Anna Wojciechowska⁴

Abstract

Of the big mammal taxa, the brown bear (*Ursus arctos*) is one of a few surviving species and one of the two largest terrestrial carnivorans that have successfully exploited caves. Greenish and blueish patches were collected in August 2016 from the cave walls and pine twigs in the pseudokarstic Główniowa Nyża Cave in the High Tatra Mountains, southern Poland. These materials were cultured and the first appearance of airborne microorganisms (algae and cyanobacteria) during two-three months of cultivation were observed. Overall, 24 species were identified using light microscopy and transmission electron microscopy. The highest number (10) of documented species belonged to Cyanobacteria with the genus *Gloeocapsa* the most diverse. We identified ten Chlorophyta species. Only four taxa of diatoms were found. No correlation between species diversity and physical parameters (temperature and humidity) was found. The materials containing airborne microorganisms growing on the granite walls were most probably brought in by wind, whereas the ones on the twigs were brought in by wind and/or by the bear. The presence of *Ursus arctos* does influence distribution of airborne microorganisms.

Introduction

Caves represent very specific, extreme terrestrial habitats, where growth of airborne microorganisms and vascular plants are limited by unfavorable abiotic factors. They present composite micro-ecosystems that include bacteria, cyanobacteria, algae, fungi, lichens, liverworts, and mosses, in different proportions depending on the environmental conditions. Dayner and Johansen (1991), Pedersen (2000) and Popović et al. (2015) suggested that reduced light intensity, low nutrients, and absence of seasonality are the predominant features that influence distribution and composition of aerial algal and cyanobacterial assemblages in caves, while Mulec et al. (2008) stated that temperature, humidity, and flowing water also play a role in the colonization of aerial habitats. It is possible that animals, and in particular bears, can transport different spores into caves, and an example of such phenomenon is the Główniowa Nyża Cave in the High Tatra Mountains, Poland. This cave was discovered in March 2011 by Janusz Łukaszczyk Głowoń while observing a female bear with cubs. The plan and description of cave was prepared by Tomasz Zwijacz-Kozica in collaboration with J. Łukaszczyk Głowoń, M. Strączek Helios, and F. Zięba, during the bears absence. The Główniowa Nyża Cave continues to be used for brown bear hibernation.

Ursus arctos is a large brown bear with the widest distribution of any living ursid. The brown bear occurs in the coniferous, mixed, and deciduous forest zones of Europe, however, the bear seasonally visits the tundras and arctic heaths above the timberline. Zedrosser et al. (2001) described the Carpathian population of brown bears in Slovakia, Poland, Ukraine, and Romania which includes about 8,000 bears and is the second largest in Europe. All bear populations are protected by the Habitat Directive in Europe which is compulsory for all EU countries. Almost all the bears in Europe live in large transboundary populations in eastern or northern Europe (Zedrosser et al., 2001). Nielsen et al. (2010) stated that in different regions of the world hibernating bears use various places to build their dens. Linnell et al. (2000) described wintering brown bears in natural caves or in rock cavities, dens dug in snow cover, and also hidden in rotten trees. The European brown bear is omnivorous, but feeds chiefly on vascular plants. Grasslands and shrublands integrated with forests, subalpine meadows, and alpine communities are typical habitat for bears and in particular *Ursus arctos* (Nietfeld et al., 1985). There is the risk of mistaking a briefly exploited summer den for a true bear hibernation site (Mysterud, 1983).

Airborne algae and cyanobacteria are known to colonize non-aquatic habitats including exposed bedrock (Rindi et al., 2010; Ress and Lowe, 2013), soil, terrestrial bryophytes, tree bark, rocks, and anthropogenic structures (Neustupa and Štifterová, 2013). These pioneer species modify the rock surface by producing carbonic acid during respiration

¹Department of Botany, Institute of Biology, Jan Kochanowski University, Świętokrzyska 15, 25-406 Kielce, Poland; email: marcinko@kielce.com.pl

²Tatra National Park, Kuźnice 1, 34-500 Zakopane, Poland

³Division of Plant Pathology and Mycology, Department of Plant Protection, Wrocław University of Environmental and Life Sciences, Grunwaldzki 24a, 53-363 Wrocław, Poland

⁴Department of Geobotany and Landscape Planning, Faculty of Biology and Environmental Protection, Nicolas Copernicus University, Lwowska 1, 87-100 Toruń, Poland

^CCorresponding author: marcinko@kielce.com.pl

(Smith and Olson, 2007). Airborne microorganisms are generally characterized by small size, high resistance to desiccation, specific preferences for pH, tolerating low nutrient levels, high conductivity, and most of them can be considered as cosmopolitan and distributed worldwide (Falasco et al., 2014). Gorbushina and Broughton (2009) suggested that airborne microorganisms are exposed to harsher and more variable environmental conditions than their aquatic counterparts where the surrounding water usually buffers abrupt changes of radiation and temperature. Many algal species living in aerial habitats are known to produce extracellular mucilage which aids in water retention (Gerrath, 2003). This mucilage contains a considerable amount of moisture and is common in airborne cyanobacterial genera, such as *Nostoc*, *Gloeotheca*, *Gloeocapsa*, and *Aphanocapsa*. Johansen et al. (1983) found that mucilage-producing cyanobacteria and green algae are the first colonizers on moist rock faces, and other algal species begin to colonize the mucilage. Algal cells have been found to be transported by wind, water, and animals, such as birds, bears, and humans (Kristiansen, 1996). Wind is mainly responsible for the atmospheric distribution of airborne microorganisms supplying new inoculum to barren substrata, thus contributing to the cosmopolitan distribution of many microorganisms (Gorbushina 2007). The ecological success of airborne microorganisms in environmentally-harsh habitats such as caves or building facades depends on many factors (Karsten et al., 2007). The nutrients used by organisms to survive, grow, and reproduce, can be supplied by rain, water, snow, aerosols, dust or soil particles, and big animals such as bears. The phototrophs can be transported the same way as the nutrients. In our study we defined the diversity of airborne microorganisms in the Główniowa Nyża Cave (High Tatra Mountains, Poland) and we explored morphological adaptations to microhabitat preference. We hypothesize that the presence of *Ursus arctos* influences distribution of airborne microorganisms.

Materials and Methods

Cave Description

The pseudokarstic Główniowa Nyża Cave is located in the High Tatra Mountains of Poland, in the Orla Ściana above the Roztoka Valley in the municipality of Bukowina Tatrzńska (Fig. 1). It was discovered in 29 March 2011 by Janusz Łukaszczyk during observation of a female bear with cubs coming out from the cave after wintering. Due to the necessity to protect the bear wintering place, the exact cave location is not given here. The cave entrance is exposed NE, and its measurements are: width 0.8 m, height 0.9 m, length 4.3 m, and it is situated at 1605 m a.s.l., but the relative height above the Roztoka Valley is 250 m (Fig. 2). The rocky cave bottom is covered by the plant materials brought in by the bear. The cave was formed on a slit in granitoids of the crystalline High Tatras, on a tectonic fracture. The cave is dry and illuminated by the daylight coming through the cave entrance. Its climate depends on outside atmospheric conditions. In the cave light zone close to the entrance, lit by sunlight and well-oxygenated, grow mosses, lichens, grasses, and ferns. Inside the cave the traces of wintering *Ursus arctos* such as the bear's den built with fur, mosses, grasses, and small tree twigs (*Picea abies*, *Pinus cembra* and *Pinus mugo*), excrement, marks of claws, and fur on the cave walls can be observed. In the whole cave one can find the insects and spiders whose presence confirm good ecological cave conditions (relatively high temperature, humidity, and availability of nutrients).

Sampling

In total, 3 samples were collected in August 2016 from the cave walls (granite A and B) and from twigs of *Pinus cembra* or *Pinus mugo* found inside the cave. The accurate identification of pine twigs was impossible due to the damage inflicted by bear, because the twigs were part of the bear's den. Each sample (greenish and blueish coloured patches) was scraped from cave walls or from pine twigs, placed into labeled sterile plastic bag, and transported to the lab. Material was transferred into Petri dishes with fresh agarized (1%) nutrient Bold's Basal Medium (Bischoff and Bold, 1963), and cultured at 20 °C in a 12-hour light/12-hour dark cycle at 3000 $\mu\text{Em}^{-2}\text{s}^{-1}\text{lx}$ provided by 40 W cool fluorescent tubes. A microscopic study of cultures began from the first appearance of microorganisms growth during two-three months of cultivation. All the phototrophs were observed in living states and identified using a light microscope Jenamed 2 (Carl Zeiss Jena). The cells for transmission electron microscopy (TEM) were processed according to Massalski et al. (1995) and microphotographs were taken with a TESLA BS 600. Airborne algae and cyanobacteria were identified using the following literature: Anagnostidis and Komárek (1988), Ettl and Gärtner (1995), Komárek and Anagnostidis (2005), and Rindi et al. (2010).

Measurement of Physical Parameters

Temperature T , relative humidity RH , and dew points DP were measured using the Extech Temperature Humidity Meter and Vellman DMV 1300 Luxmeter from September 26, 2017 to October 12, 2017. These parameters were measured 67 times at each sampling site on the same day. For each parameter the mean value with standard error was calculated (Fig. 3).

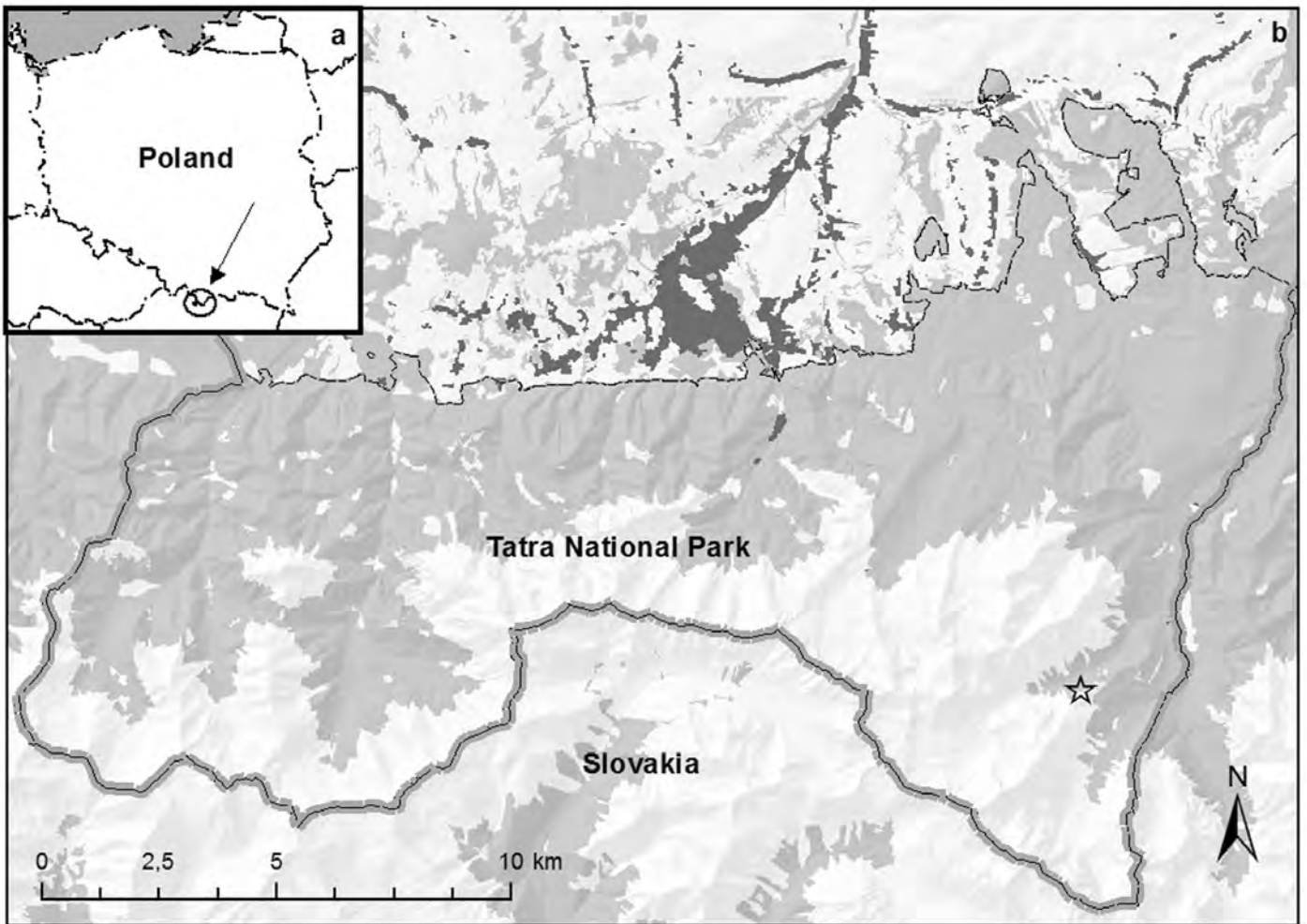


Figure 1. Map of Poland showing the location of the Główniowa Nyża Cave. A - A view of the High Tatra Mountains, southern Poland, B - A view of the Tatra National Park with marked location of cave (black star).

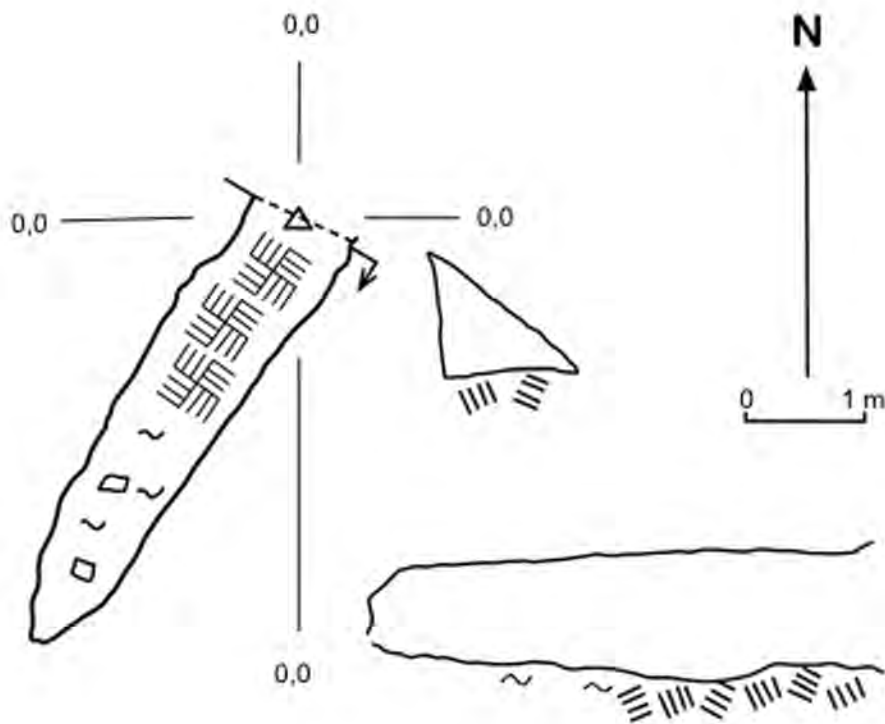


Figure 2. Survey of Główniowa Nyża Cave showing a corridor of the cave throughout the length of the cave profile; reproduced from Zwijacz-Kozica (2011). The symbols: four lines all labeled 0.0 are indicating entrance to the cave (origin of the local coordinate system); 3 sketches show: 1 – cave profile, 2 (small triangle) - cross section of the cave entrance (direction indicated by arrow on the cave), 3 - cross section of whole cave; soil - clusters of parallel lines.

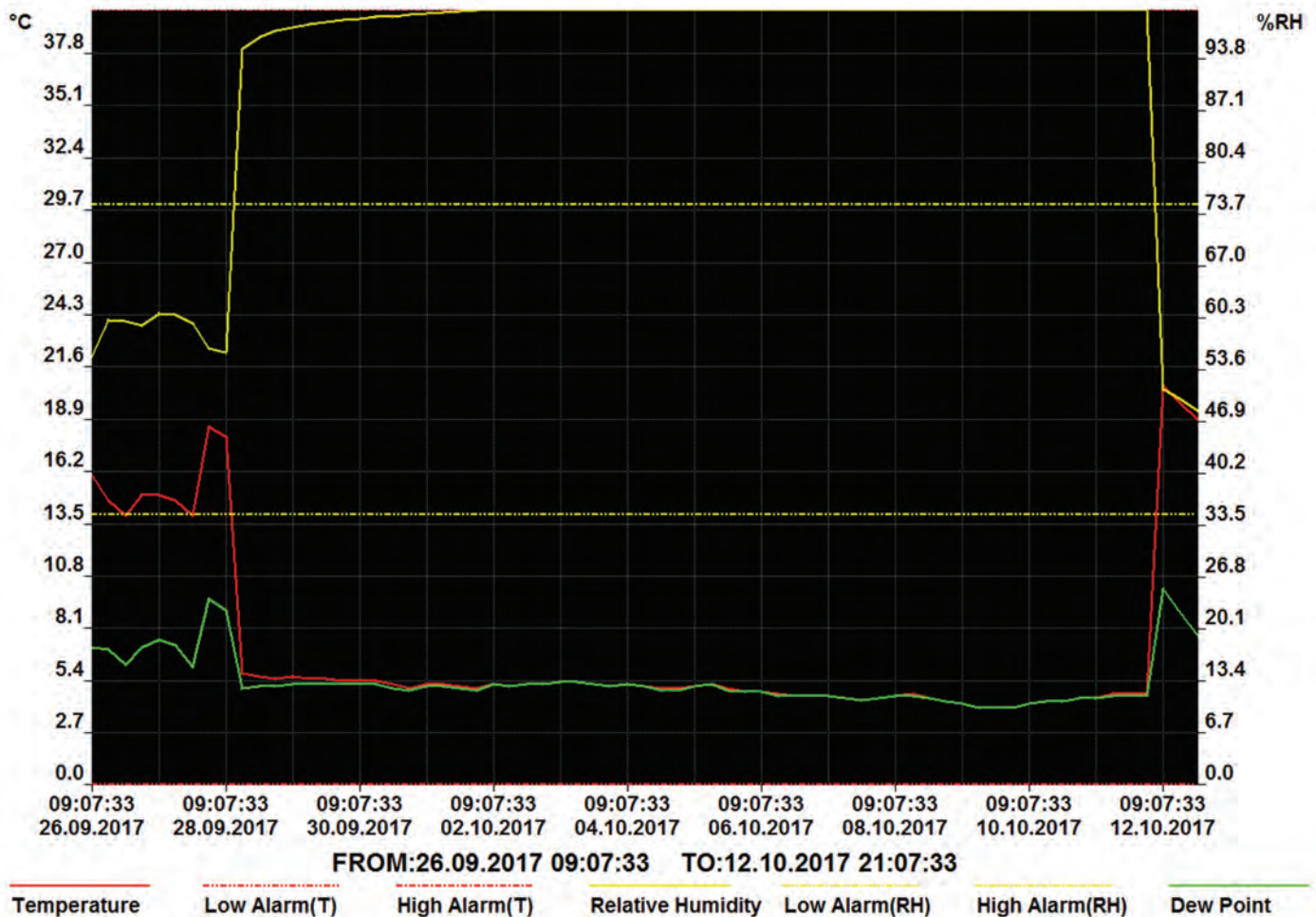


Figure 3. Plot of temperature, relative humidity and dew point values for the cave (from 26 September to 12 October 2017). Two sensors were installed in the bear's den.

Statistical Analysis

Microhabitat data analysis were presented as diagrams using software Statistica 9.0 (StatSoft Inc., 2009). The diagrams showed basic statistics for temperature, relative humidity, and dew point, i.e. average, standard error (SE) and standard deviation (SD) in the Główniowa Nyża Cave. Airborne algae and cyanobacteria species composition and frequency data recorded on three sampling sites (granite A and B, and pine twigs) were subjected to indirect analysis. PCA (Principal Component Analysis) were performed using Canoco 5.0 (ter Braak and Šmilauer, 2012). A graphical representation of this analysis was diagramed, where the vectors indicated sampling sites (particular species were marked by geometric symbols). The species names consisted of three letters of a generic name, dot, and three letters of a species name.

Results and Discussion

Temperature, relative humidity, and dew point were different across sampling sites, with average values 5.0 ± 18.0 , 48.3 ± 99.9 % and 4.0 ± 9.0 respectively (Fig. 4). The lowest T value (5°C) was in September, and highest (18°C) in October. The highest RH value was measured in the brown bear den (99.9 %) because the humidity sensor was placed inside of the den in which were bear excrements and urine, while the lowest RH value (48.3 %) was close to the cave entrance. The highest DP value was 4.0 and the lowest was 9.0. The presence of brown bear, temperature, and relative humidity were almost constant at all sampling sites, presumably due to their proximity. It is impossible to state whether all the measurements were taken during the presence of bear in the den. The measurements were recorded continuously regardless the bear presence or absence. While the average humidity of the majority of caves in Central Europe is about 85–95 % and the average temperature is in the range $5\text{--}8^\circ\text{C}$, whereas in the Główniowa Nyża Cave, the temperature and humidity at all sampling sites was higher. This dependency was due to the fact that all sampling sites were relatively close to the entrance where T and RH are influenced by the outside climatic conditions.

In total, 24 species of airborne algae and cyanobacteria were found in the pseudokarstic Główniowa Nyża Cave. The dominant group of phototrophs colonizing cave walls and pine twigs were the green algae and cyanobacteria. Ten

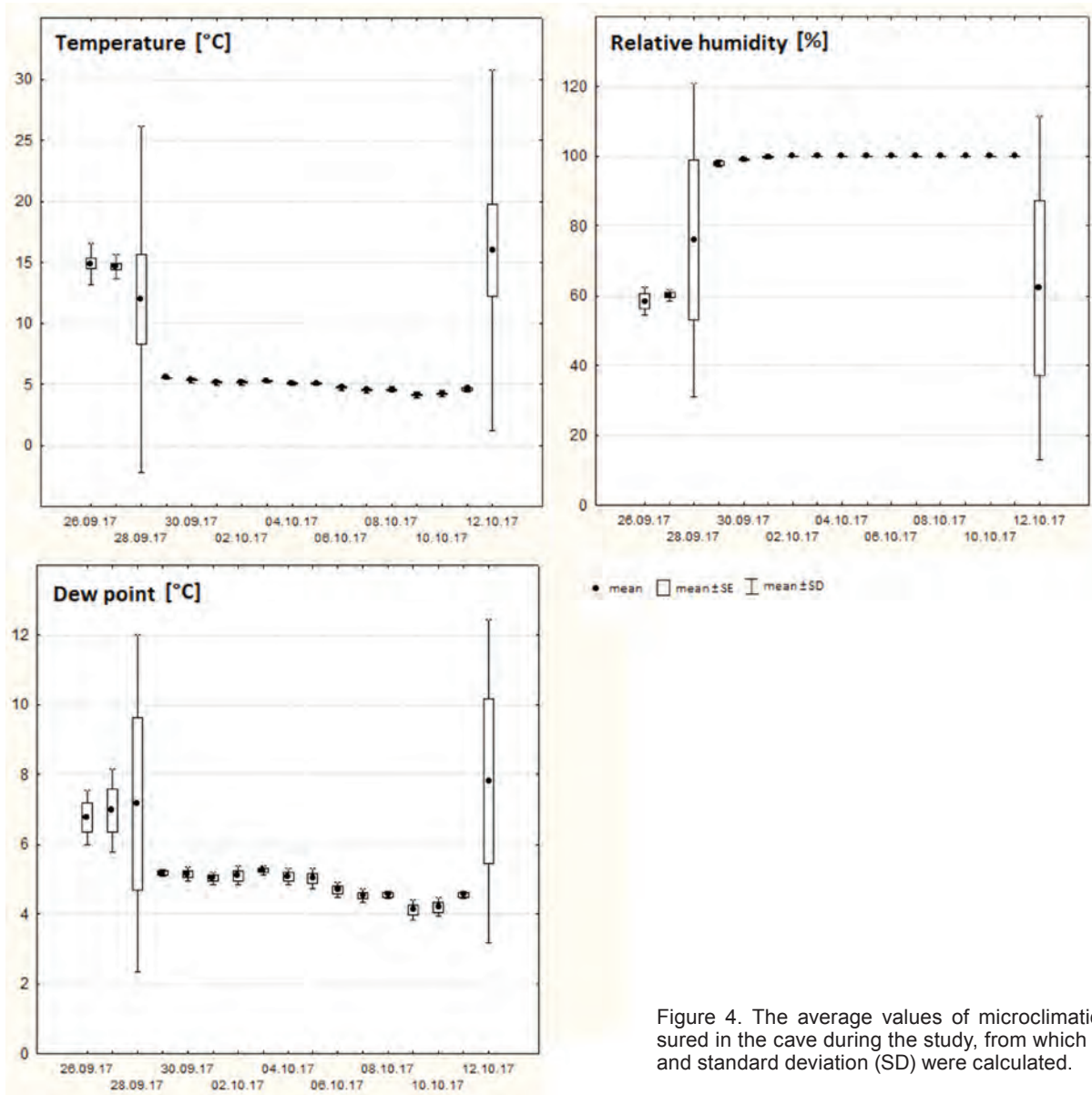


Figure 4. The average values of microclimatic parameters measured in the cave during the study, from which standard error (SE) and standard deviation (SD) were calculated.

Chlorophyta including genera: *Apatococcus*, *Asterochloris*, *Chroococcidiopsis*, *Coccomyxa*, *Klebsormidium*, *Pseudococcomyxa*, and *Stichococcus* were observed both on the cave walls and on the twigs, while *Desmodesmus olivaceus* and *Trentepohlia aurea* were present only on the cave walls (Figs 5-6). These species are typical for different lithophytic substrates in temperate zones. In our laboratory we observed that *Apatococcus minor* grew successfully on solid media (agar) which better mimics its natural growth conditions. It is not able to compete and is rapidly overgrown by other species. *Apatococcus minor* is characterized by different lifestyles and survival strategies, so it is classified as a K-strategist with low growth and mortality rates, long lifespans, and efficient resource utilization capacities (MacArthur and Wilson, 1967). Other airborne algal genera, such as *Coccomyxa* and *Stichococcus* exhibited two or three-fold higher growth rates under the described culture conditions (Gustavs et al., 2010). Consequently, the ecological success of these green algae do not originate from competitive strength based on growth rate but from long-time survival under harsh environmental conditions.

Only four airborne, cosmopolitan and widespread diatoms: *Brachysira* sp., *Hantzschia* sp., *Orthoseira roeseana*, and *Pinnularia borealis*, were identified. Diatoms living in the Główniowa Nyża Cave are generally characterized by small size, high resistance to desiccation, specific preferences for pH, and tolerating low nutrient levels. Therefore diatoms were not a significant contribution to the biodiversity of this caves microorganisms. Falasco et al. (2014) and Lauriol et al. (2006) stated that the size of the cave has an important effect on air circulation, and influence the diatom diversity in the deeper zones of caves. The Główniowa Nyża Cave is characteristic of small caves with only one main

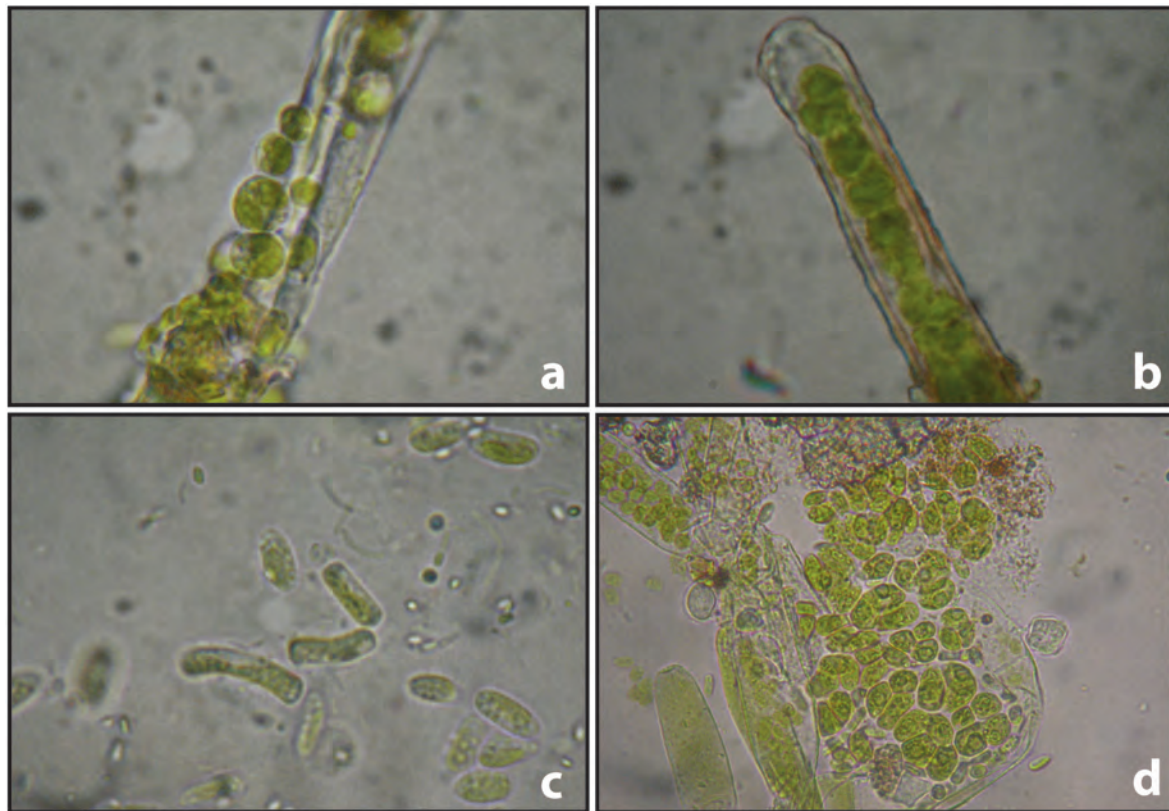


Figure 5. Culturable airborne algae from Główniowa Nyża Cave: a-b *Klebsormidium dissectum*, c - *Klebsormidium flaccidum*, d - *Desmococcus olivaceus*. Scale bars 10 μ m.

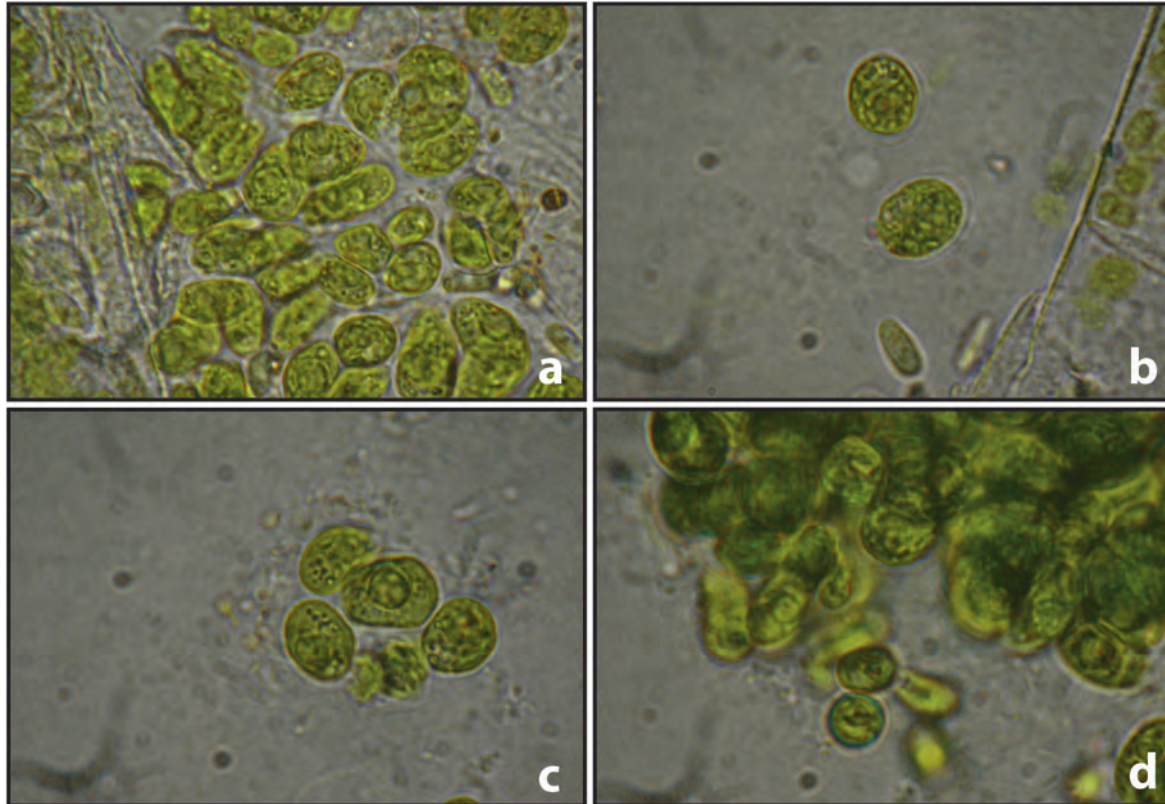


Figure 6. Green algae cells grown aerophytically on a BBM agar slant (Light Microscope view). a-b *Coccomyxa brevis*, c-d *Pseudococcomyxa ellipsoidea*. Scale bars 10 μ m.

entrance and is typical for brown bear hibernacula. It is possible that colonization of diatom spores being transported by air through the main entrance of cave were hampered because of high temperature and low humidity. Diatoms generally deposit on cave speleothems consequently to air condensation on the walls (Mulec and Kosi, 2009). Water circulation also plays an important role in the cave colonization. Diatom species entering the cave with water are generally adapted to oligotrophic conditions (Falasco et al., 2014). Krammer and Lange-Bertalot (1991) and Germain (1981) described *Orthoseira roeseana* as aerophilous and xerotic diatom species. It is commonly found on wet walls, moist stones and rocks, mosses, and even on the wet banks of the riparian vegetation (Houk, 2003), and in alkaline areas (Wehr and Sheath, 2003). Falasco et al. (2014) and Garbacki et al. (1999) reported that this species was usually in caves in the liminar zone, exposed to natural light, and Roldán and Hernández-Mariné (2009) found *Orthoseira roeseana* on artificially illuminated walls. It seems to be adapted to variable environments, on different substrates, both rocks and mosses, and was also found on a woody surface close to the main entrance (Škaloud, 2009). Our study confirmed this species presence only on the pine twigs. *Pinnularia borealis* is typically an aerophilous and epiphytic species (Taylor et al., 2007), often anemophilous (Krammer, 2000). It is one of the most frequently recorded taxa on submerged bryophytes (Van de Vijver and Beyens, 1997), occurring in wild caves close to the main entrance on very wet walls (Garbacki et al., 1999), but Hoffmann and Darienko (2005) also recorded it in caves opened for tourism. In the Główniowa Nyża Cave *Pinnularia borealis* was observed only sporadically on the pine twigs.

Cyanobacterial species were found mainly on the cave walls but only two taxa. *Chroococcus ercegovicii* and *Gloeocapsa bififormis*, were present on pine twigs. Ten cyanobacteria taxa in the genera *Aphanocapsa*, *Chroococcus*, *Gloeocapsa*, *Gloeotheca*, *Nostoc*, and *Scytonema* were found. The members of *Nostocales* are typical cyanobacteria among cave microhabitats. The members of the order Oscillatoriales are usually characteristic for caves, however there were not present in the studied cave. Among cyanobacteria, *Aphanocapsa muscicola* was found on the wall in the Główniowa Nyża Cave, but this species occurs in other microhabitats such as soil substrate, bryophytes, and rocks (Matuła et al., 2007). This species according to John et al. (2011) is very abundant on slightly basic substrata, shaded habitats, and is a component of some cyanobacterial mats. During laboratory cultivation, microscopic analyses revealed the presence of atypical cyanobacterial structure, such as single cells embedded in mucilage of dark green color, whereas *Aphanotheca saxicola* grows on wet rock surfaces forming mucilaginous blue-green thallus. This species found in the studied cave is also known from ornamental pools and fountains (Vinogradova, 1999) and as an epilithic cyanobacterium on rocky shores (Nagarkar, 1998). *Gloeocapsa atrata* among mosses is widespread on wet rocks and Główniowa Nyża Cave walls, and less commonly known from wet soil (John et al., 2011). During laboratory cultivation, microscopic analyses revealed the cells of *Gloeocapsa atrata* occurring in subcolonies with individual envelopes surrounded by colorless mucilaginous envelopes. *Gloeocapsa bififormis* in laboratory cultivation formed irregular colonies, dirty yellow or brownish, and yellow mucilaginous envelopes. The fact that three species *Gloeocapsa* genus were present at the Główniowa Nyża Cave indicates that the airborne microorganisms colonization on the walls is at an intermediate stage, and this agrees with Pentecost (1992), who considered all these species as pioneers in rock colonization. *Gloeotheca palea* grew on wet rocks and other granite surfaces, sometimes among mosses. *Nostoc commune* is the dominant species responsible for the formation of thick mats containing other airborne algae in the cave. The comparison between the cyanobacteria and algae from Główniowa Nyża Cave and three caves in Serbia (Popović et al. 2015), shows that in all four caves there is an abundance of Cyanobacteria, with chroococcalean taxa prevailing and species of the genus *Gloeocapsa*, which occur in various habitats with many different ecological characteristics, indicating its tolerance to a wide range of environmental conditions. Most of the documented cyanobacteria from the investigated caves were typical aerophytic species.

The occurrence frequency of every recorded species based on the observation of 3 samples from each sampling site is shown in Table 1. The ultrastructure of airborne algae and cyanobacteria cells was documented using TEM. The PCA analysis pointed out that micro-environmental factors such as temperature and water availability, and the type of materials used to build the bear's den influenced the distribution of the algae and cyanobacteria. The PCA analysis clearly distinguished the species associated with the brown bear's activity and the spruce twigs in the bear's den (Fig. 7) as presented on one side of the graph, while on the other side of the graph were cyanobacteria collected on the cave granite walls.

Airborne microorganisms can also be observed on hard substrates such as granite. Studies of algal and cyanobacteria on this substrate are very scarce and were carried out previously in Spain (Rifon-Lastra and Noguerol-Seoane, 2001), in Slovakia (Uher, 2010) and in the southern part of Ukraine (Mikhailyuk, 2013). Mikhailyuk and Darienko (2011) studied the epilithic, chasmoendolithic and epiphytic algae from granite outcrops in the south of Ukraine. The results showed that algae never formed macroscopic growth on bare surfaces and occurred only in 40% of the cultivated samples. Cavernicolous airborne microorganisms are rather rich and diverse. Vinogradova and Mikhailyuk (2009) pointed out that algae numbers in speleoecotopes from 340 species (Coûté and Chauveau, 1994) to 542 (Draganov, 1977), among them cyanobacteria account up to 60 % and the rest of the taxonomic groups vary from 1 % to 20 %. Albertano

Table 1. The list of the documented airborne algal and cyanobacterial species in the Główniowa Nyża Cave. Occurrence frequency: 1 = 20 %; 2 = 40 %; 3 = 60 %; 4 = 80 %; 5 = 100 % (after Popović et al., 2015).

Taxa	Granite A	Pine Twigs	Granite B
Chlorophyta			
<i>Apatococcus minor</i> Brand		1	
<i>Asterochloris pyriformis</i> Tschermak-Woess		3	1
<i>Chroococcidiopsis edaphica</i> Johansen et Flechtner		1	
<i>Coccomyxa brevis</i> (Vischer) Gärtner & Schragi	2	2	
<i>Desmococcus olivaceus</i> Brand			4
<i>Klebsormidium dissectum</i> (Gay) Ettl & Gärtner		3	
<i>Klebsormidium flaccidum</i> var. <i>lubricum</i> (Chodat) Ettl & Gärtner	1	1	
<i>Pseudococcomyxa ellipsoidea</i> Hindák		2	
<i>Stichococcus allas</i> Reisingl	2	2	
<i>Trentepohlia aurea</i> (Linnaeus) Martius	3		
Heterokontophyta			
Bacillariophyceae			
<i>Brachysira</i> sp.	1	1	
<i>Hantzschia</i> sp.		2	2
<i>Orthoseira roeseana</i> (Rabenhorst) Pfitzer		2	
<i>Pinnularia borealis</i> Ehrenberg		1	
Cyanophyta			
<i>Aphanocapsa muscicola</i> (Meneghini) Wille	2		
<i>Aphanothece saxicola</i> Nägeli			2
<i>Chroococcus ercegovicii</i> Komárek & Anagnostidis	1	2	
<i>Gloeocapsa atrata</i> Kützing	1		3
<i>Gloeocapsa biformis</i> Ercegovic	4	4	
<i>Gloeocapsa rupicola</i> Kützing	2		3
<i>Gloeothece palea</i> (Kützing) Rabenhorst	2		5
<i>Nostoc commune</i> Vaucher ex Bornet & Flahault	5		5
<i>Nostoc</i> sp.			2
<i>Scytonema mirabile</i> Bornet	2	2	

et al. (2003) suggested that in well illuminated caves, cyanobacteria, diatoms, and chlorophytes generally colonize lit rock walls causing physical and chemical damage. Pusz et al. (2018) described airborne fungal spores in five bear dens located within Tatra National Park in southern Poland. Thirteen species of fungi were cultured from which seven taxa were present in the Główniowa Nyża Cave.

In the Główniowa Nyża Cave, airborne algae and cyanobacteria are dominant organisms, and similar species are frequently encountered in European caves (Berberousse et al., 2006). These microorganisms were pioneer species because of their ability to grow diazotrophically (Gallon et al., 1991). Other members of the Oscillatoriales are well-adapted to extremely low irradiance compared to other filamentous cyanobacteria. Albertano et al. (2000) reported the occurrence of cyanobacteria on both marble and granite monuments in different Mediterranean countries. The dominant presence of filamentous cyanobacteria in stable conditions of low-light intensity and high relative humidity has been reported for different caves (Martinez and Asencio, 2010; Roldán and Hernández-Mariné, 2009). *Nostoc* is a cosmopolitan terrestrial genus that can endure desiccation, as well as very low temperatures (Dodds et al., 1995).

Mulec (2012) suggested that heterotrophic microorganisms tend to colonize parts of caves where nutrients have been introduced, such as areas near surface openings, underground rivers, sediments, and surfaces associated with animal excrement. However, Bastian et al. (2009) stated that many caves naturally face increased input of organic matter, while others are subjected to high anthropogenic impact due to drainage of polluted water into the underground or extensive tourist visits of show caves. The airborne algae and cyanobacteria in the Główniowa Nyża Cave can be subject to harsh environmental conditions such as an inconsistent availability of moisture, relative increased temperature, and the presence of brown bear. Airborne algae and cyanobacteria can survive frequent and prolonged periods

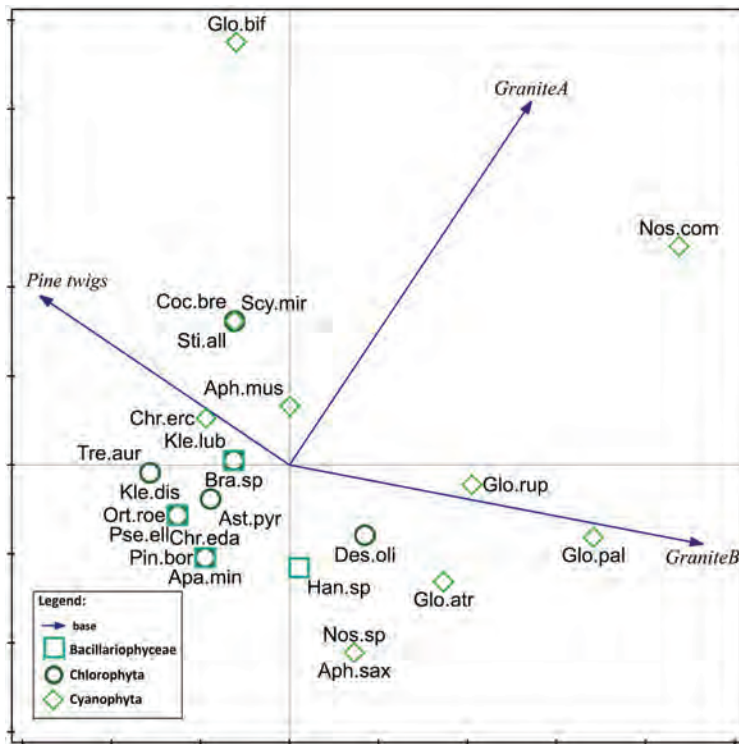


Figure 7. Principal Component Analysis (PCA) of sampling sites based on environmental parameters. The substrates (granite A, granite B and pine twigs) are marked with vectors and microorganisms as geometrical figures: b - square – diatoms (Bacillariophyceae), circle – green algae (Chlorophyta), rhomb – cyanobacteria (Cyanophyta). The 1st ordination axis accounted for 55.6 % of the total variability of data. Abbreviations of species names in Fig. 7 consist of three letters of a generic name and three letters of a species name.

Abbreviations of species names: *Apatococcus minor* (Apa. min.); *Aphanocapsa muscicola* (Aph. mus.); *Aphanothece saxicola* (Aph. sax.); *Asterochloris pyriformis* (Ast. pyr.); *Brachysira* sp. (Bra. sp.); *Chroococciopsis edaphica* (Chr. eda.); *Coccomyxa brevis* (Coc. bre.); *Chroococcus ercegovicii* (Chr. erc.); *Desmococcus olivaceus* (Des. oli.); *Hantzschia* sp. (Han. sp.); *Gloeocapsa atrata* (Glo. atr.); *Gloeocapsa bififormis* (Glo. bif.); *Gloeocapsa rupicola* (Glo. rup.); *Gloeothece palea* (Glo. pal.); *Klebsormidium dissectum* (Kle. dis.); *Klebsormidium flaccidum* var. *lubricum* (Kle. lub.); *Nostoc commune* (Nos. com.); *Nostoc* sp. (Nos. sp.); *Orthoseira rooseana* (Ort. roe.); *Pinnularia borealis* (Pin. bor.); *Pseudococcomyxa ellipsoidea* (Pse. ell.); *Scytonema mirabile* (Scy. mir.); *Stichococcus allas* (Sti. all.); *Trentepohlia aurea* (Tre. aur.).

of desiccation, and moisture availability has been found to be an important factor regulating the algal abundance in these habitats (Lopez-Bautista et al., 2007). Cyanobacteria have been found to dominate communities in aerial habitats (Matthes-Sears et al., 1999) and are also often the first algal colonizer in cave aerial habitats. The tolerance of many cyanobacterial species to a wide range of moisture and light may contribute to their dominance (Whitton and Potts, 2000), and they are able to survive and recover more quickly from desiccation than other microorganism (De Winder et al., 1989).

Species dispersal may play a role in similarities seen between the green algae, cyanobacteria, and diatoms of this cave. Airborne algae have been shown to be easily transported by the wind and animals. Taxa that can withstand desiccation have the potential to survive aerial transport. Many algal species from aerial habitats produce extracellular mucilage which allows them to withstand periods of desiccation (Gerrath, 2003). UV radiation can also influence the survival of cells in aerial transport. Ehling-Schultz et al. (1997) suggested that ability of cyanobacteria to not only withstand desiccation but also to produce photoprotective pigments gives them a competitive advantage for longer distance aerial transport. Johansen et al. (1983) and Röss and Lowe (2013) found that mucilage-producing cyanobacteria and green algae are the first colonizers on moist rock faces, and once established, other species begin to colonize the mucilage. Nutrient availability may play a role in shaping the structure of aerial algae due to possible nutrient limitation in these habitats (Johansen et al., 1983). The ecological phenomena seem to have an influence on the distribution of airborne microalgae in the Cave.

Conclusion

24 species of airborne microorganisms were cultivated from samples collected from various habitats in the pseudokarstic Główniowa Nyża Cave in the High Tatra Mountains, southern Poland. These phototrophs using LM and TEM microscopy were identified only from cultivated samples, but not directly from field specimens. In the present work, the diversity of algae and cyanobacteria as the main phototrophic microorganisms colonizing the cave surfaces were studied. There was no correlation between species diversity and physical parameters (temperature and humidity). An investigation of the diversity of airborne microorganisms and presence of brown bear in the Główniowa Nyża Cave were conducted for the first time in Poland.

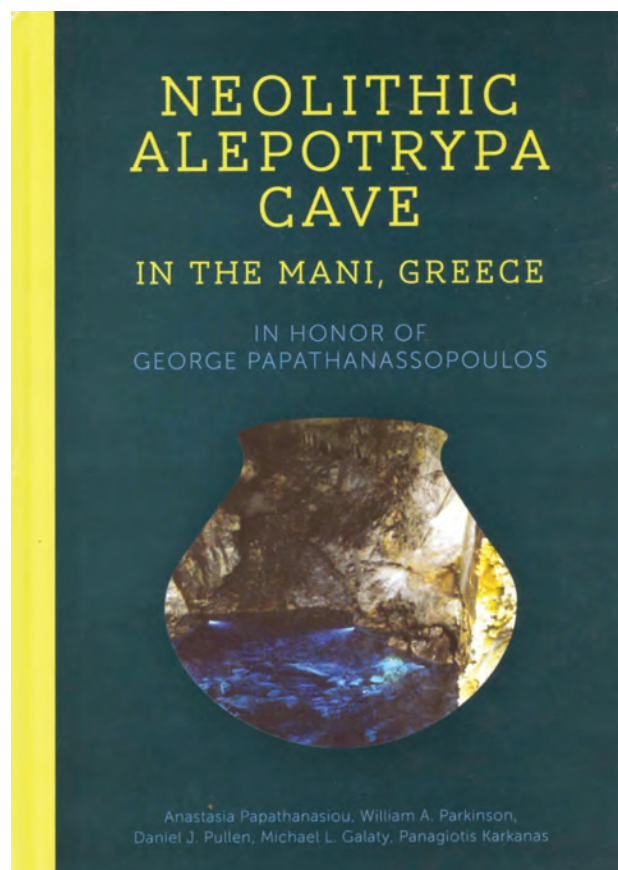
Acknowledgements

We thank Prof. Andrzej Massalski for valuable comments on the manuscript, and PhD Piotr Rafalski for the useful discussion about the statistical methods. Thanks go to anonymous reviewers for improving the manuscript.

References

- Albertano, P., Moscone, D., Palleschi, G., Hermosin, B., Saiz-Jimenez, C., Sanchez-Moral, S., Hernández-Mariné, M., Urzú, C., Groth, I., Schroeckh, V., Saarela, M., Mattila-Sandholm, T., Gallon, J.R., Graziottin, F., Bisconti, F. and Giuliani, R., 2003, Cyanobacteria attack rocks (CATS): Control and preventive strategies to avoid damage caused by cyanobacteria and associated microorganisms in Roman hypogean monuments: *in* Saiz-Jimenez, C., ed, *Molecular Biology and Cultural Heritage*, Lisse: Swets and Zeitlinger, p. 151–162.
- Albertano, P., Bruno, L., D'Ottavi, D., Moscone, D. and Palleschi, G., 2000, Effect of photosynthesis on pH variation in cyanobacterial biofilms from Roman catacombs: *Journal of Applied Phycology*, v. 12, p. 279–384. <https://doi.org/10.1023/A:1008149529914>.
- Anagnostidis, K. and Komárek, J., 1988, Modern approach to the classification system of Cyanophytes. 3. Oscillatoriales: *Archiv für Hydrobiologie*, Supplement, v. 80, p. 327–472.
- Barberousse, H., Tell, G., Yepremian, C. and Couté, A., 2006, Diversity of algae and cyanobacteria growing on building facades in France: *Algalogical Studies*, v. 120, no. 1, p. 81–105. <https://doi.org/10.1127/1864-1318/2006/0120-0081>.
- Bastian, F., Alabouvette, C. and Saiz-Jimenez, C., 2009, The impact of arthropods on fungal community structure in Lascaux Cave: *Journal of Applied Microbiology*, v. 106, p. 1456–1462. <https://doi.org/10.1111/j.1365-2672.2008.04121.x>.
- Bischoff, H.W. and Bold, H.C., 1963, *Phycological Studies IV. Some soil algae from Enchanted Rock and related algal species*: University of Texas Publications, Austin, no. 6318, p. 1–95.
- Coûté, A.D. and Chauveau, O., 1994, Algae: *in* Juberthie, C. and Decu, V., eds, *Encyclopaedia biospeologica Tome 1*. Société de Biospéologie, Moulis, Bucarest, p. 371–380.
- Dayner, D.M. and Johansen, J.R., 1991, Observations on the algal flora of Seneca Cavern, Seneca County, Ohio: *Ohio Journal of Science*, v. 91, no. 3, p. 118–121.
- De Winder, B., Matthijs, H.C.P. and Mur, L.R., 1989, The role of water retaining substrata on the photosynthetic response of three drought tolerant phototrophic micro-organisms isolated from a terrestrial habitat: *Archives of Microbiology*, v. 152, p. 458–462. <https://doi.org/10.1007/BF00446929>.
- Dodds, W.K., Gudder, D.A. and Mollenhauer, D., 1995, The ecology of Nostoc: *Journal of Phycology*, v. 31, no. 1, p. 2–18. <https://doi.org/10.1111/j.0022-3646.1995.00002.x>.
- Draganov, S., 1977, Taxonomic structure of cave algal flora: *in* Proc. 7th International Congress of Speleology, Sheffield, England, p. 155–156.
- Ehling-Schultz, M., Bilger, W. and Scherer, S., 1997, UV-B-induced synthesis of photoprotective pigments and extracellular polysaccharides in the terrestrial cyanobacterium *Nostoc commune*: *Journal of Bacteriology*, v. 179, no. 6, p. 1940–1945. <https://doi.org/10.1128/jb.179.6.1940-1945.1997>.
- Ettl, H. and Gärtner, G., 1995, *Syllabus der Boden-, Luft- und Flechtenalgen*: Gustav Fischer, Stuttgart, Jena, New York, p. 1–721.
- Falasco, E., Ector, L., Isaia, M., Wetzell, C.E., Hoffmann, L. and Bona, F., 2014, Diatom flora in subterranean ecosystems: a review: *International Journal of Speleology*, v. 43, no. 3, p. 231–251. <https://doi.org/10.5038/1827-806X.43.3.1>.
- Gallon, J.R., Hashem, M.A. and Chaplin, A.E., 1991, Nitrogen fixation by *Oscillatoria* sp. under autotrophic and photoheterotrophic conditions: *Journal of General Microbiology*, v. 137, p. 31–39. <https://doi.org/10.1099/00221287-137-1-31>.
- Garbacki, N., Ector, L., Kostikov, I. and Hoffmann, L., 1999, Contribution to the study of the flora of caves in Belgium: *Belgian Journal of Botany*, v. 132, no. 1, p. 43–76.
- Germain, H., 1981, Flore des Diatomophycées eaux douces et saumâtres du Massif Armoricain et des contrées voisines d'Europe occidentale: Collection „Faunes et Flores Actuelles“, Société Nouvelles des Editions Boublée, Paris, p. 1–444.
- Gerrath, J.F., 2003, Conjugating green algae and desmids: *in* Wehr, J.D. and Sheath, R.G., eds, *Freshwater algae of North America. Ecology and classification*: Elsevier, New York, p. 353–382. <https://doi.org/10.1016/B978-012741550-5/50010-6>.
- Gorbushina, A., 2007, Life on the rocks: *Environmental Microbiology*, v. 9, p. 1613–1631. <https://doi.org/10.1111/j.1462-2920.2007.01301.x>.
- Gorbushina, A.A. and Broughton, W.J., 2009, Microbiology of the atmosphere-rock interface: how biological interactions and physical stresses modulate a sophisticated microbial ecosystem: *Annual Review of Microbiology*, v. 63, p. 431–450. <https://doi.org/10.1146/annurev.mi-cro.091208.073349>.
- Gustavs, L., Eggert, A., Michalik, D. and Karsten, U., 2010, Physiological and biochemical responses of green microalgae from different habitats to osmotic and matric stress: *Protoplasma*, v. 243, p. 3–14. <https://doi.org/10.1007/s00709-009-0060-9>.
- Hoffmann, L. and Darienko, T., 2005, Algal biodiversity on sandstone in Luxembourg: *Ferrantia*, v. 44, p. 99–101.
- Houk, V., 2003, Atlas of freshwater centric diatoms with a brief key and descriptions. Part I. Melosiraceae, Orthosiraaceae, Paraliaceae and Aulacoseiraceae: *Czech Phycology Supplement*, v. 1, p. 1–112.
- Johansen, J.R., Rushfort, S.R., Orbendorfer, R., Fungladda, N. and Grimes, J.A., 1983, The algal flora of selected wet walls in Zion National Park, Utah, USA: *Nova Hedwigia*, v. 38, p. 765–808.
- John, D.M., Whitton, B.A., and Brook, A.J., 2011, *The Freshwater Algal Flora of the British Isles: An Identification Guide to Freshwater and Terrestrial Algae*: Cambridge University Press, Cambridge, p. 41–896.
- Karsten, U., Lembcke, S. and Schumann, R., 2007, The effects of ultraviolet radiation on photosynthetic performance, growth and sunscreen compounds in aeroterrestrial biofilm algae isolated from building facades: *Planta*, v. 225, p. 991–1000. <https://doi.org/10.1007/s00425-006-0406-x-Source>.
- Komárek, J. and Anagnostidis, K., 2005, Cyanoprokaryota 2. Oscillatoriales: *in*: Büdel, B., Krienitz, L., Gärdner, G. and Schagerl, M., eds, *Süßwasserflora von Mitteleuropa 19/2*, Elsevier, Spektrum, Heidelberg, p. 1–759.
- Krammer, K., 2000, The genus *Pinnularia*: *in*: Lange-Bertalot, H. ed, *Diatoms of Europe. Diatoms of the European Inland Waters and Comparable Habitats*, Ruggel, ARG Gantner Verlag, v.1, p. 703.
- Krammer, K. and Lange-Bertalot, H., 1991, *Bacillariophyceae*. 3. *Centrales, Fragilariaceae, Eunotiaceae*: *in*: Ettl, H., Gerloff, J., Heynig, H. and Mollenhauer, D. eds, *Süßwasser von Mitteleuropa*, Stuttgart. Band 2/3, Gustav Fischer Verlag, Stuttgart, p. 576.
- Kristiansen, J., 1996, Dispersal of freshwater algae – a review: *Hydrobiologia*, v. 336, p. 151–157. <https://doi.org/10.1007/BF00010829>.
- Lauriol, B., Prévost, Cl. and Lacelle, D., 2006, The distribution of diatom flora in ice caves of the northern Yukon Territory, Canada: relationship to air circulation and freezing: *International Journal of Speleology*, v. 35, no. 2, p. 83–92. <http://doi.org/10.5038/1827-806X.35.2.4>.
- Linnell, J.D.C., Barnes, B., Swenson, J.E., Andersen, R., 2000, How vulnerable are denning bears to disturbance?: *Wildlife Society Bulletin*, v. 28, p. 400–413.
- Lopez-Bautista, J.M., Rindi, F. and Casamatta, D., 2007, The systematics of subaerial algae: *in*: Seckbach, J. ed, *Algae and Cyanobacteria in Extreme Environments*: p. 599–617. https://doi.org/10.1007/978-1-4020-6112-7_33.
- MacArthur, R.H. and Wilson, E.O., 1967, *The Theory of Island Biogeography*: University Press, Princeton, p. 215.

- Martinez, A. and Asencio, A.D. 2010, Distribution of cyanobacteria at the Gelada Cave (Spain) by physical parameters: *Journal of Cave and Karst Studies*, v. 72, p. 11–20. <https://doi.org/10.4311/jcks2009lsc0082>.
- Massalski, A., Mrozińska, T. and Olech, M., 1995, *Lobococcus irregularis* (Boye-Pet.) Reislgl var. *antarcticus* var.nov. (Chlorellales, Chlorophyta) from King George Island, South Shetland Islands, Antarctica and its ultrastructure: *Nova Hedwigia*, v. 61, p. 199–206.
- Matthes-Sears, U., Gerrath, J.A., Gerrath, J.F. and Larson, D.W., 1999, Community structure of epilithic and endolithic algae and cyanobacteria on cliffs of the Niagara Escarpment: *Journal of Vegetation Science*, v. 10, no. 4, p. 587–598. <https://doi.org/10.2307/3237193>.
- Matuła, J., Pietryka, M., Richter, D. and Wojtuń, B., 2007, Cyanoprokaryota and algae of Arctic terrestrial ecosystems in the Hornsund area, Spitsbergen: *Polish Polar Research*, v. 28, no. 4, p. 283–316.
- Mikhailyuk, T.I., 2013, Terrestrial algae from the granite outcrops of River Valleys of the Ukraine: *International Journal on Algae*, v. 15, no. 4, p. 313–332. <https://doi.org/10.1615/InterJAlgae.v15.i4.20>.
- Mikhailyuk, T.I. and Darienko, T.M., 2011, Algae of terrestrial habitats of NNP Gutsulschina: *Phytosociocentre*, p. 142–151.
- Mulec, J., 2012, Lampenflora, in: White, W.B. and Culver, D.C. eds, *Encyclopedia of Caves*: Academic Press, Amsterdam, p. 451–456. doi: 10.1016/B978-0-12-383832-2.00064-5.
- Mulec, J. and Kosi, G., 2009, Lampenflora algae and methods of growth control: *Journal of Cave and Karst Studies*, v. 71, no. 2, p. 109–115.
- Mulec, J., Kosi, G. and Vrhovšek, D., 2008, Characterization of cave aerophytic algal communities and effects of irradiance levels on production of pigment: *Journal of Cave and Karst Studies*, v. 70, no. 1, p. 3–12.
- Mysterud, I., 1983, Characteristics of summer beds of European brown bears in Norway: *International Conference on Bear Research and Management*, v. 5, p. 1–208. <https://doi.org/10.2307/3872540>.
- Nagarkar, S., 1998, New records of marine cyanobacteria from rocky shores of Hong Kong: *Botanica Marina*, v. 41, no. 6, p. 527–542. <http://doi:10.1515/botm.1998.41.1-6.527>.
- Nestupa, J. and Štifterová, A., 2013, Distribution patterns of subaerial corticolous microalgae in two European regions: *Plant Ecology and Evolution*, v. 146, p. 279–289. <https://doi.org/10.5091/plecevo.2013.862>.
- Nielsen, S.E., McDermid, G.J., Stenhouse, G.B. and Boyce, M.S., 2010, Dynamic wildlife habitat models: seasonal foods and mortality risk predict occupancy-abundance and habitat selection in grizzly bears: *Biological Conservation*, v. 143, no. 7, p. 1623–1634. <https://doi.org/10.1016/j.biocon.2010.04.007>.
- Niefeld, M.J., Wilk, K. Woolnough and Hoskin, B., 1985, Wildlife habitat requirement summaries for selected wildlife species in Alberta: Wildlife resource inventory unit, Alberta Energy and Natural Resources. ENR Technical Report Number T/23.
- Pedersen, K., 2000, Exploration of deep intraterrestrial microbial life: current perspective: *MiniReview, FEMS Microbiology Letters*, v. 185, p. 9–16. <https://doi.org/10.1111/j.1574-6968.2000.tb09033.x>.
- Pentecost, A., 1992, A note on the colonization of limestone rocks by *cyanobacteria*: *Archiv für Hydrobiologie*, v. 124, p. 167–172.
- Popović, S., Subakov Simić, G., Stupar, M., Unković, N., Predojević, D., Jovanović, J. and Ljaljević, G., 2015, Cyanobacteria, algae and microfungi present in biofilm from Božana Cave (Serbia): *International Journal of Speleology*, v. 44, no. 2, p. 141–140. <https://doi.org/10.5038/1827-806X.44.2.4>.
- Pusz, W., Baturo-Cieśniewska, A. and Zwijacz-Kozica, T. 2018, Culturable Fungi in Brown Bear Cave Dens: *Polish Journal of Environmental Studies*, v. 27, no. 1, p. 247–255.
- Pusz, W., Baturo-Cieśniewska, A. and Zwijacz-Kozica, T., 2017, Culturable fungi in brown bear cave dens: *Polish Journal of Environmental Studies*, v. 27, no. 1, p. 1–9.
- Ress, R.J. and Lowe, R.L., 2013, Contrast and comparison of aerial algal communities from two distinct regions in the U.S.A., the Great Smoky Mountains National Park (TN) and the Lake Superior region: *Fottea*, v. 13, no. 2, p. 165–172. <https://doi.org/10.5507/fof.2013.014>.
- Rifon-Lastra, A. and Nogueroles-Seoane, A., 2001, Green algae associated with the granite walls of monuments in Galicia (NW Spain): *Cryprogamie Algologie*, v. 22, p. 305–326. [https://doi.org/10.1016/S0181-1568\(01\)01069-8](https://doi.org/10.1016/S0181-1568(01)01069-8).
- Rindi, F., Allali, H.A., Lam, D.W. and López-Bautista, J.M., 2010, An overview of the biodiversity and biogeography of terrestrial green algae: in: Rescigno, V. and Maletta, S. eds, *Biodiversity hotspots*. Nova Science Publishers, New York, p. 105–122.
- Roldán, M. and Hernández-Mariné, M., 2009, Exploring the secrets of the three-dimensional architecture of phototrophic biofilms in caves: *International Journal of Speleology*, v. 38, p. 41–53. <https://doi.org/10.5038/1827-806X.38.1.5>.
- Škaloud, P., 2009, Species composition and diversity of aero-terrestrial algae and cyanobacteria of the Boreč Hill ventaroles: *Fottea*, v. 9, p. 65–80. <https://doi.org/10.5507/fof.2009.006>.
- Smith, T. and Olson, R., 2007, A taxonomic survey of Lamp flora (Algae and Cyanobacteria) in electrically lit passages within Mammoth Cave National Park, Kentucky: *International Journal of Speleology*, v. 36, no. 2, p. 105–114. <https://doi.org/10.5038/1827-806X.36.2.6>.
- Taylor, J.C., Harding, W.R. and Archibald, C.G.M., 2007, *An Illustrated Guide to Some Common Diatom Species from South Africa*: Water Research Commission, Pretoria, Report TT 282/07, 34 + 12 p. and 178 pls.
- Ter Braak, C.J.F. and Šmilauer, P., 2012, *Canoco Reference Manual and User's Guide: Software for Ordination (version 5.0)*: Microcomputer Power (Ithaca, NY, USA), p. 496.
- Uher, B., 2010, Cyanobacteria and algae as significant actors of biodeterioration: Saarbrücken, LAP Lambert Academic Publishing AG and Co. KG, p. 161.
- Van de Vijver, B. and Beyens, L., 1997, The epiphytic diatom flora of mosses from Strømness Bay area, South Georgia: *Polar Biology*, v. 17, p. 492–501. <https://doi.org/10.1007/s003000050148>.
- Vinogradova, O.N., 1999, Species composition and distribution of Cyanophyta in water bodies of the Mountain Crimea (Ukraine): *International Journal on Algae*, v. 1, no. 2, p. 76–87. <https://doi.org/10.1615/InterJAlgae.v1.i2.70>.
- Vinogradova, O.N. and Mikhailyuk, T.I., 2009, Algal flora of the caves and grottoes of the National Nature Park "Podilsky Tovtry" (Ukraine): *International Journal on Algae*, v. 11, p. 289–404. <https://doi.org/10.1615/InterJAlgae.v11.i3.80>.
- Vinogradova, O.N., Wasser, S.P. and Nevo, E., 2009, Algae of the Sefunim Cave (Israel): species, diversity affected by light, humidity and rock stresses: *International Journal on Algae*, v. 11, no. 2, p. 99–116. <https://doi.org/10.1615/InterJAlgae.v11.i2.10>.
- Wehr, J.D. and Sheath, R.G., 2003, *Freshwater habitats of algae*: in: Wehr, J.D. and Sheath, R.G. eds, *Freshwater algae of North America: ecology and classification*, Academic Press, San Diego.
- Whitton, B.A., 2012, *Ecology of Cyanobacteria II. Their Diversity in Space and Time*: Springer Science+Business Media B.V., p. 706. <https://doi.org/10.1007/978-94-007-3855-3>.
- Whitton, B.A. and Potts, M., 2000, *The ecology of cyanobacteria. The diversity in time and space*: Springer Netherlands, p. 669. <https://doi.org/10.1007/0-306-4685507>.
- Zedrosser, A., Dahle, B., Swenson, J. and Gerstl, N., 2001, Status and management of the brown bear in Europe: *Ursus*, v. 12, p. 9–20.
- Zwijacz-Kozica, T., 2011, Protected or not protected, Tatra Mountains: *Tatra National Park*, p. 56–58.



Neolithic Alepotrypa Cave in the Mani, Greece: in honor of George Papathanassopoulos

Papathanasiou, A., Parkinson, W.A., Pullen, D.J., Galaty, M.L., and Karkanis, P. (eds.), 2018, 1950 Lawrence Rd., Havertown, PA 19083, Oxbow Books, 464 p., 8.3 x 11.7 inches, Hardcover: ISBN 9781785706486, \$110.00, Digital: ISBN 9781785706493.

This book is written for archaeologists and includes detailed, scholarly descriptions of excavations made in Alepotrypa Cave, at Diros Bay, Lakonia, Greece. It commemorates work done there by George Papathanassopoulos from 1970 to 2006. The cave was used during the Neolithic c 6000 to 3200 BC after which the cave entrance collapsed sealing the cave until recent times. This significantly increased the importance of the Neolithic material in the cave by preserving biological material, large numbers of artifacts, undisturbed deposits and the large floor space used by past humans. It is the richest site of its kind in Greece and in fact in Europe. The cave has an outer and an inner section which ends in a lake and was used as living space and for burials.

There are 23 chapters by various authors beginning with an introduction to the area. Other chapters concentrate on specific topics such the sequence of absolute radiocarbon dates, the distribution of human bones often reburied in prominent piles, imported chipped obsidian tools, pottery, grinding tools and bone awls. The chapters include careful catalogs with photos of what was found along with interpretations. Examination of human bones showed people had chronic nutritional deficiency and led lives of strenuous physical activity living to an average age of about 29 years. From examination of biological remains, it was found they had domesticated animals and ate mainly sheep, goats and pigs. There is also strong evidence for dairy goods. Grains were ground but were not stored in the cave. The archeology shows that the Neolithic people repeatedly left artifacts as well as human bones in similar arrangements suggesting ritual and a continuous remembrance of the dead.

The book contains a great deal of information and interesting interpretations; however, because the book is very detailed, it would appeal most to those specializing in archaeology. It is not a regional interpretation, but specific to one cave. Reproduction of artifacts and drafting are excellent, and many graphs and tables are included to supplement the text.

Reviewed by Margaret Palmer, 619 Winney Hill Rd., Oneonta, NY 13820

GUIDE TO AUTHORS

The *Journal of Cave and Karst Studies* is a multidisciplinary journal devoted to cave and karst research. The *Journal* is seeking original, unpublished manuscripts concerning the scientific study of caves or other karst features. Authors do not need to be members of the National Speleological Society, but preference is given to manuscripts of importance to North American speleology.

LANGUAGES: The *Journal of Cave and Karst Studies* uses American-style English as its standard language and spelling style, with the exception of allowing a second abstract in another language when room allows. In the case of proper names, the *Journal* tries to accommodate other spellings and punctuation styles. In cases where the Editor-in-Chief finds it appropriate to use non-English words outside of proper names (generally where no equivalent English word exist), the *Journal* italicizes them. However, the common abbreviations i.e., e.g., et al., and etc. should appear in roman text. Authors are encouraged to write for our combined professional and amateur readerships

CONTENT: Each paper will contain a title with the authors' names and addresses, an abstract, and the text of the paper, including a summary or conclusions section. Acknowledgments and references follow the text. Manuscripts should be limited to 6,000 words and no more than 10 figures and 5 tables. Larger manuscripts may be considered, but the *Journal* reserves the right to charge processing fees for larger submissions.

ABSTRACTS: An abstract stating the essential points and results must accompany all articles. An abstract is a summary, not a promise of what topics are covered in the paper.

STYLE: The *Journal* consults The Chicago Manual of Style on most general style issues.

REFERENCES: In the text, references to previously published work should be followed by the relevant author's name and date (and page number, when appropriate) in brackets. All cited references are alphabetical at the end of the manuscript with senior author's last name first, followed by date of publication, title, publisher, volume, and page numbers. Geological Society of America format should be used (see http://www.geosociety.org/documents/gsa/pubs/GSA_RefGuide_Examples.pdf). Please do not abbreviate periodical titles. Web references are acceptable when deemed appropriate. The references should follow the style of: Author (or publisher), year, Webpage title: Publisher (if a specific author is available), full URL (e.g., <http://www.usgs.gov/citguide.html>), and the date the website was accessed in brackets. If there are specific authors given, use their name and list the responsible organization as publisher. Because of the ephemeral nature of websites, please provide the specific date. Citations within the text should read: (Author, Year).

SUBMISSION: Manuscripts are to be submitted via the PeerTrack submission system at <http://www.edmgr.com/jcks/>. Instructions are provided at that address. At your first visit, you will be prompted to establish a login and password, after which you will enter information about your manuscript and upload your manuscript, tables, and figure files. Manuscript files can be uploaded as DOC, WPD, RTF, TXT, or LaTeX. Note: LaTeX files should not use any unusual style files; a LaTeX template and BiBTeX file may be obtained from the Editor-in-Chief. Table files can be uploaded as DOC, WPD, RTF, TXT, or LaTeX files and figure files can be uploaded as TIFF, AI, EPS, or CDR files. Extensive supporting data may be placed on the *Journal's* website as supplemental material at the discretion of the Editor-in-Chief. The data that are used within a paper must be made available upon request. Authors may be required to provide supporting data in a fundamental format, such as ASCII for text data or comma-delimited ASCII for tabular data.

DISCUSSIONS: Critical discussions of papers previously published in the *Journal* are welcome. Authors will be given an opportunity to reply. Discussions and replies must be limited to a maximum of 1000 words and discussions will be subject to review before publication. Discussions must be within 6 months after the original article appears.

MEASUREMENTS: All measurements will be in Systeme Internationale (metric) except when quoting historical references. Other units will be allowed where necessary if placed in parentheses and following the SI units.

FIGURES: Figures and lettering must be neat and legible. Figure captions should be on a separate sheet of paper and not within the figure. Figures should be numbered in sequence and referred to in the text by inserting (Fig. x). Most figures will be reduced, hence the lettering should be large. Photographs must be sharp and high contrast. Figures must have a minimum resolution of 300 dpi for acceptance. Please do not submit JPEG images.

TABLES: See <http://caves.org/pub/journal/PDF/Tables.pdf> to get guidelines for table layout.

COPYRIGHT AND AUTHOR'S RESPONSIBILITIES: It is the author's responsibility to clear any copyright or acknowledgement matters concerning text, tables, or figures used. Authors should also ensure adequate attention to sensitive or legal issues such as land owner and land manager concerns or policies and cave location disclosures.

PROCESS: All submitted manuscripts are sent out to at least two experts in the field. Reviewed manuscripts are then returned to the author for consideration of the referees' remarks and revision, where appropriate. Revised manuscripts are returned to the appropriate Associate Editor who then recommends acceptance or rejection. The Editor-in-Chief makes final decisions regarding publication. Upon acceptance, the senior author will be sent one set of PDF proofs for review. Examine the current issue for more information about the format used.

Journal of Cave and Karst Studies

Volume 81 Number 1 March 2019

CONTENTS

Article	1
Observations on the Population Ecology of the Cave Salamander, <i>Eurycea lucifuga</i> (Rafinesque, 1822) <i>J. Gavin Bradley and Perri K. Eason</i>	
Article	9
Geological and Hydrogeological Effective Factors in the High Permeability Zones of Several Dam Sites of the Zagros Region, Iran <i>Behnaz Shabab Boroujeni, Javad Ashjari and Haji Karimi</i>	
Article	25
Caves in Space <i>John Mylroie</i>	
Article	33
Relict Drainage Effects on Distribution and Morphometry of Karst Depressions: A Case Study from Central Taurus (Turkey) <i>Mehmet Furkan Şener, Muhammed Zeynel Öztürk</i>	
Article	44
Formation Mechanisms for the Largest Sandstone Sinkhole in Ohio <i>Joshua A. Novello and Ira D. Sasowsky</i>	
Article	57
The Relationship between Presence of Brown Bear (<i>Ursus arctos</i>) and Diversity of Airbone Algae and Cyanobacteria in the Glowoniowa Nyża Cave, Tartra Mountains, Poland <i>Joanna Czerwik-Marcinkowska, Tomasz Zwiłacz-Kozica, Wojciech Pusz, and Anna Wojciechowska</i>	
Book Review	68
Neolithic Alepotrypa Cave in the Mani, Greece: in Honor of George Papathanassopoulos <i>Reviewed by Margaret Palmer</i>	

Visit us at www.caves.org/pub/journal